1. Report No.	2. Government Accession No.	3. Recipient's Catalog No.
FHWA/TX-02/2123-2		

4. Title and Subtitle	5. Report Date
DEVELOPMENT OF AN ANALYSIS PROCEDURE FOR LOAD-ZONING PAVEMENTS	November 2001
	6. Performing Organization Code

7. Author(s)	8. Performing Organization Report No.
Emmanuel G. Fernando and Wenting Liu	Report 2123-2

9. Performing Organization Name and Address	10. Work Unit No. (TRAIS)
Texas Transportation Institute The Texas A&M University System College Station, Texas 77843-3135	11. Contract or Grant No. Project No. 0-2123

12. Sponsoring Agency Name and Address	13. Type of Report and Period Covered
Texas Department of Transportation Research and Technology Implementation Office P. O. Box 5080 Austin, Texas 78763-5080	Research: September 1998 - August 1999 14. Sponsoring Agency Code

15. Supplementary Notes

Research performed in cooperation with the Texas Department of Transportation and the U.S. Department of Transportation, Federal Highway Administration.
Research Project Title: Develop a Method for Determining Allowable Loads on Load-Zoned Pavements - Phase II

16. Abstract

Most load-zoned roads in Texas are still posted with a gross vehicle weight (GVW) limit of 58,420 lbs, corresponding to the legal load limit at the time these roads were designed and built. Since the load from a vehicle is transmitted to the pavement through its axles, establishing load limits based on axle load and axle configuration is a more rational approach than the one presently used. Realizing the need for a better methodology of load-zoning pavements, the Texas Department of Transportation funded a project to develop a procedure for evaluating load restrictions on the basis of axle load and axle configuration. This report documents the development of the load-zoning analysis procedure. Research efforts conducted at the Texas Transportation Institute led to the development of the Program for Load-Zoning Analysis (PLZA) that pavement engineers may use to evaluate the need for load restrictions and to determine, as appropriate, the single and tandem axle load limits based on a user-prescribed reliability level.

To predict the induced pavement response under surface wheel loads, PLZA uses a layered elastic pavement model that permits users to characterize pavement materials as linear or nonlinear. The predicted horizontal strain at the bottom of the asphalt layer, and the vertical strain at the top of the subgrade are used to evaluate pavement performance. To combine the effects of different axle loads and axle configurations, PLZA uses Miner's hypothesis of cumulative damage to predict service life and the probability of pavement failure within a prescribed analysis period. This report explains the methodology for load-zoning and demonstrates its application using data collected on in-service pavements.

17. Key Words	18. Distribution Statement
Load-Zoning, Axle Load Limits, Nondestructive Testing, Pavement Evaluation, Pavement Performance Prediction	No restrictions. This document is available to the public through NTIS: National Technical Information Service 5285 Port Royal Road Springfield, Virginia 22161

19. Security Classif.(of this report)	20. Security Classif.(of this page)	21. No. of Pages	22. Price
Unclassified	Unclassified	90	

DEVELOPMENT OF AN ANALYSIS PROCEDURE FOR LOAD-ZONING PAVEMENTS

by

Emmanuel G. Fernando
Associate Research Engineer
Texas Transportation Institute

and

Wenting Liu
Assistant Research Scientist
Texas Transportation Institute

Report 2123-2
Project Number 0-2123
Research Project Title: Develop a Method for Determining Allowable Loads on Load-Zoned Pavements - Phase II

Sponsored by the
Texas Department of Transportation
In Cooperation with the
U.S. Department of Transportation
Federal Highway Administration

November 2001

TEXAS TRANSPORTATION INSTITUTE
The Texas A&M University System
College Station, Texas 77843-3135

DISCLAIMER

The contents of this report reflect the views of the authors, who are responsible for the facts and accuracy of the data presented. The contents do not necessarily reflect the official views or policies of the Texas Department of Transportation (TxDOT) or the Federal Highway Administration (FHWA). This report does not constitute a standard, specification, or regulation, nor is it intended for construction, bidding, or permit purposes. The engineer in charge of the project was Dr. Emmanuel G. Fernando, P.E. # 69614.

ACKNOWLEDGMENTS

The work reported herein was conducted as part of a research project sponsored by TxDOT and FHWA. The objective of the study was to develop an automated procedure for evaluating the need for load restrictions and to determine, as appropriate, the allowable axle load limits along a given route based on predicted performance. The authors gratefully acknowledge the support and guidance of the project director, Joe Leidy of the Materials and Pavements Section of TxDOT. In addition, the contributions of the following individuals are recognized and sincerely appreciated:

1. Billy Pigg of the Waco district and Mark McClanahan of the Tyler district provided personnel and equipment to the field evaluation of load-zoned pavements conducted in this project.
2. Seong-Wan Park and Lee Gustavus of the Texas Transportation Institute (TTI) collected field data on load-zoned pavements and conducted laboratory tests on material samples taken from these pavements.

TABLE OF CONTENTS

LIST OF FIGURES

Figure Page

Figure Page

LIST OF TABLES

Table Page

CHAPTER I
INTRODUCTION

Overweight and oversized vehicles play an important role in economic development. The productivity in the movement of goods can certainly be enhanced if truckers are allowed to use highways at the vehicles' peak operating capacities. However, the consequent increase in truck loadings will accelerate the deterioration of highways and bridges. Unless additional funds are available to upgrade existing highways to higher standards or to pay for the increased maintenance and resurfacing costs due to accelerated deterioration, pavements will reach their service lives much earlier than originally planned. Thus, there are laws empowering state authorities to post load restrictions on highways, particularly those not built to accommodate today's heavier truck traffic.

In Texas, there are approximately 17,500 miles of load-zoned pavements, comprising more than 20 percent of the number of centerline miles on the state-maintained system. These pavements are primarily low-volume farm-to-market roads (FMs) constructed in the 1950s, at a time when legal load limits were lower than they are now. Like most governments, Texas does not have the money to upgrade all existing load-zoned pavements to accommodate present truck traffic, nor is this justifiable for many of these pavements because of the continuing low traffic volumes. To do so would divert funds from higher priority highway and bridge improvement projects.

The effects of oversized/overweight vehicles have been studied in numerous investigations (*1*-*8*). In this regard, Park and Fernando (*9*) have reviewed load-zoning practices in Texas and other agencies. Their review showed that existing procedures vary between road authorities. Many of the guidelines in place were developed from years of experience and typically rely on deflection measurements to establish the need for load restrictions and the magnitudes of load limits. In many agencies, these determinations are based on empirical correlations between pavement deflections and pavement life. The review also showed that load limit postings vary between highway agencies, from seasonal to year round, and from the simple use of gross vehicle weight (GVW) limits, to the combined specification of gross vehicle and axle load limits.

Most load-zoned roads in Texas are still posted with a GVW limit of 58,420 lbs, corresponding to the legal load limit at the time these roads were designed and built. Since the load from a vehicle is transmitted to the pavement through its axles, determining load limits on the basis of axle load is a better approach than the one presently used. Under the policy of uniform GVW posting, a vehicle may be within the specified load limit but still be damaging roads because of high axle loads. Conversely, the gross vehicle weight may be above the posted load limit, but still cause less deterioration if the vehicle load is distributed through the axles in such a way that the imparted pavement stresses are minimized. Thus, axle load limits may actually encourage the use of alternative vehicle configurations that will allow truckers to transport goods more efficiently while at the same time minimizing the damage done to the pavement.

Developing policies to regulate the operations of oversized/overweight trucks is a complex problem as these policies have far-reaching political, social, economic, and environmental implications. Many factors enter into the equation. For example, load limits affect the amount of freight that can be moved on any given trip. Assuming constant payload, increasing load limits will result in fewer trips, allowing truckers to maximize their operating efficiency. This may lead to reductions in vehicle operating costs brought about by fuel savings, a potential benefit to the environment. Further, the savings in vehicle operating costs may be passed on to the consumer in terms of lower prices. On the other hand, the increased load limits may lead to accelerated pavement deterioration since the reduction in trips may not be enough to offset the increase in pavement damage per vehicle trip due to increased axle loads. In view of the already limited resurfacing budgets available to transportation agencies and the backlog of projects that already exists, increased load limits will likely lead to degradation of the highway infrastructure. Without additional funds to pay for the extra wear and tear on the state's highways and bridges, all road users will eventually suffer due to increased vehicle operating costs and increased travel time associated with deteriorated pavements. However, coming up with a mechanism to raise needed revenue is not easy.

Evaluating the complex political, social, economic, and environmental effects of oversized/overweight vehicles is beyond the scope of the present study. In conducting this project, researchers focused on the engineering aspects of the problem to develop a rational

methodology for evaluating load restrictions on the basis of axle load and axle configuration. The development efforts resulted in the Program for Load-Zoning Analysis (PLZA) that is described in the user's guide prepared by Fernando and Liu (*10*). The present report documents the development of this computer program. It is divided into the following chapters:

1. Chapter I provides background on the objective and scope of this project;
2. Chapter II presents the methodology used by researchers to develop the program for load-zoning analysis;
3. Chapter III presents a sensitivity analysis of predicted pavement life using the performance models in PLZA;
4. Chapter IV illustrates the application of the computer program using data from selected test sites; and
5. Chapter V summarizes the findings from the project and provides recommendations for implementing PLZA.

The appendix presents penetration curves from dynamic cone penetrometer tests conducted by researchers on the pavement sections used to demonstrate the application of the load-zoning analysis procedure.

CHAPTER II
METHODOLOGY FOR EVALUATING LOAD RESTRICTIONS

A load-zoning analysis will generally address the following questions:

1. Is there a need for posting load limits on a given route?
2. If load restrictions are necessary, what axle load limits should be used?

The framework that researchers used to develop PLZA incorporates these two steps in the load-zoning analysis. The authors adopted this approach because most load-zoning evaluations in recent years have pertained to the removal of existing load limits on roads that have been upgraded through rehabilitation or reconstruction. The districts make every effort to rehabilitate an existing load-zoned road to a higher standard to accommodate truck traffic at the legal load limits; thus, it is expected that most applications will relate to the applicability of removing existing load limits, rather than to posting new load limits.

The methodology that researchers developed for evaluating load restrictions is based on predicting the effects of load limits on pavement performance. Figure 1 illustrates the framework the researchers used to develop the load-zoning analysis program. In the procedure developed, pavement engineers must first characterize the route they will analyze. This step is done using existing capabilities within TxDOT, which include the application of ground penetrating radar (GPR) to estimate pavement layer thicknesses, and the backcalculation of layer moduli from falling weight deflectometer (FWD) measurements. The authors recommend a GPR survey on the route to establish the variations in layer thickness. This survey should be conducted at the beginning of the evaluation for the following purposes:

1. to detect possible changes in pavement cross-section along the route and divide the route into analysis segments, as appropriate;
2. to establish the need for cores or dynamic cone penetrometer (DCP) data to supplement the radar survey and identify locations where coring or DCP measurements should be made; and

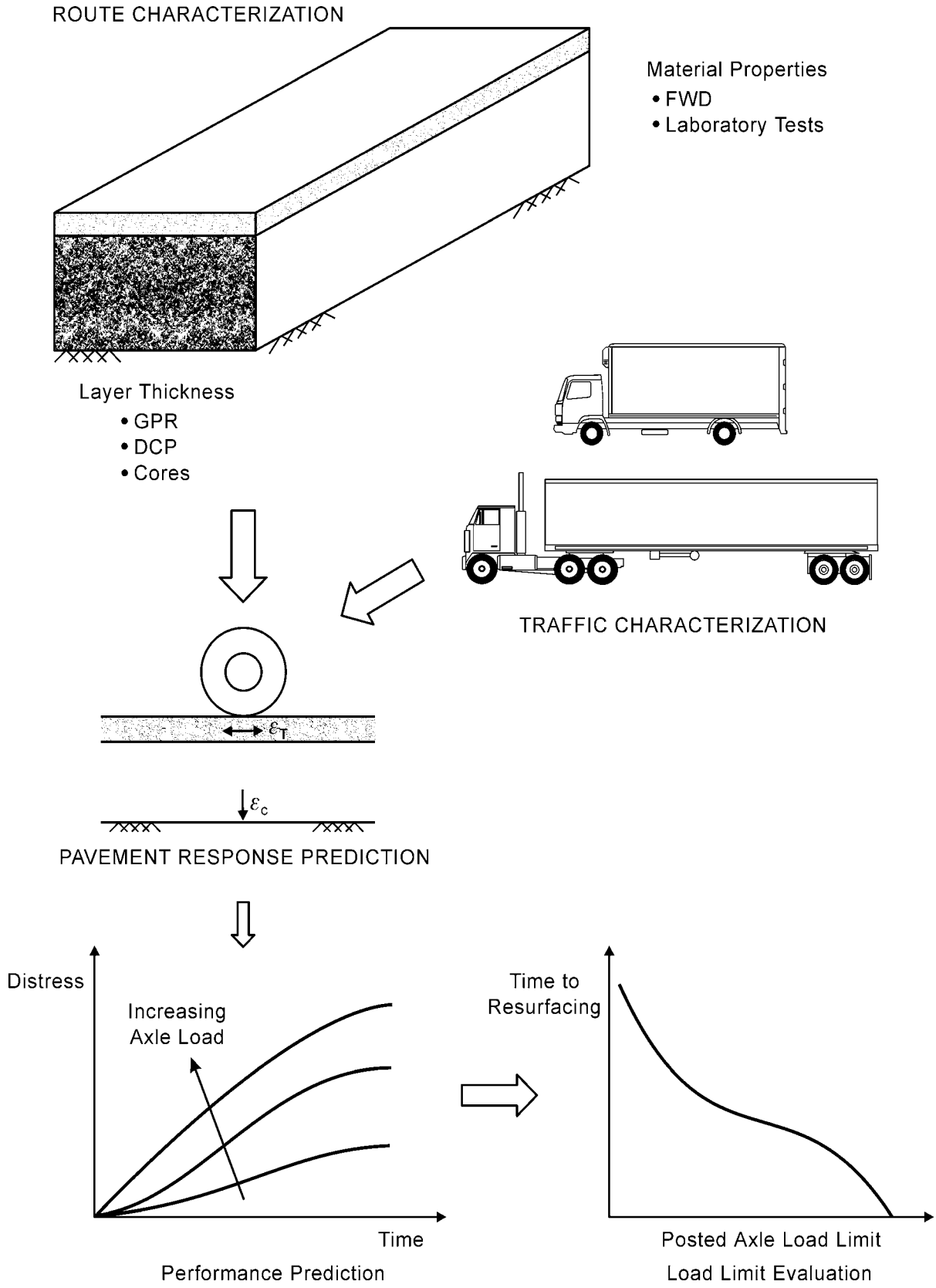

Figure 1. Framework Used to Develop Program for Load-Zoning Analysis.

3. to establish the locations of FWD measurements consistent with pavement section changes identified from the radar survey.

In addition, pavement engineers must characterize the traffic load distribution on a given route. In this regard, they may request truck traffic data from the Transportation Planning and Programming (TP&P) division of TxDOT. The beginning and ending average daily traffic (ADT) values, directional factor, and percent trucks are normally tabulated by TP&P in the *Traffic Analysis for Highway Design* report that it provides in response to requests from districts or the Materials and Pavements section of TxDOT's Construction Division. The data reported are used in the analysis procedure, along with an estimate of the average number of axle groups per truck, the percent single axles, and the percent tandem axles, to predict the cumulative single and tandem axle load applications during the specified design period. PLZA uses the predicted cumulative load applications to evaluate the need for load restrictions, and the applicable single and tandem axle load limits, as appropriate. In this analysis, PLZA predicts pavement response to wheel loading using the layered elastic model in the Program to Analyze Loads Superheavy (PALS) developed by Jooste and Fernando (*11*). PLZA provides the option of modeling the nonlinear behavior observed in pavement materials. This capability becomes particularly important for thin-surfaced pavements, which comprise a big portion of the highway network in Texas. For these pavements, a nonlinear analysis will provide a more realistic prediction of the stresses induced under loading (*11*). PLZA models the nonlinearity or stress-dependency of pavement materials using the following equation by Uzan (*12*):

$$E = K_1\, pa \left(\frac{\theta}{pa}\right)^{K_2} \left(\frac{\tau_{oct}}{pa}\right)^{K_3} \qquad (1)$$

where,

E = layer modulus,

θ = bulk stress,

τ_{oct} = octahedral shear stress,

pa = atmospheric pressure (14.5 psi), and

K_1, K_2, K_3 = material constants determined from resilient modulus testing.

Given the principal stresses, σ_1, σ_2, and σ_3, predicted from layered elastic theory, the first stress invariant and octahedral shear stress are determined from the following equations:

$$\theta = \sigma_1 + \sigma_2 + \sigma_3 \tag{2}$$

$$\tau_{oct} = \frac{1}{3}\sqrt{(\sigma_1 - \sigma_2)^2 + (\sigma_2 - \sigma_3)^2 + (\sigma_3 - \sigma_1)^2} \tag{3}$$

The relationship given by Eq. (1) is often referred to as the Universal Soil Model because it can be used to characterize the resilient properties of both fine-grained and coarse-grained soils. Because of this feature, researchers decided to use the model in PLZA. The coefficients, K_1, K_2, and K_3, may be determined from laboratory tests using the procedure developed by the American Association of State Highway and Transportation Officials (AASHTO). This test method, designated as AASHTO T 292-91, is applicable for untreated base/subbase, and subgrade materials. Since the calculated stresses are normalized with respect to the atmospheric pressure, the K_1, K_2, and K_3 coefficients are dimensionless.

In their study, Jooste and Fernando (*11*) found that the coefficient K_1 has the most influence on the predicted resilient modulus. Figure 2 illustrates this finding. The figure shows the predicted resilient moduli for a granular base material at three different values of K_1. The data shown were calculated assuming a pavement with a 4-inch-thick asphalt concrete surface layer overlying an 8-inch-thick granular base. Values of 0.6 and !0.3 were assumed for the parameters K_2 and K_3, respectively, for the base material.

For a given curve, it is observed that the resilient modulus increases with increasing wheel load, illustrating the hardening effect of increasing confinement on the predicted resilient modulus. This hardening effect is associated with the K_2 term of Eq. (1) given by:

$$K_2 \ term = \left(\frac{\theta}{pa}\right)^{K_2} \tag{4}$$

As the wheel load increases, the confining pressure also increases, resulting in higher predicted values for the resilient modulus. However, the octahedral shear stress also increases with increasing wheel load, which will tend to decrease the resilient modulus.

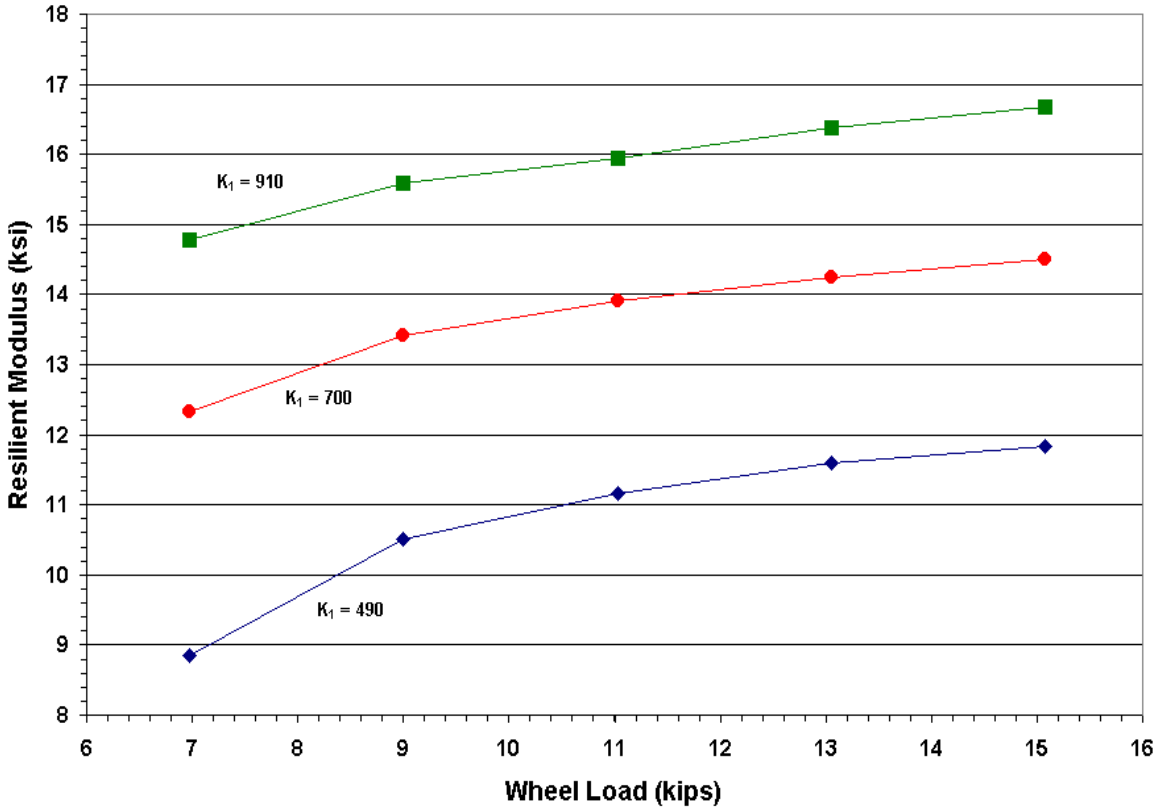

Figure 2. Variation of Predicted Resilient Modulus with K_1 (*11*).

For the pavement and range of wheel loads considered in Figure 2, the predicted increase in confinement with higher wheel load compensates for the softening effect of the octahedral shear stress. Thus, the resilient modulus is predicted to increase with higher wheel load. However, the opposite trend may be obtained for other pavements (such as thin pavements), where the softening effect of the octahedral shear stress may be more pronounced. Readers may discern the hardening effect of higher confinement and the softening effect of higher octahedral shear stress from Figure 3. The K_3 term in the figure is equal to:

$$K_3\ term = \left(\frac{\tau_{oct}}{pa}\right)^{K_3} \quad (5)$$

Note that, as the wheel load increases, the K_2 term increases because of higher confinement. However, the octahedral shear stress also increases so that the K_3 term diminishes with

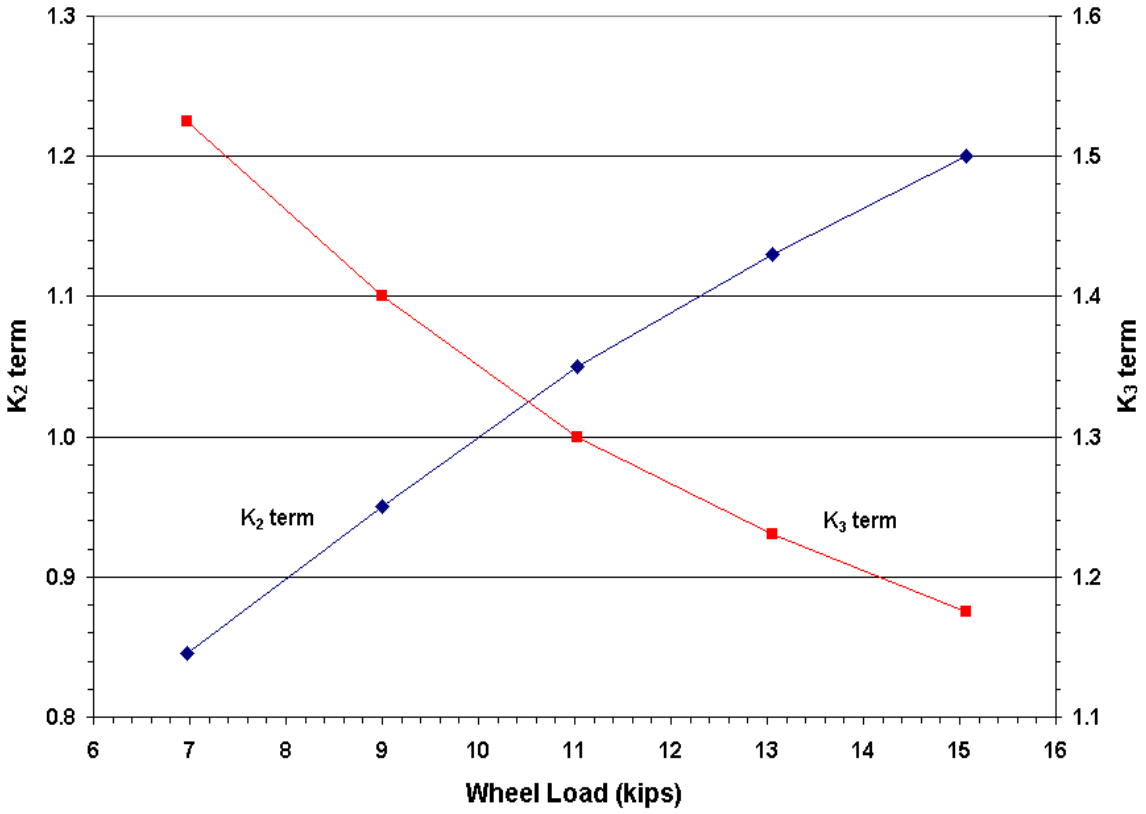

Figure 3. Illustration of the Hardening Effect Due to Increasing Confinement and the Softening Effect Due to J_{oct} (*11*).

higher wheel loads. Consequently, while the effect of higher K_1 is generally to increase the predicted resilient modulus, the effects of K_2 and K_3 depend on the interactions between these coefficients, the applied loads, and the pavement geometry. The tendency of a material to stiffen with increasing confinement is related to K_2. However, this tendency is counteracted by the softening effect under increasing shear, as controlled by the coefficient K_3. The greater the tendency of a material to stiffen under increasing confinement, the higher the effect of K_2. Similarly, the greater the tendency of a material to soften under shear, the higher the effect of K_3. The effects of these coefficients on the resilient modulus are also affected by the applied loads and pavement geometry due to the effects of these latter factors on the induced stresses.

Titus-Glover and Fernando (*13*) tested a number of untreated base and subgrade materials used in Texas and provided values of K_1, K_2, and K_3 at different moisture levels. Tables 1 and 2 show the coefficients for different materials determined from their tests.

Table 1. Laboratory Values of K_1, K_2, and K_3 for Untreated Granular Materials (13).

Material Type	K_1			K_2			K_3		
	- opt.[1]	at opt.	+ opt.[2]	- opt.	at opt.	+ opt.	- opt.	at opt.	+ opt.
Caliche	1443	888	477	1.18	0.83	0.19	0.00	0.00	0.00
Iron Ore Gravel	2816	3271	211	0.60	0.49	0.56	0.00	0.00	0.00
Shell Base	827	815	753	1.10	0.60	0.78	0.00	0.00	0.00
Crushed Limestone	1498	1657	—	0.90	0.90	—	-0.33	-0.33	—
Average	1646	1658	480	0.95	0.71	0.51	-0.33	-0.33	0.00
Std. Dev.	725	988	221	0.22	0.17	0.24	0.00	0.00	0.00

[1] From tests run at moisture contents below optimum
[2] From tests conducted at moisture contents above optimum

Table 2. Laboratory Values of K_1, K_2, and K_3 for Subgrade Materials (13).

Material Type	K_1			K_2			K_3		
	- opt.	at opt.	+ opt.	- opt.	at opt.	+ opt.	- opt.	at opt.	+ opt.
Sand	3118	6434	6319	0.44	0.51	0.40	0.00	0.00	-0.03
Sandy Gravel	11,288	1574	—	0.63	0.67	—	-0.10	-0.28	—
Lean Clay	4096	105	776	0.00	0.32	0.10	-0.27	0.10	-0.55
Fat Clay	200	263	440	0.66	1.25	0.66	-1.47	-0.50	-0.17
Silt	824	1172	998	1.19	0.52	0.50	-0.11	-0.20	-0.10
Averages for Sandy Materials	7203	4004	6319	0.53	0.59	0.40	-0.05	-0.14	-0.03
Standard Deviation for Sandy Materials	4085	2430	0	0.09	0.08	0.00	0.05	0.14	0.00
Averages for Clayey Materials	1707	513	738	0.62	0.70	0.42	-0.62	-0.20	-0.27
Standard Deviation for Clayey Materials	1709	470	229	0.49	0.40	0.24	0.61	0.24	0.20

Pavement engineers may use the data shown in these tables to estimate the values of the K_1, K_2, and K_3 coefficients when resilient modulus data from laboratory tests are not available.

In practice, a falling weight deflectometer survey is conducted over the route to be evaluated. Thus, to conduct a load-zoning analysis using PLZA, the engineer inputs the K_2 and K_3 values. K_1 is then estimated using the prescribed K_2 and K_3 coefficients with the modulus backcalculated from FWD data. Note that the program permits the engineer to model a given material as linear or nonlinear elastic. For a linear elastic material, the coefficients K_2 and K_3 in Eq. (1) are zero, and K_1 is directly determined from the backcalculated modulus.

PLZA uses the predicted pavement response, specifically the horizontal strain at the bottom of the asphalt layer, and the vertical strain at the top of the subgrade to predict the service life for a given pavement, axle load, and axle configuration. In predicting pavement performance, the Asphalt Institute equations for fatigue cracking and rutting are used (*14*). The service life based on fatigue cracking, $(N_f)^c$, is predicted from the equation:

$$(N_f)^c = 7.95 \times 10^{-2} \left(\frac{1}{\varepsilon_{ac}}\right)^{3.29} \left(\frac{1}{E_{ac}}\right)^{0.854} \quad (6)$$

where,

ε_{ac} = predicted tensile strain at the bottom of the asphalt surface layer, and

E_{ac} = asphalt concrete modulus.

Equation (6) is used in the Asphalt Institute's thickness design manual (*15*) and predicts the number of load applications prior to development of 20 percent fatigue cracking based on total pavement area (*14*). The service life based on rutting is determined from:

$$(N_f)^r = 1.365 \times 10^{-9} \left(\frac{1}{\varepsilon_{sg}}\right)^{4.477} \quad (7)$$

where,

ε_{sg} = predicted vertical compressive strain at the top of the subgrade, and

$(N_f)^r$ = number of allowable load applications based on a limiting rut depth criterion of 0.5 inches (*14*).

In the load-zoning analysis, the strains induced under loading are predicted at a number of lateral offsets beneath the wheel loads, as shown in Figure 4. These positions correspond to the outside tire edge, middle of a tire, inside tire edge, and midway between the dual tires for a single axle configuration. For a tandem axle assembly, the strains are also predicted at these lateral offsets beneath the dual tires and at a distance of half the axle spacing. PLZA uses the maximum predicted asphalt tensile strain and subgrade compressive strain to predict the allowable number of axle load repetitions for a given axle configuration.

To determine the service life in years, the load-zoning program computes the ratio of the expected number of yearly load applications (from the traffic characterization) to the allowable number of load repetitions (from the performance prediction). This ratio is an estimate of the life consumed per year for a given axle configuration and load. Assuming Miner's hypothesis of cumulative damage (*16*), the damage ratios are summed to predict the yearly service life consumption. Getting the reciprocal of this sum gives the predicted service life, in years, for each failure criterion. It also defines a point on the load limit chart illustrated at the bottom right corner of Figure 1. The analysis program defines other points on the chart in a similar fashion.

In evaluating load limits, the analysis program includes an option for adjusting the cumulative single and tandem axle load repetitions that are expected to use the route during the prescribed design period. The researchers recognize that load limits affect the amount of freight that a truck may move on any given trip. To consider this effect, PLZA provides the option of adjusting the expected cumulative axle load applications with changes in axle load limits. The adjustment is carried out assuming the following:

1. The total payload carried by trucks using the route remains constant, and
2. The ratio of single to tandem axle load repetitions is maintained.

The total payload is determined based on the legal load limits. Thus, for lower limits, the expected number of applications will increase since truckers will have to make more trips to move the same total payload. Conversely, the cumulative load repetitions will decrease if axle load limits are raised. The engineer may also decide not to adjust the expected axle load repetitions with changes in load limits. Under this assumption, lowering load limits means

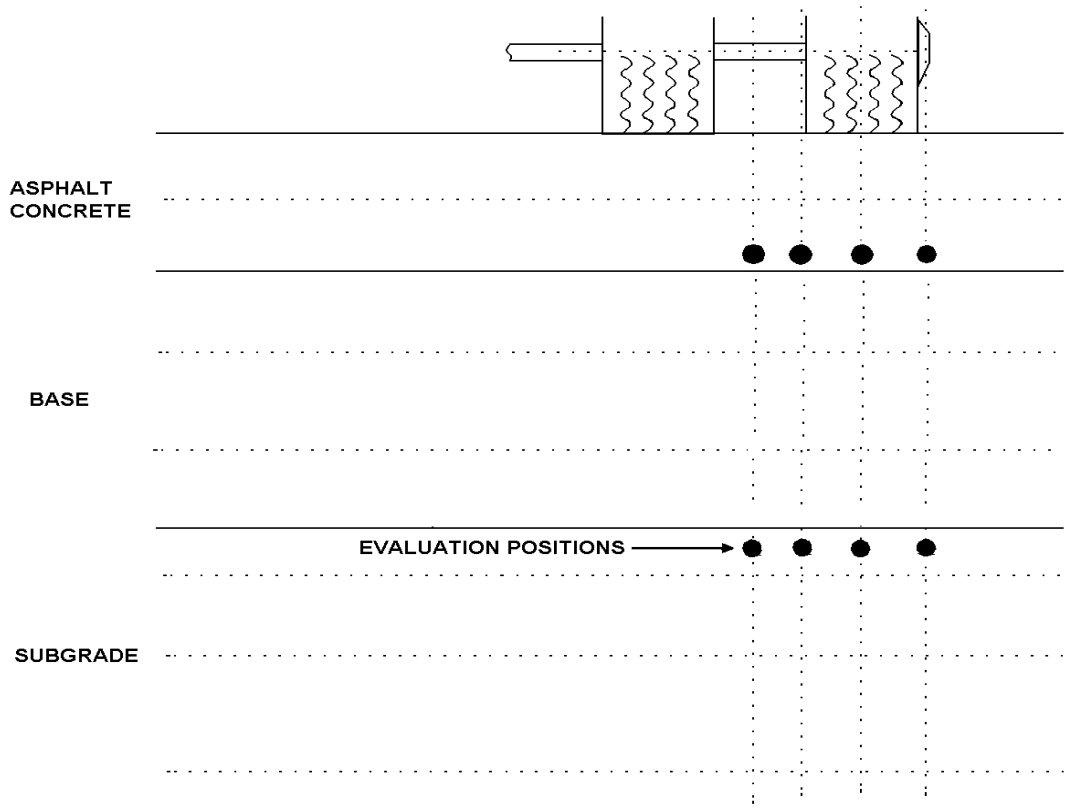

Figure 4. Locations where Strains are Predicted for Evaluating Pavement Life.

that less payload may be moved on the given roadway, implying that to carry the same payload, truckers need to find alternative routes.

In the framework used, axle load restrictions are established based on the minimum service life or time to next resurfacing required by the pavement engineer. As explained previously, the evaluation of performance uses data from characterization of the route, principally, FWD and layer thickness information. Due to variability in materials and layer thicknesses, predictions of pavement life will vary accordingly along the route. To consider this variability, PLZA uses the service life predictions to compute the probability that the service life will be less than the required life, T_r, specified by the engineer. This approach is illustrated conceptually in Figure 5, which shows a hypothetical distribution of predicted service lives, T_f. For a given set of single and tandem axle load limits, the analysis program determines the probability of premature failure, P_{fail}, assuming that the predicted service lives

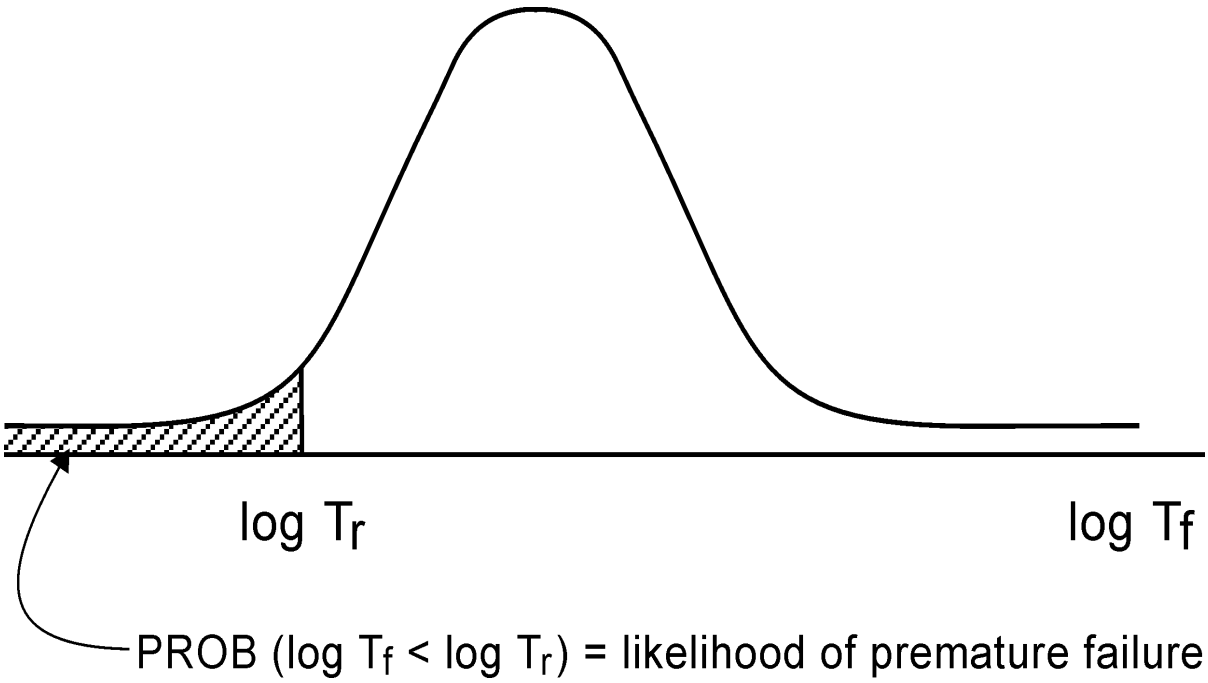

Figure 5. Conceptual Illustration of Reliability Evaluation to Establish Axle Load Restrictions.

follow a lognormal distribution. This probability is indicated by the shaded area in Figure 5. From this estimate, the analysis program evaluates pavement reliability as 1 ! P_{fail}.

The reliability from PLZA is used to establish the need for load restrictions and to determine single and tandem axle load limits, as appropriate. Specifically, the computed reliability is compared with the desired or target value that may be tied to the roadway functional classification. Table 3 presents suggested levels of reliability according to the AASHTO pavement design guide (*17*). From this table, a desired reliability level within the range of 50 to 80 percent may be appropriate to evaluate axle load restrictions on the low-volume farm-to-market roads typical of most load-zoned roads in Texas. On the other hand, existing load-zoned roads that have been upgraded through rehabilitation or reconstruction may require a higher level of reliability, within the range of 70 to 90 percent, particularly if the improvements were made in anticipation of an increase in the level of use of the facility. Note that the reliability is determined for each distress criterion. PLZA then takes the minimum of the computed reliability levels for fatigue cracking and rutting, and compares

Table 3. Suggested Levels of Reliability for Various Functional Classifications (*17*).

Functional Class	Recommended Reliability Level (percent)	
	Urban	Rural
Interstate and other freeways	85 – 99.9	80 – 99.9
Principal arterials	80 – 99	75 – 95
Collectors	80 – 95	75 – 95
Local	50 – 80	50 – 80

this value with the desired reliability level to establish the need for load restrictions, and to determine, as appropriate, the single and tandem axle load limits for the route.

CHAPTER III
SENSITIVITY ANALYSIS OF PREDICTED PAVEMENT LIFE

This chapter presents a sensitivity analysis of predicted pavement life based on the Asphalt Institute performance models (*14*) presented in Chapter II. Researchers conducted the sensitivity analysis for the following reasons:

1. to evaluate the effects of pavement design factors on predicted pavement life;
2. to identify pavement design variables that are important in the load-zoning analysis; and
3. to verify whether the effects of design variables on predicted performance are consistent with engineering experience and practice.

The results from this analysis are useful to identify options an engineer may take with respect to upgrading an existing load-zoned road to permit truckers to operate their vehicles at the legal load limits. To conduct the sensitivity analysis, the authors assumed the thin, medium and thick pavement structures shown in Table 4. For each pavement, the design factors were varied from the base or reference levels shown in the table. Specifically, each factor was varied by ±20 percent from its reference level, while holding the other factors at their corresponding base levels. The researchers then used the Asphalt Institute performance models to predict the change in pavement life with each change in the design factor. For this purpose, researchers used the predicted number of allowable 18-kip equivalent single axle loads (ESALs) to evaluate the effects of the design variables considered in the sensitivity analysis.

Figures 6 to 11 illustrate the effects of the design variables on predicted pavement life for each pavement structure and distress criterion included in the analysis. The vertical bars in each figure illustrate the relative importance of the design variables. The height of each bar corresponds to the change in predicted pavement life as the given variable is varied from the low to the high level, while the other variables are held at their base or reference levels. The horizontal line denotes the predicted life when all factors are at their reference levels.

Table 4. Pavement Structures Used in the Sensitivity Analysis[1].

Pavement Structure	Asphalt Modulus (ksi)	Base Modulus (ksi)	Subgrade Modulus (ksi)	Asphalt Thickness (inches)	Base Thickness (inches)
Thin	250	25	8	3	6
Medium	500	50	12	5	10
Thick	750	75	16	7	14

[1] Each factor was varied ±20 percent from the base or reference level shown in this table.

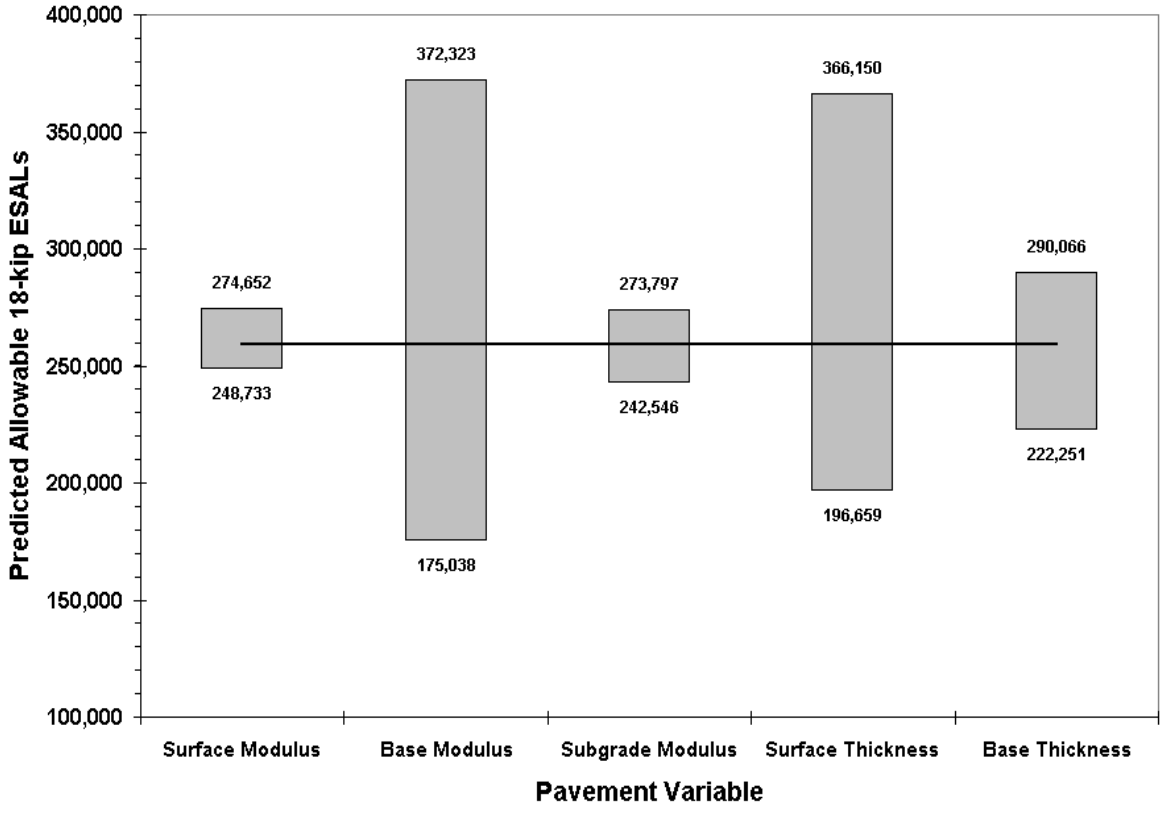

Figure 6. Effects of Design Variables on Predicted Pavement Life Based on Fatigue Cracking (Thin Pavement Structure).

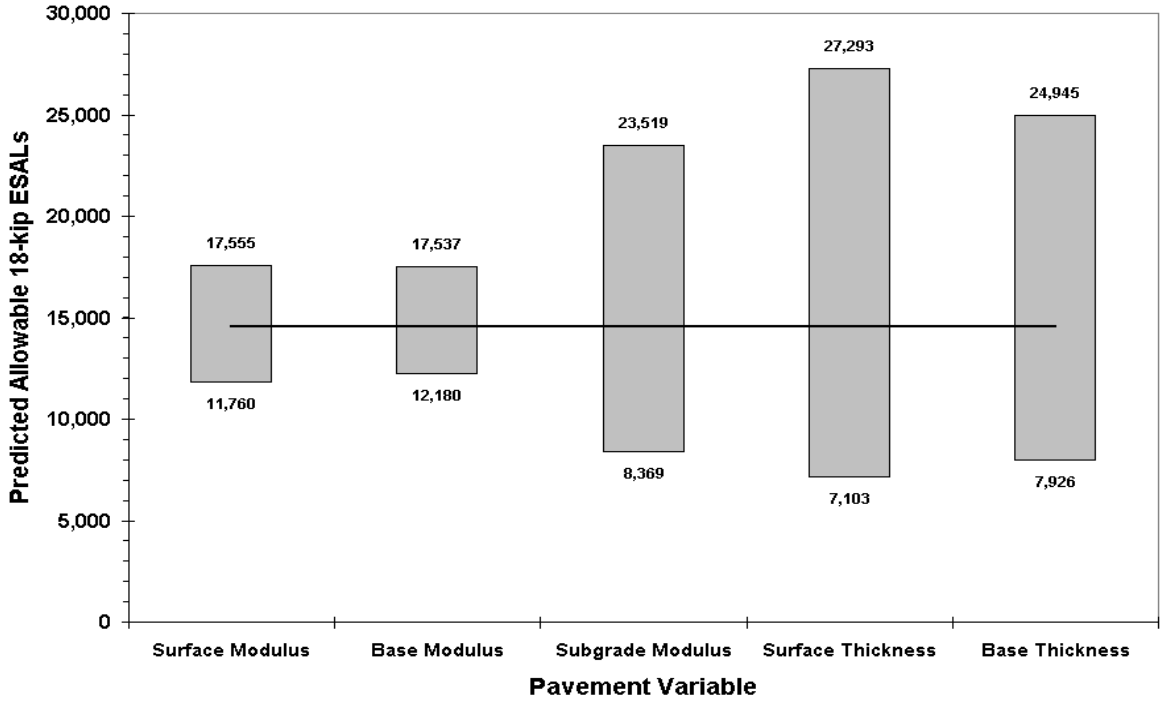

Figure 7. Effects of Design Variables on Predicted Pavement Life Based on Rutting (Thin Pavement Structure).

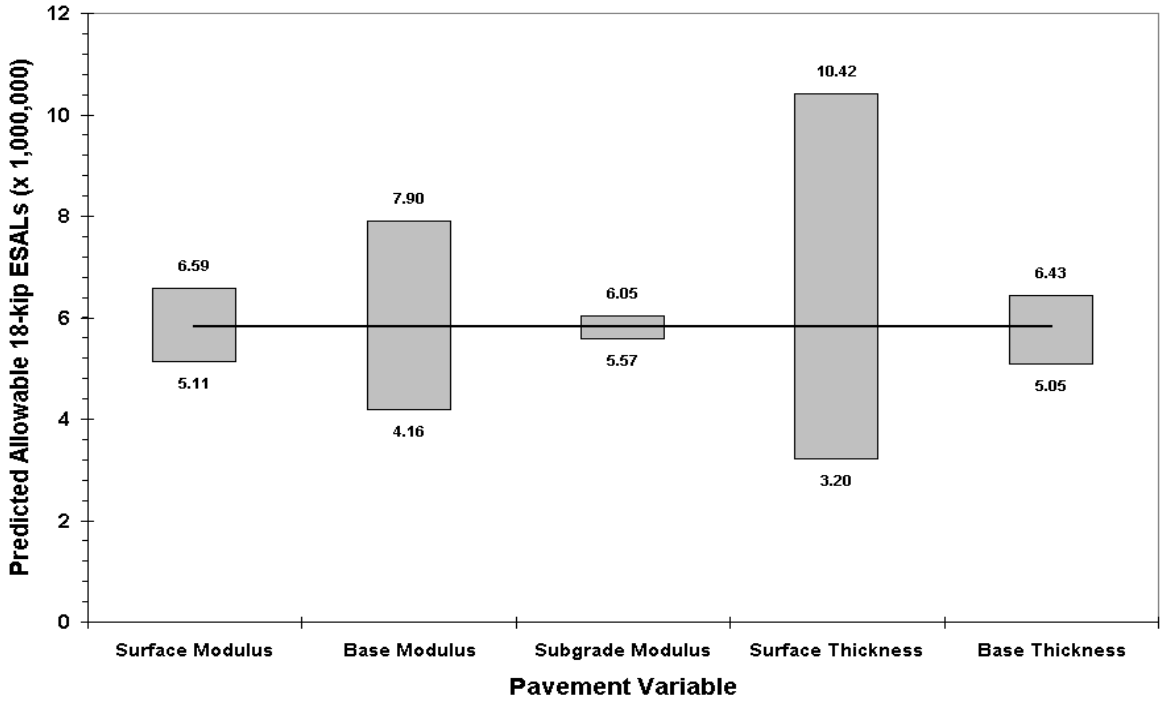

Figure 8. Effects of Design Variables on Predicted Pavement Life Based on Fatigue Cracking (Medium Pavement Structure).

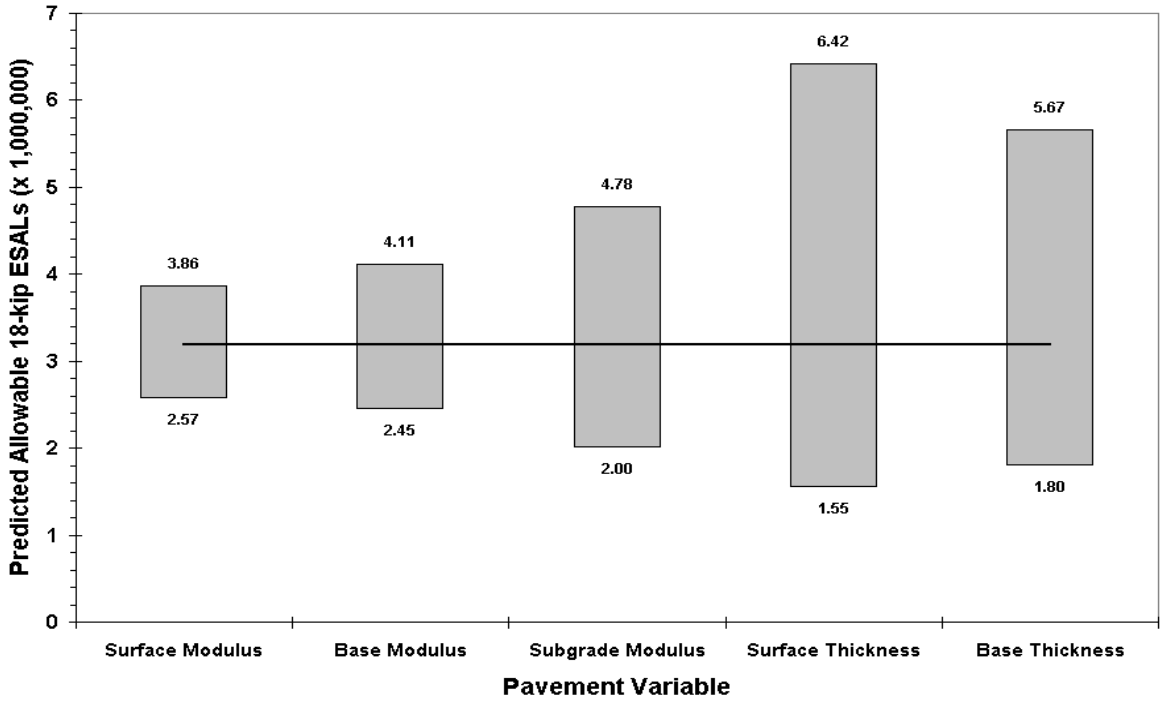

Figure 9. Effects of Design Variables on Predicted Pavement Life Based on Rutting (Medium Pavement Structure).

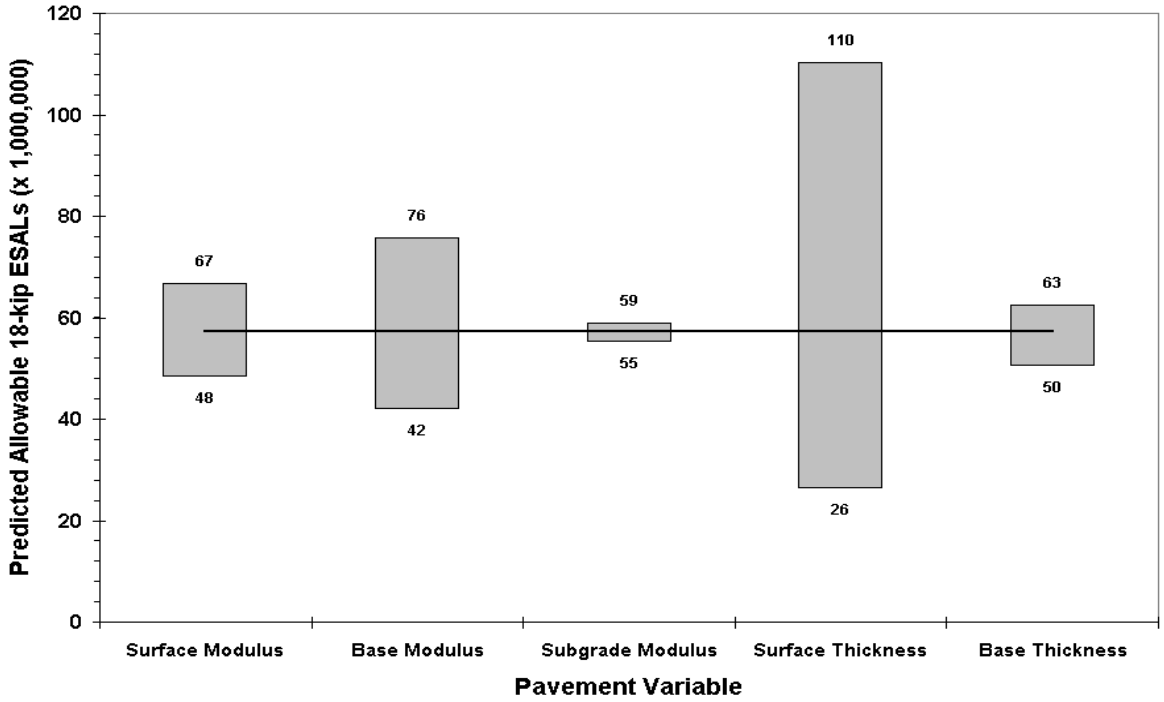

Figure 10. Effects of Design Variables on Predicted Pavement Life Based on Fatigue Cracking (Thick Pavement Structure).

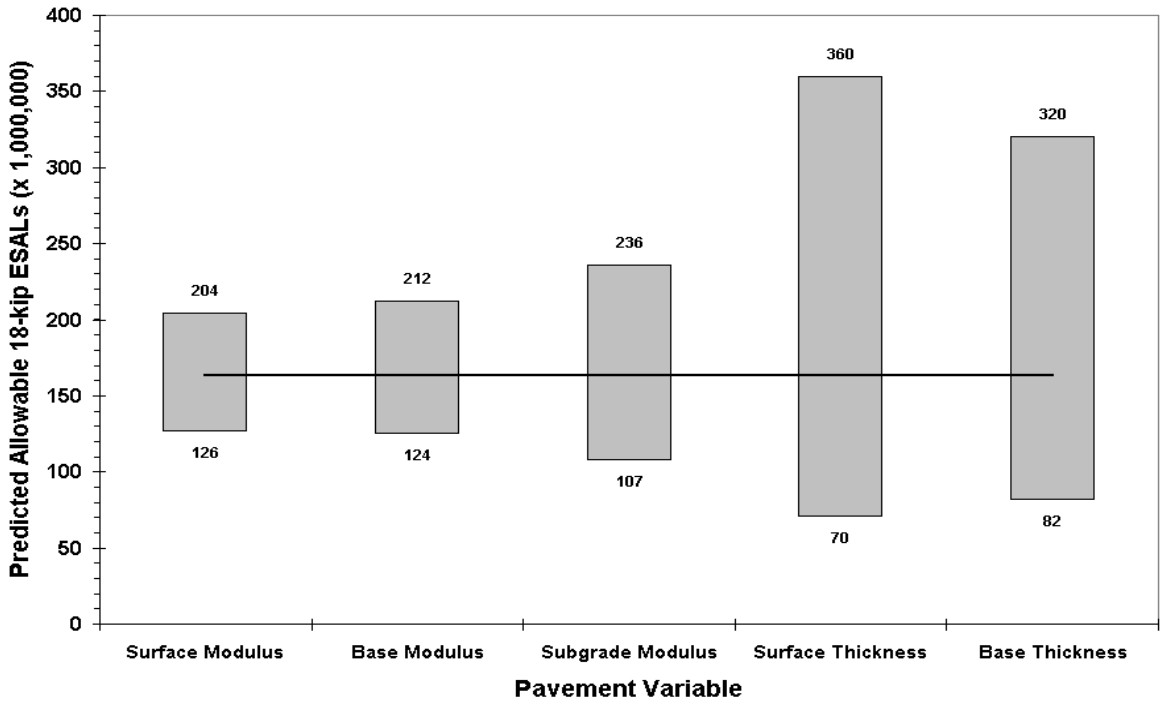

Figure 11. Effects of Design Variables on Predicted Pavement Life Based on Rutting (Thick Pavement Structure).

To show the direction of the effect, the predicted pavement lives are noted in the figures. Specifically, the number at the bottom of each bar is the predicted life at the low level (&20 percent), while the number at the top of the bar is the corresponding prediction at the high level (+20 percent) of the design variable. In addition, Table 5 shows the effects of changes in the design variables in terms of the predicted changes in pavement life, while Table 6 provides the relative rankings of the design variables based on their effects. From these results, the authors make the following observations:

1. For the pavement structures used in the sensitivity analysis, the predicted pavement life varies directly with the design variables. Figures 6 to 11 show a reduction in the predicted service life as the design variable is varied by &20 percent from its reference level. Conversely, the predicted pavement life increases as each factor is changed by +20 percent.
2. The predicted fatigue life for the thin pavement is influenced by the base modulus, surface thickness, and base thickness, and to a lesser degree, by the subgrade and surface moduli. The effects of surface thickness and base modulus

Table 5. Change in Predicted Pavement Life with Change in Design Variable.

Pavement Structure	Design Variable	Level[1]	Percent Change in Predicted Life	
			Fatigue Cracking	Rutting
Thin	Surface Modulus	Low	&4.1	&19.3
		High	+5.9	+20.5
	Base Modulus	Low	&32.5	&16.4
		High	+43.5	+20.4
	Subgrade Modulus	Low	&6.5	&42.6
		High	+5.6	+61.4
	Surface Thickness	Low	&24.2	&51.3
		High	+41.2	+87.3
	Base Thickness	Low	&14.3	&45.6
		High	+11.8	+71.2
Medium	Surface Modulus	Low	&12.2	&19.4
		High	+13.2	+21.2
	Base Modulus	Low	&28.5	&23.1
		High	+35.6	+29.0
	Subgrade Modulus	Low	&4.4	&37.2
		High	+3.8	+50.0
	Surface Thickness	Low	&45.0	&51.3
		High	+78.9	+101.4
	Base Thickness	Low	&13.2	&43.6
		High	+10.4	+77.7
Thick	Surface Modulus	Low	&15.6	&22.5
		High	+16.6	+25.1
	Base Modulus	Low	&26.6	&23.8
		High	+32.3	+29.9
	Subgrade Modulus	Low	&3.6	&34.3
		High	+3.1	+44.3
	Surface Thickness	Low	&54.2	&57.0
		High	+92.9	+120.5
	Base Thickness	Low	&12.0	&50.1
		High	+9.2	+96.0

[1] Low level is at &20% of the reference value for the given pavement. High level is at +20%.

Table 6. Relative Rankings of Design Variables.

Distress	Pavement Structure	Design Variable					
		Level[1]	Surface Modulus	Base Modulus	Subgrade Modulus	Surface Thickness	Base Thickness
Fatigue Cracking	Thin	Low	5	1	4	2	3
		High	4	1	5	2	3
	Medium	Low	4	2	5	1	3
		High	3	2	5	1	4
	Thick	Low	3	2	5	1	4
		High	3	2	5	1	4
	Average Rank		3.7	1.7	4.8	1.3	3.5
Rutting	Thin	Low	4	5	3	1	2
		High	4	5	3	1	2
	Medium	Low	5	4	3	1	2
		High	5	4	3	1	2
	Thick	Low	5	4	3	1	2
		High	5	4	3	1	2
	Average Rank		4.7	4.3	3.0	1.0	2.0

[1] Low level is at &20% of the reference value for the given pavement. High level is at +20%.

are also significant for the medium and thick pavement structures. Since fatigue life is inversely related to the asphalt tensile strain from Eq. (6), this observation reflects the significant reduction in the predicted tensile strain with a thicker surface or stiffer base, and vice versa. The authors note that fatigue life is inversely related to the modulus of the surface mix in Eq. (6). However, this inverse relationship is counteracted by the reduction in the predicted tensile strain with a stiffer mix. Thus, the predicted change in fatigue life may be positive or negative depending on the magnitude of the change in surface modulus and the corresponding change in the asphalt tensile strain determined from layered elastic theory. For the pavement structures used in the sensitivity analysis, the predicted fatigue life varied in the same direction as the change in surface modulus.

3. Overall, Table 6 indicates that the fatigue life predicted from Eq. (6) is influenced the most by the surface thickness and the base modulus, and to a lesser degree, by the base thickness and surface modulus. The subgrade modulus exhibited an appreciable effect only for the thin pavement.
4. On the basis of rutting, Figures 6 to 11 show that predicted pavement life is influenced significantly by all of the design variables. In particular, the surface thickness, base thickness, and subgrade modulus are observed to have the most impact on the predicted life, which varied in the same direction as the change in each design variable.
5. Figures 6 to 11 show that the rut depth criterion governs the predicted pavement life for the thin and medium pavements, while the fatigue criterion governs the service life for the thick pavement. Since most roads that undergo a load-zoning analysis fall under the thin and medium categories, this observation implies that, for roads comparable to the pavements analyzed, rutting will likely control the load restrictions, based on the Asphalt Institute performance equations.

In summary, the sensitivity analysis gave results that are consistent with engineering practice and experience, in the researchers' opinion. In terms of options to rehabilitate existing load-zoned roads to carry legal load limits, the results from this analysis imply that increasing the surface thickness and/or improving the base material are primary options an engineer should consider to improve the expected fatigue life of the roadway. The effect of these changes on predicted pavement response is to reduce the bending effect under load, and the tensile strain at the bottom of the surface mix. Theoretically, this reduction in tensile strain translates to a higher number of load repetitions prior to crack initiation. In addition, the increase in surface thickness adds to the number of load repetitions for crack propagation. Thus, the net result of these changes is an increase in the predicted fatigue life of the pavement.

On the basis of the rut depth criterion, the primary options an engineer should consider are to increase the surface thickness and/or base thickness, and to improve the subgrade through stabilization or replacement with a better material. The effect of these changes is to reduce the compressive strain at the top of the subgrade, resulting in a predicted increase in pavement life.

CHAPTER IV
APPLICATION OF LOAD-ZONING ANALYSIS PROCEDURE

SITE SELECTION

With assistance from TxDOT, researchers from the Texas Transportation Institute evaluated a number of load-zoned pavements using the analysis procedure presented in Chapter II. For this task, the project director contacted a number of districts to establish test sections for the evaluation. From these initial contacts, he identified four load-zoned pavements in the Waco and Tyler districts. Preliminary testing consisted of GPR surveys conducted by the project director using TxDOT's air-launched GPR system. Researchers analyzed the radar data to establish the variation of layer thickness and dielectric profiles along the pavements surveyed. From this analysis, the project director and researchers identified uniform sections within the load-zoned pavements that could potentially be used to demonstrate the application of the load-zoning methodology.

Researchers then conducted a visual inspection of each route to select test sections for this demonstration. In making the selections, the pavement condition and geometry of the route were considered. Since the procedure to evaluate load restrictions is tied to remaining life, the project director and researchers believed it necessary to pick sections that showed minimal or no visual distress. Evaluating pavements that exhibit rutting, cracking, and patching may simply verify the need for rehabilitation instead of a need for load restrictions.

In addition to pavement condition, researchers considered the geometry of the route. For safety reasons during field testing, they selected test sections along straight tangents, away from winding curves or hills that were found along the load-zoned pavements surveyed on this project. Thus, four test sections were selected from the GPR analysis and initial site inspections. Table 7 shows the test sections researchers used to demonstrate the application of the load-zoning procedure. The remainder of this chapter presents the evaluation of the selected test sections.

Table 7. Test Sections Established for Load-Zoning Analysis.

Roadway	County	Lane	Section Length (miles)	Start of Section
FM 437	Bell	K1	0.2	1.2 miles south of US 190 in Rogers
FM 933	Hill	K1	0.6	2.5 miles south of Aquilla
FM 1805	Smith	K1	0.5	1.1 miles south of FM 1253 in Jamestown
FM 751	Van Zandt	K1	0.6	4.5 miles south of Hunt-Van Zandt county line

PAVEMENT STRUCTURAL EVALUATION

Figures 12 to 15 show the GPR data collected along the load-zoned pavements, and identify the test sections evaluated by researchers. These figures show color representations of the GPR traces generated using TxDOT's COLORMAP program (*18*) developed by TTI. The reflections at the top of each figure come from the bottom of the surface layer or top of base, from which researchers made estimates of the asphalt thickness. However, researchers were unable to determine the base thickness from the GPR data. The reasons for this are two-fold. On FM 437, Figure 12 shows that the reflections appearing after the top of the base exhibit highly variable arrival times. It is difficult to establish, from the data alone, that these reflections originate from the bottom of the base. To conclude this without ground truth information would be rash, in the researchers' opinion. On the other test sites, no reflections are observed after the bottom of the surface layer, which precludes the prediction of base thickness from GPR. Consequently, TTI researchers conducted DCP tests to determine the layering from the penetration curves and establish layer thicknesses for the FWD and load-zoning analyses.

DCP Tests

On all four test sections, researchers initially drilled through the surface mix until the drill bit started bringing out base material. Loose material from drilling was then removed to expose the top of the base, and they measured the surface thickness. The diameter of the hole researchers drilled was approximately 1.9 inches. Since the surface layer is thin at all

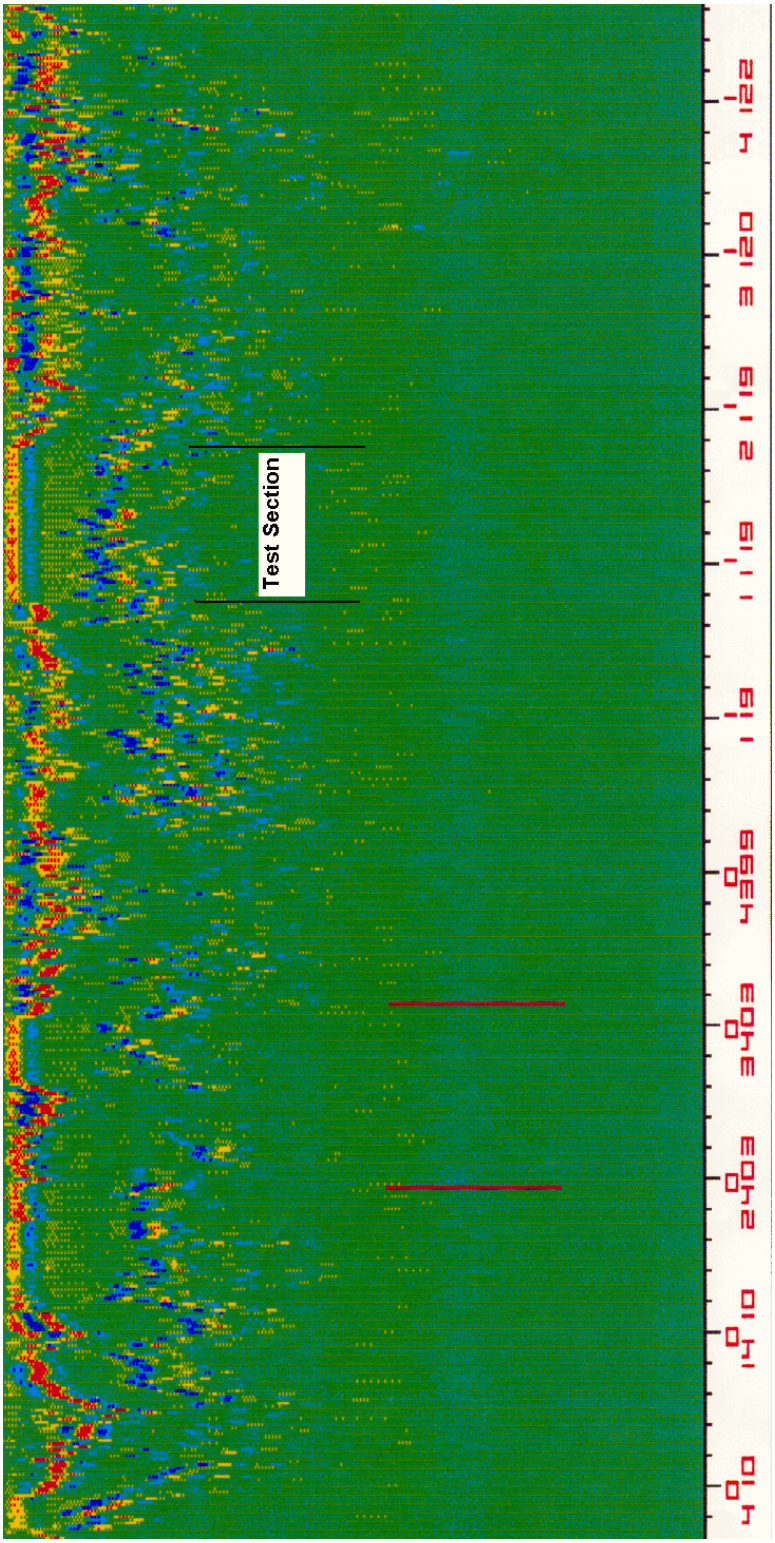

Figure 12. GPR Data Collected along FM 437.

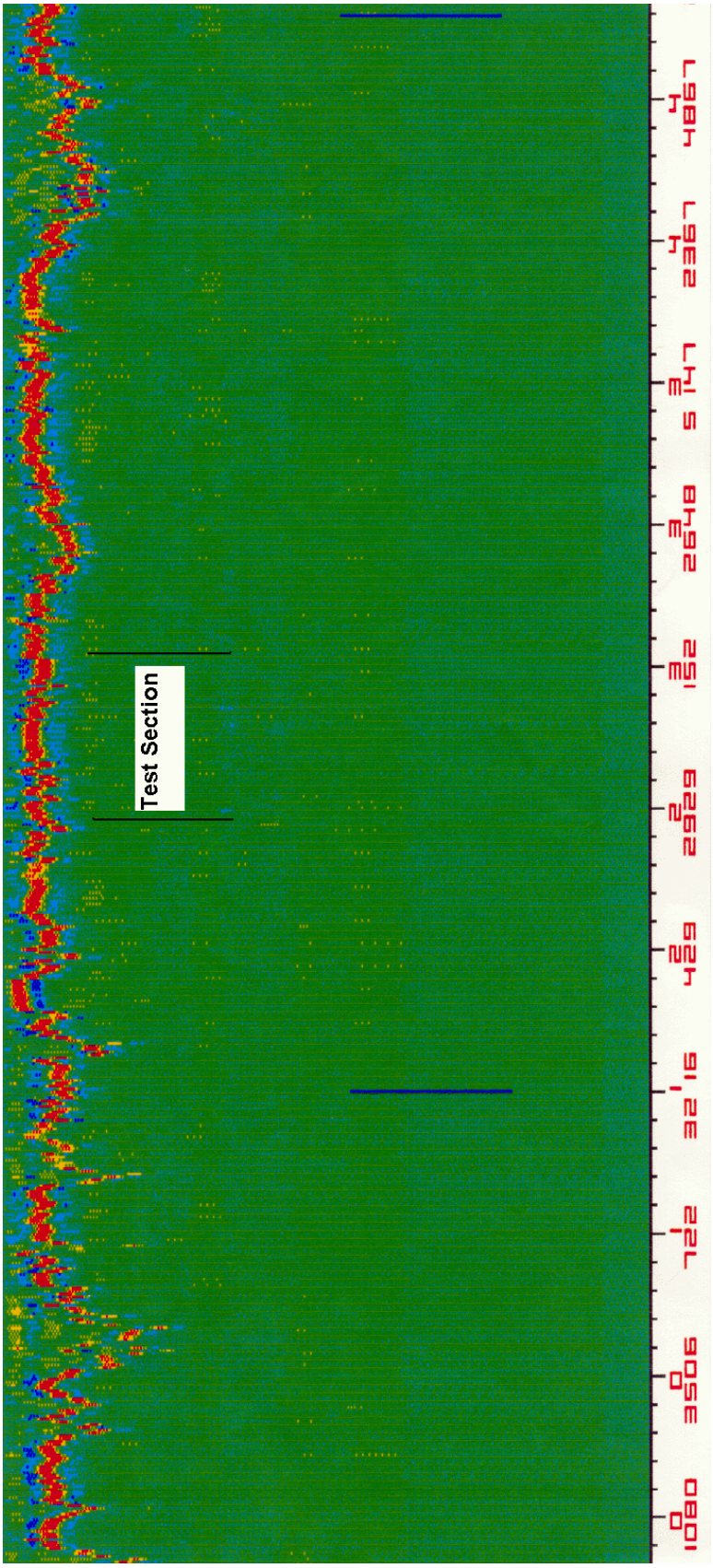

Figure 13. GPR Data Collected along FM 933.

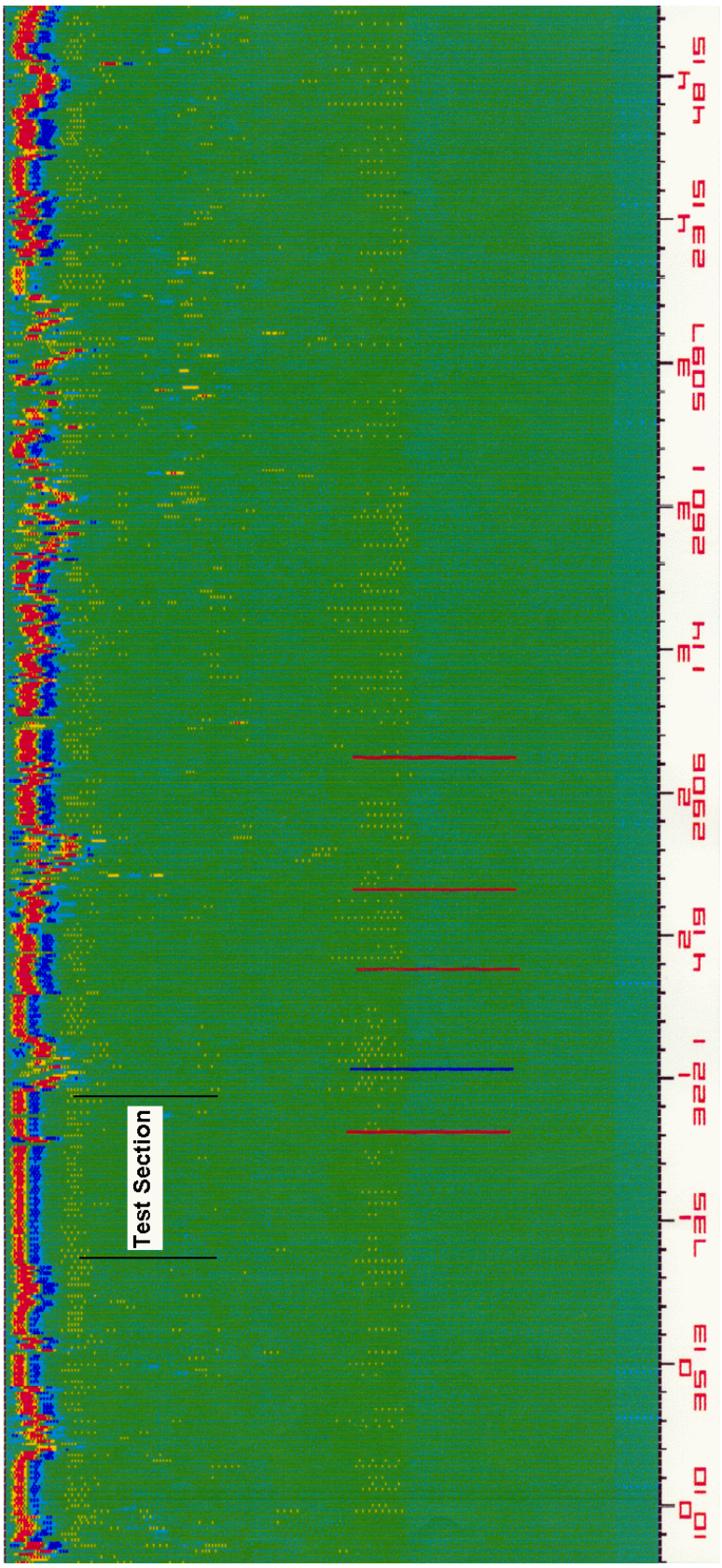

Figure 14. GPR Data Collected along FM 1805.

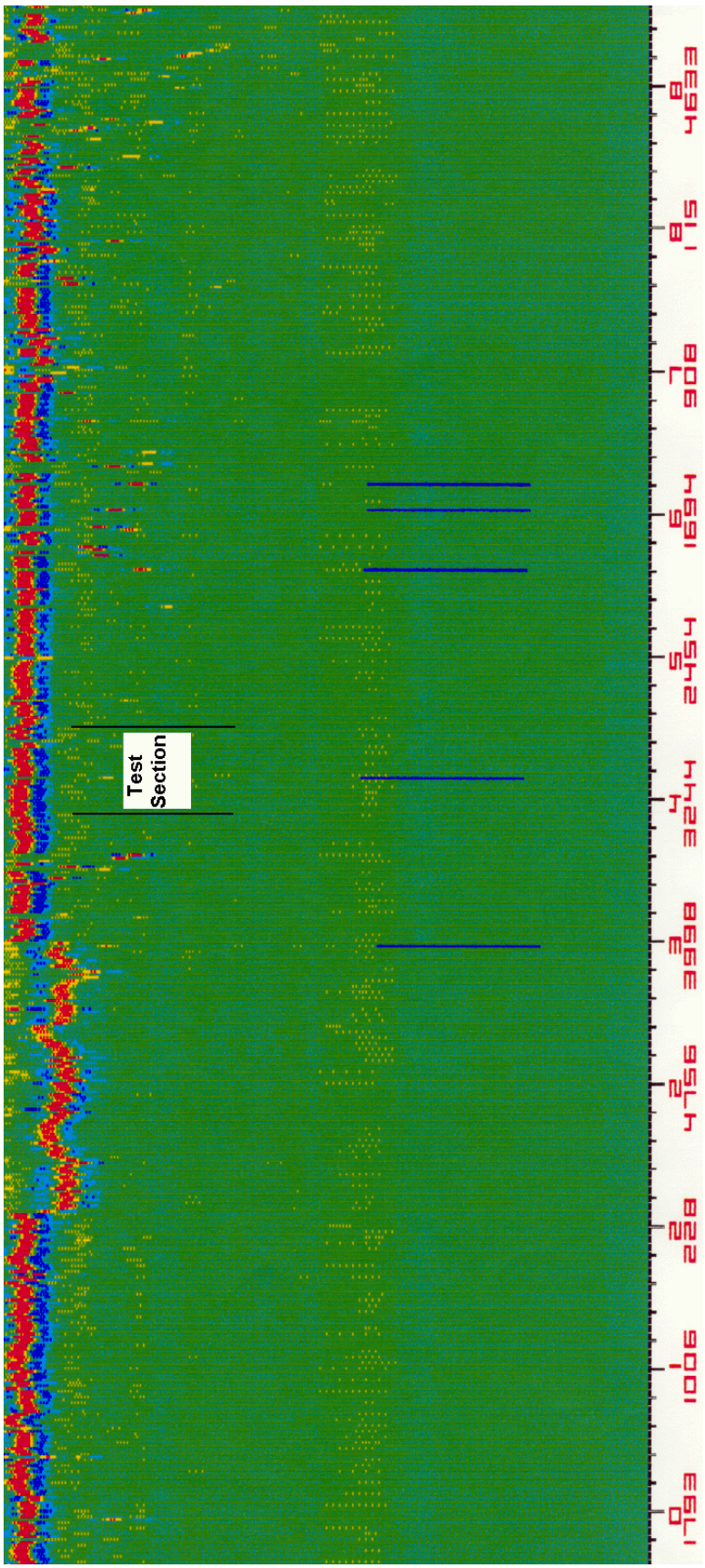

Figure 15. GPR Data Collected along FM 751.

four sections, finding the asphalt/base interface and measuring the surface thickness from inside the hole did not prove difficult. Researchers then placed the DCP inside the hole and started testing at the base layer. In most cases, the DCP was driven through the pavement for a depth of 30 to 36 inches. The appendix presents the penetration curves determined from the DCP testing.

Along FM 437, researchers found it difficult to penetrate the base layer. Because of this, the decision was made to drill through the base. It was from this drilling, when asphalt-stabilized material was observed coming out of the hole, that researchers first suspected that the existing pavement may be sitting on top of an old road. Researchers also found it difficult to penetrate this layer. As a result, the pavement layering at this test section could not be determined from the DCP. However, as this road was scheduled for rehabilitation, researchers were able to establish the layering at this site from coring reports provided by the Waco district and from a trench dug at one station along the test section. The coring data, as well as the trench cut at the site, verified that an old pavement was underneath the existing roadway. This old pavement consisted of a loose asphalt layer overlying a gravel base.

Table 8 shows the layer thicknesses determined at locations where FWD measurements were made at the four test sections. On FM 437, the subbase thickness given in the table corresponds to the old pavement noted previously. Between this old pavement and the surface is an unusually thin layer of flexible base that appears to be Austin chalk according to the Waco pavement design engineer.

On FM 933, FM 1805, and FM 751, researchers established the pavement layering below the surface mix from the DCP data collected at these sites. By identifying where the slope changes occur on the penetration curve, researchers made estimates of layer thickness as illustrated in Figure 16. Researchers used the thickness data given in Table 8 to backcalculate layer moduli from the FWD data using the MODULUS program (*19*).

Materials Sampling

At each section, a maintenance foreman from the district dug a trench at a selected station so that researchers could verify the layering at the site and identify the materials comprising the pavement. Trenching was done after completion of FWD and DCP tests, using a backhoe from the district. The FWD deflections and DCP data were used to

Table 8. Layer Thicknesses at Locations of FWD Measurements on Test Sections.

Location of Test Section	Station	Layer Thickness (inches)		
		Surface	Base	Subbase
FM 437	1+900	2.4	3.2	18.9
	2+000	1.2	2.9	14.8
	2+050	1.3	1.7	15.8
	2+100	1.2	3.2	13.0
	2+150	1.2	3.2	13.0
	2+200	1.2	3.2	13.0
FM 933	30+460	2.0	15.0	
	30+260	2.6	11.8	6.8
	30+060	2.6	18.3	
	29+860	2.6	19.6	
	29+660	3.2	10.6	12.2
	29+460	3.0	13.0	10.5
FM 1805	0	1.1	8.9	
	100	1.2	6.4	13.4
	200	1.1	8.7	17.8
	300	1.1	8.3	19.4
	400	1.1	12.9	8.0
	500	1.1	4.3	8.6
	600	2.1	3.9	7.0
	700	1.0	18.1	
	800	1.0	9.2	4.2
FM 751	0	1.9	11.5	
	100	2.1	15.5	
	200	2.0	10.2	
	300	2.6	9.0	
	400	2.4	11.8	
	500	2.4	8.9	
	600	2.9	8.0	
	700	3.2	9.9	
	800	3.5	7.5	
	900	3.3	9.8	
	1000	3.2	8.9	

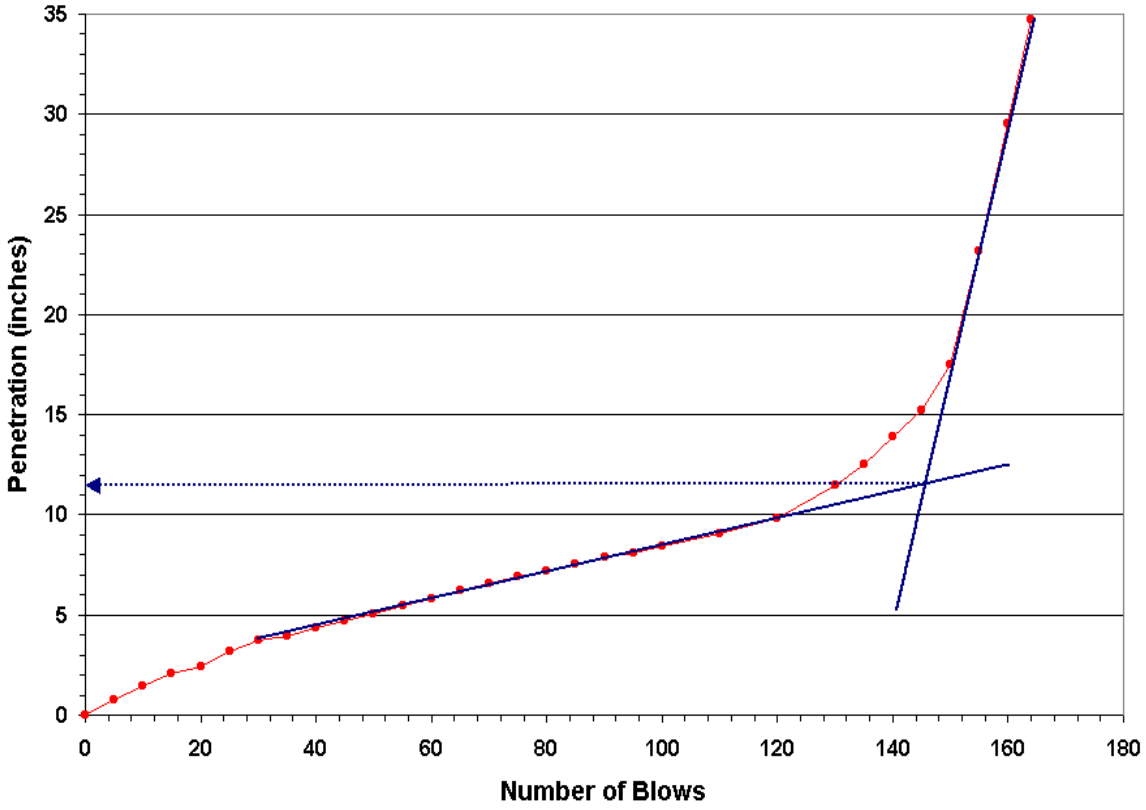

Figure 16. Estimating Layer Thickness from DCP Data.

pick the station where materials were sampled. Specifically, researchers selected the station at each site that exhibited the highest FWD deflections and/or DCP penetration rate.

The gradation, Atterberg limits, and field moisture content of the materials sampled were determined in the laboratory. Figures 17 to 23 show the gradation curves determined from the laboratory tests. The particle size analyses of base and subgrade materials larger than the #200 sieve were conducted by wet sieving. For particles smaller than the #200 sieve, TxDOT's Horiba laser diffraction particle size distribution analyzer was used following test method Tex-238-F.

Researchers note that no subgrade samples were obtained from FM 437. As discussed earlier, this roadway is underlain by an old pavement, which ranged in thickness from 13 to about 19 inches. Digging up the old pavement would have created a trench that significantly required more material to backfill and patch. However, based on

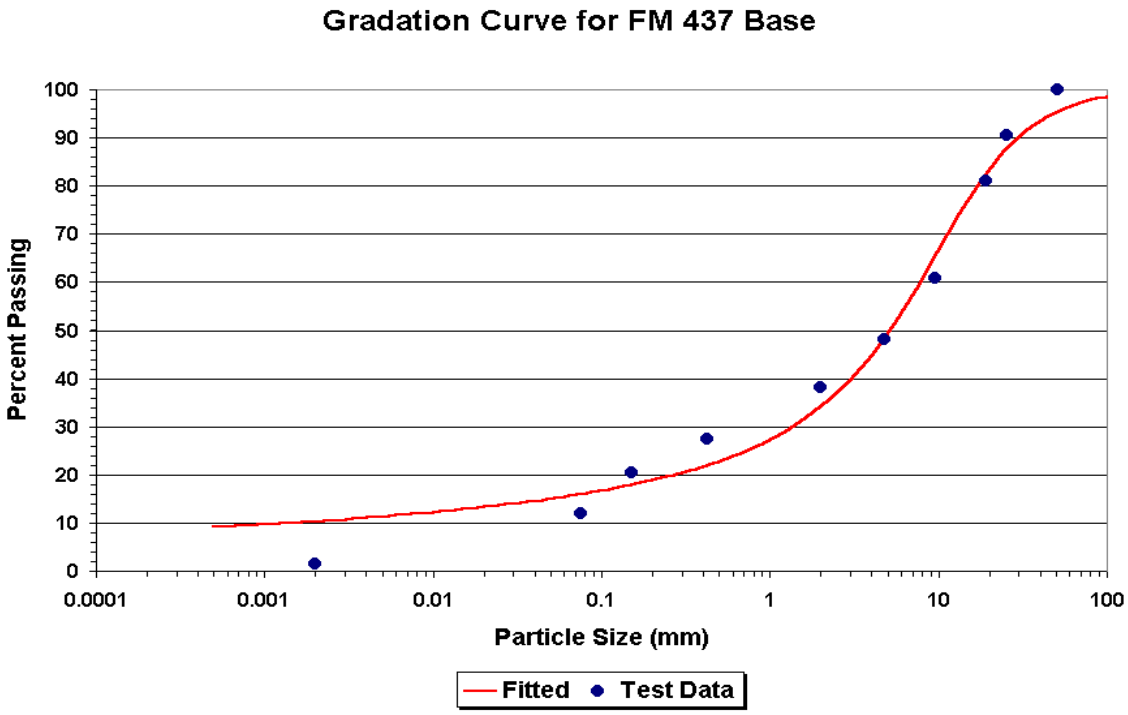

Figure 17. Gradation of Base Material Sampled from FM 437.

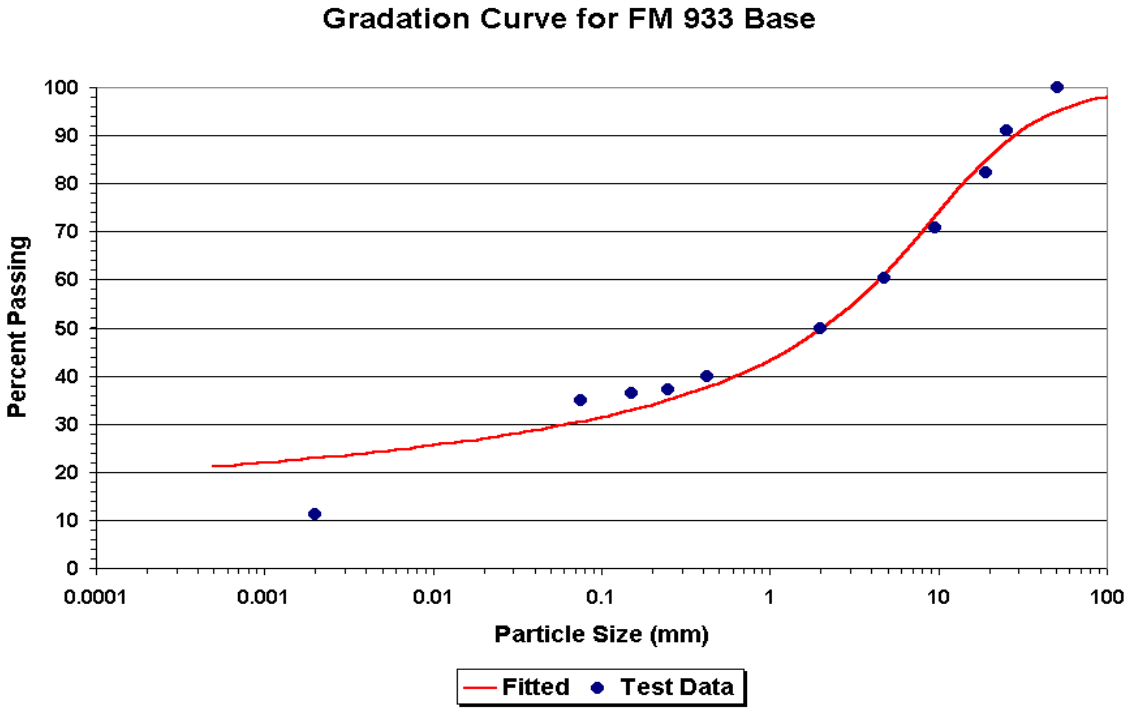

Figure 18. Gradation of Base Material Sampled from FM 933.

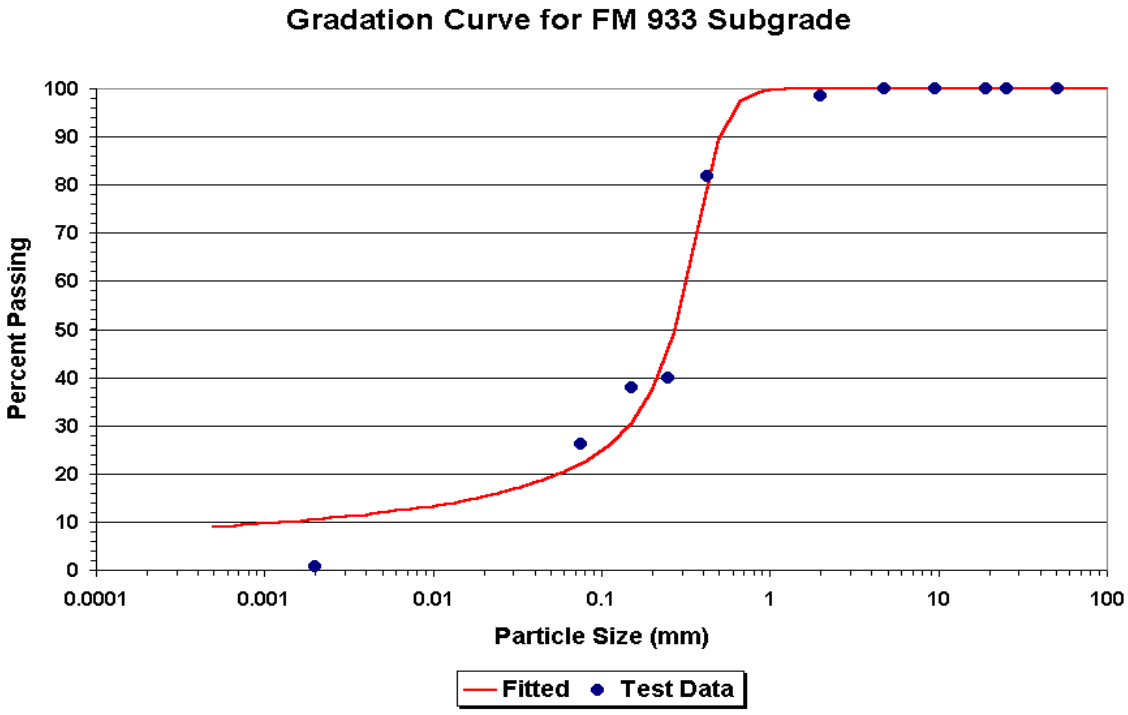

Figure 19. Gradation of Subgrade Material Sampled from FM 933.

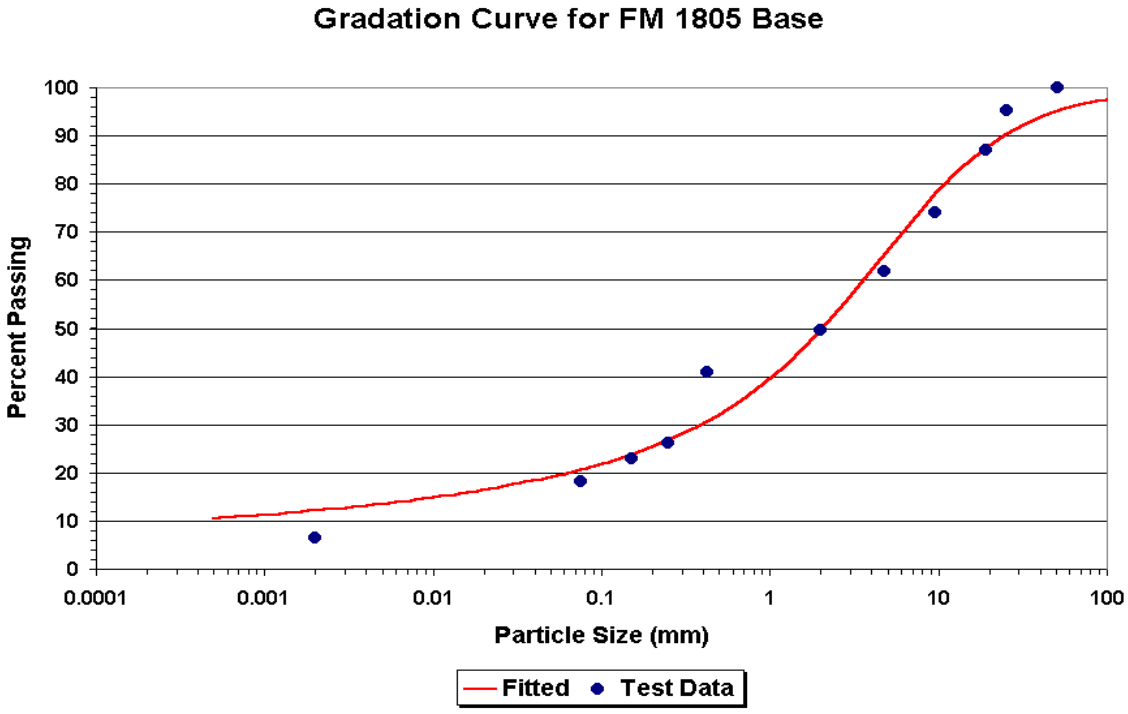

Figure 20. Gradation of Base Material Sampled from FM 1805.

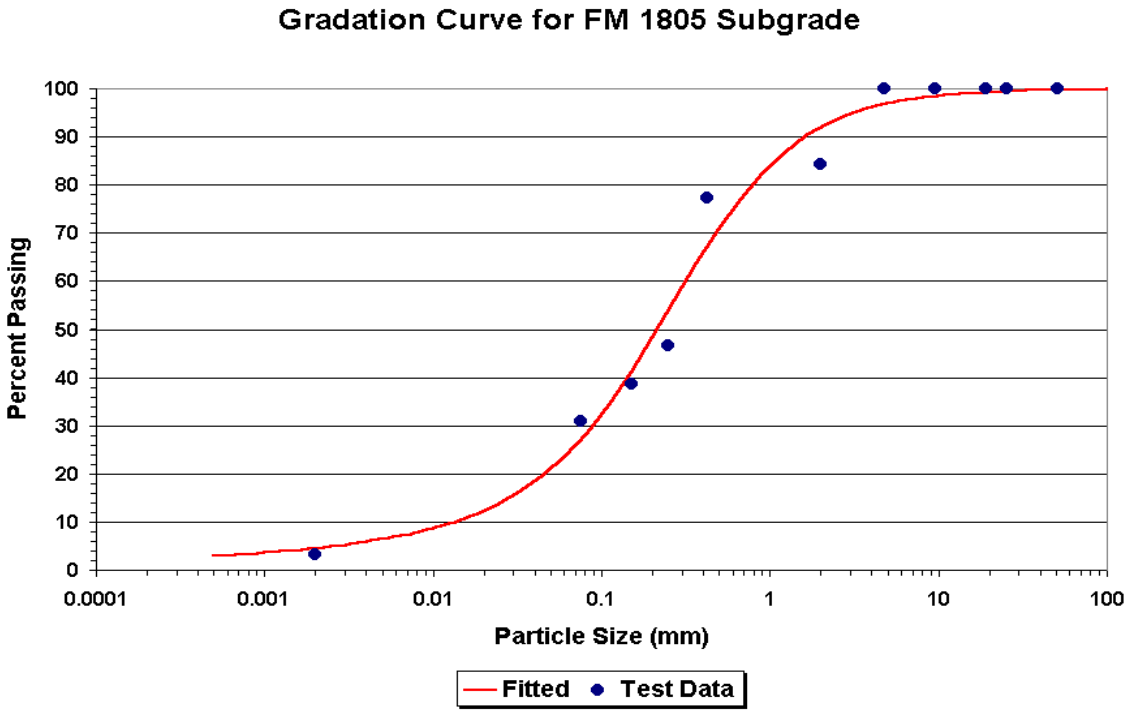

Figure 21. Gradation of Subgrade Material Sampled from FM 1805.

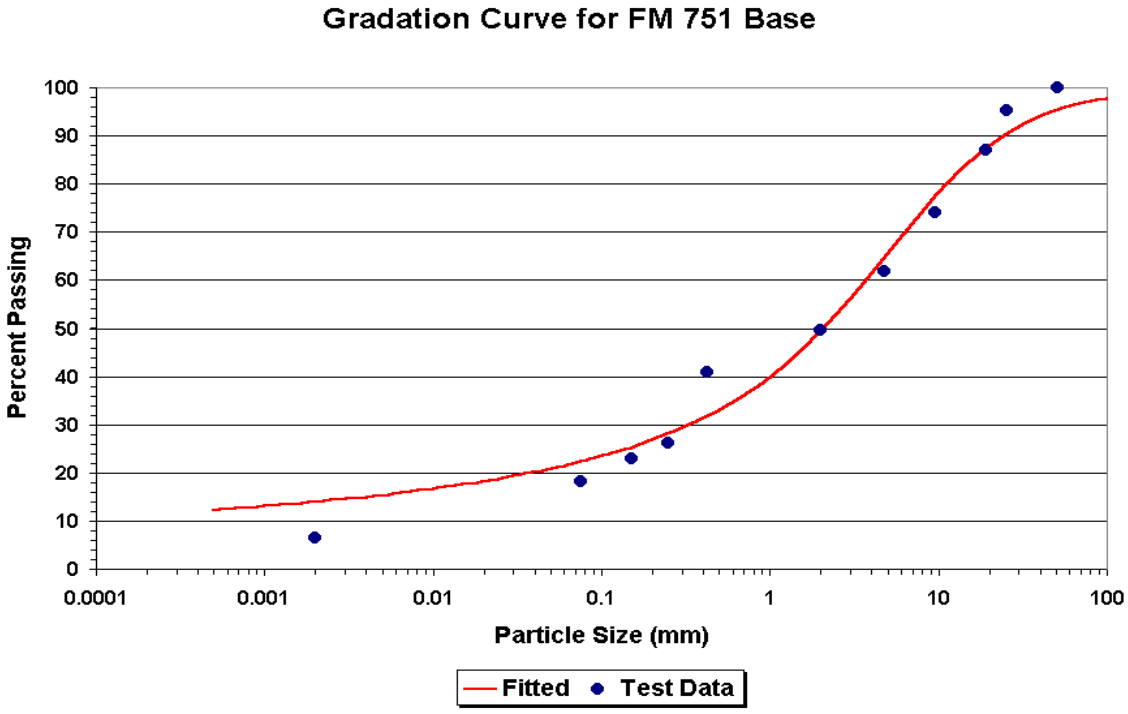

Figure 22. Gradation of Base Material Sampled from FM 751.

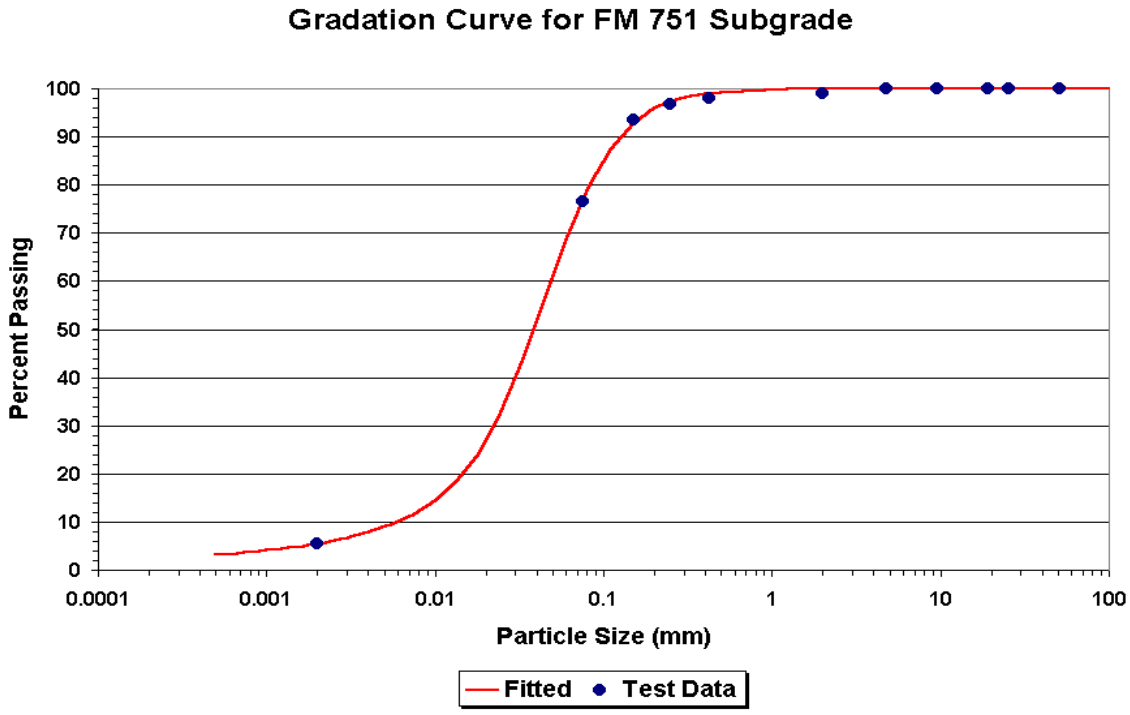

Figure 23. Gradation of Subgrade Material Sampled from FM 751.

information from the Bell County soil map (*20*), researchers identified the native soil at the site to be clay. The coring log on FM 437 also showed this information.

Table 9 presents the Atterberg limits of the sampled materials. The Atterberg limits, in conjunction with the gradation curves, were used to classify the materials based on the AASHTO soil classification system. Table 9 gives the resulting classifications. For subgrade materials, the soil types shown in the table were obtained from the Bell, Hill, Smith, and Van Zandt County soil maps (*20*-*23*). As shown in the footnotes to Table 9, the Atterberg limits determined from laboratory tests on subgrade samples from FM 933, FM 1805, and FM 751 agree with the corresponding information obtained from the respective county soil surveys.

Table 10 presents the field moisture contents of the sampled materials. Researchers used a nuclear density gauge in the field to estimate the moisture contents of the base and subgrade layers. In addition, they placed samples of the materials inside plastic bags for moisture content determinations in the laboratory. As the reader may observe from Table 10, the moisture contents determined in the field and in the laboratory are quite comparable.

Table 9. Atterberg Limits and Soil Classifications of Materials Sampled.

Location of Test Section	Layer	Liquid Limit (LL)	Plasticity Index (PI)	AASHTO Soil Classification	Soil Type
FM 437	Base	12.45	0.89	A-1-b (0)	Austin chalk
FM 933	Base	26.91	13.04	A-2-6 (1)	crushed limestone
FM 1805	Base	21.78	5.06	A-1-b (0)	iron ore gravel
FM 751	Base	21.30	5.01	A-1-b (0)	crushed limestone
FM 437[1]	Subgrade	55 – 80	40 – 50	A-7-6	clay
FM 933[2]	Subgrade	11.96	non-plastic (NP)	A-2-4 (0)	Bastsil loamy fine sand
FM 1805[3]	Subgrade	19.75	3.24	A-2-4 (0)	fine sandy loam
FM 751[4]	Subgrade	26.55	15.96	A-6 (9)	Wilson silt loam

[1] Information given on FM 437 subgrade is from Bell County soil survey (*20*).
[2] Based on Hill County soil survey (*21*), the soil at the site has LL < 20 and PI from NP to 4.
[3] Based on Smith County soil survey (*22*), the soils at the site have LL < 32 and PI from NP to 10.
[4] Based on Van Zandt County soil survey (*23*), the soil at the site has LL from 26 to 38 and PI from 11 to 20.

Table 10. Field Moisture Contents of Base and Subgrade Materials.

Location of Test Section	Layer	Moisture Content (percent)	
		Field	Laboratory
FM 437	Base	N/A	4.62
FM 933	Base	8.60	8.98
FM 1805	Base	12.05	13.47
FM 751	Base	8.20	8.12
FM 933	Subgrade	5.50	4.74
FM 1805	Subgrade	13.80	13.29
FM 751	Subgrade	19.70	21.22

FWD Testing

TxDOT collected FWD deflections along the outside wheelpath of each test section. Tables 11 to 14 show the FWD deflections at the different stations tested. Researchers used the MODULUS program (*19*), along with the layer thicknesses determined from the DCP, to

Table 11. FWD Data Taken from FM 437 Test Section.

Station	Load (lbs)	Sensor Displacement (mils)						
		R1	R2	R3	R4	R5	R6	R7
1+900	10,690	11.19	7.68	5.37	3.94	3.11	2.37	2.00
2+000	9665	23.74	15.42	9.26	5.82	4.18	2.22	2.60
2+050	9268	24.59	14.92	8.11	4.91	3.61	3.13	2.24
2+100	9847	19.13	12.55	7.32	4.45	3.37	2.40	2.14
2+150	8982	17.31	11.24	7.05	4.61	3.44	2.74	2.14
2+200	10,194	13.52	8.96	6.15	4.42	3.43	2.63	2.14

Table 12. FWD Data Taken from FM 933 Test Section.

Station	Load (lbs)	Sensor Displacement (mils)						
		R1	R2	R3	R4	R5	R6	R7
30+460	10,161	22.60	9.38	3.80	1.89	1.24	1.01	0.82
30+260	9284	37.87	12.50	5.45	3.33	2.36	1.78	1.43
30+060	8732	46.01	16.80	6.67	3.60	2.46	1.85	1.47
29+860	9800	21.93	7.28	3.30	1.91	1.37	1.03	0.81
29+660	8883	42.31	11.89	3.66	2.05	1.45	1.13	0.94
29+460	8790	41.34	12.07	4.27	2.29	1.53	1.18	0.89

Table 13. FWD Data Taken from FM 1805 Test Section.

Station	Load (lbs)	Sensor Displacement (mils)						
		R1	R2	R3	R4	R5	R6	R7
0	10,344	38.07	13.36	5.02	2.88	2.20	1.56	1.30
100	11,182	37.26	14.24	5.74	2.98	1.83	1.31	1.11
200	10,928	38.11	14.11	5.65	3.11	2.10	1.68	1.43
300	10,872	40.37	13.69	5.41	3.34	2.07	1.49	1.15
400	10,448	46.48	14.75	4.80	3.05	2.27	1.77	1.35
500	9458	61.80	24.52	8.58	5.39	3.85	2.85	2.32
600	9304	53.53	22.82	7.11	3.24	1.99	1.55	1.28
700	9406	59.63	20.13	5.70	3.07	2.45	2.00	1.59
800	10,312	54.80	15.08	5.11	2.50	1.80	1.36	0.99

Table 14. FWD Data Taken from FM 751 Test Section.

Station	Load (lbs)	Sensor Displacement (mils)						
		R1	R2	R3	R4	R5	R6	R7
0	11,032	38.42	14.69	7.30	5.02	3.69	2.89	2.36
100	9852	37.19	13.92	6.40	4.20	3.09	2.39	2.02
200	10,101	43.67	15.57	6.14	3.91	2.89	2.26	1.90
300	10,026	40.56	15.21	6.47	4.25	3.13	2.48	2.11
400	9398	49.05	22.85	8.73	5.39	3.89	3.08	2.58
500	9700	45.11	19.50	8.67	5.47	3.94	3.15	2.63
600	9784	46.56	21.07	9.84	6.10	4.35	3.32	2.70
700	10,022	44.33	18.10	8.35	5.42	3.92	3.01	2.44
800	9648	50.53	20.44	8.91	5.50	3.98	3.07	2.56
900	9565	43.55	18.32	7.70	4.70	3.38	2.61	2.23
1000	9386	54.30	24.43	9.34	5.56	4.12	3.23	2.76

backcalculate the layer moduli from the FWD data. The results from these analyses are given in Tables 15 to 18. Researchers used the data from the pavement evaluations conducted with the FWD and DCP to assess the need for load restrictions on the sections tested and demonstrate the application of the load-zoning analysis procedure.

LOAD-ZONING ANALYSIS

Traffic Analysis

Since the load-zoning procedure is based on predicting pavement service life for the expected vehicle loadings, researchers needed traffic information on the sections tested. To get the available data, the project director requested TxDOT's Transportation Planning and Programming division to provide the standard "Traffic Analysis for Highway Design" tables for the prescribed limits of the load-zoned routes. Table 19 summarizes the traffic data provided by TP&P. Researchers used the data provided by TP&P to estimate the expected single and tandem axle load applications for the load-zoning analysis.

To evaluate the need for load restrictions, researchers assumed a required service life of 10 years. For the purpose of estimating the expected single and tandem axle load

Table 15. Backcalculated Layer Moduli on FM 437 Test Section.

Station	Backcalculated Modulus (ksi)				Error/Sensor (%)
	Surface	Base	Subbase	Subgrade	
1+900	734	545	70	16	0.85
2+000	372	1000	17	11	7.37
2+050	687	789	24	11	4.53
2+100	413	584	32	13	2.50
2+150	976	363	38	12	1.77
2+200	200	537	95	15	1.11

Table 16. Backcalculated Layer Moduli on FM 933 Test Section.

Station	Backcalculated Modulus (ksi)				Error/Sensor (%)
	Surface	Base	Subbase	Subgrade	
30+460	644	36		16	15.80
30+260	200	14	34	16	2.55
30+060	200	11		11	3.94
29+860	221	31		30	1.55
29+660	100	10	22	21	3.64
29+460	100	12	17	22	2.85

Table 17. Backcalculated Layer Moduli on FM 1805 Test Section.

Station	Backcalculated Modulus (ksi)				Error/Sensor (%)
	Surface	Base	Subbase	Subgrade	
0	300	26		18	6.46
100	300	42	12	21	0.72
200	300	32	14	21	5.19
300	300	27	15	20	3.09
400	300	20	7	25	6.29
500	300	27	6	9	5.43
600	300	20	5	13	5.09
700	300	12		18	14.71
800	300	17	6	17	6.83

Table 18. Backcalculated Layer Moduli on FM 751 Test Section.

Station	Backcalculated Modulus (ksi)			Error/Sensor (%)
	Surface	Base	Subgrade	
0	334	24	17	1.18
100	207	21	15	2.47
200	235	17	14	5.70
300	200	16	15	4.25
400	340	12	9	8.28
500	152	20	10	7.82
600	116	18	10	3.00
700	200	12	14	3.24
800	200	10	10	5.71
900	200	11	11	6.72
1000	200	10	8	8.87

Table 19. Traffic Data Provided by TP&P.

Route	Limits	Beginning 20-year ADT	Ending 20-year ADT	Directional Distribution (%)	Percent trucks in ADT	20-year 18-kip ESALs for one direction
FM 437	Rogers city limits to 1.2 miles south of US 190	1000	1400	60 – 40	10.3	306,000
FM 933	From 2.4 miles south of Aquilla city limit to 3.1 miles south of Aquilla	1800	2600	60 – 40	10.3	596,000
FM 1805	From 1.0 mile south of FM 1253 to 1.6 miles south of FM 1253	900	1500	60 – 40	9.7	286,000
FM 751	From 4.4 miles south of Hunt-Van Zandt county line to 5.1 miles south of the county line	2000	3000	60 – 40	3.6	190,000

applications during this period, the traffic growth rate was first estimated at each site using the beginning and ending 20-year ADTs in the following equation:

$$ADT_t = ADT_0 (1+g)^t \quad (8)$$

where,

ADT_t = ending ADT after t years,
ADT_0 = beginning ADT, and
g = traffic growth rate.

The growth rates determined using Eq. (8) are given in Table 20. From the traffic data, the total number of trucks in the base year may also be estimated from the equation:

$$NT_0 = ADT_0 \times 365 \times DF \times PT \quad (9)$$

where,

NT_0 = number of trucks in the design lane in the beginning or base year,
DF = directional distribution factor, and
PT = percent trucks in the ADT.

Since the number of 18-kip ESALs in 20 years is given, the number of ESALs per truck may be determined from the equation:

$$ESAL_t = NT_0 \times EF \left[\frac{(1+g)^t - 1}{g} \right] \quad (10)$$

where,

$ESAL_t$ = cumulative number of 18-kip ESALs in t years, and
EF = ESAL factor (number of ESALs per truck).

Table 20 shows the number of trucks in the base year computed from Eq. (9) and the ESAL factors determined from Eq. (10). Given g, NT_0, and EF, researchers estimated the cumulative 18-kip ESALs in 10 years from Eq. (10). These estimates are also given in Table 20.

The 18-kip ESALs in 10 years, designated as $ESAL_{10}$, is used to determine the total payload to be carried by trucks during the design period. This total payload, PL_t, in t years (kips) is simply calculated as:

Table 20. Results of Traffic Analysis.

Route	Growth Rate	Number of Trucks in Base Year	ESAL Factor	Number of 18-kip ESALS in 10 years	Total Payload in 10 Years (kips)	n_s	n_t
FM 437	0.0170	22,557	0.575	140,160	2,522,884	31,362	55,754
FM 933	0.0186	40,603	0.613	270,681	4,872,266	60,567	107,674
FM 1805	0.0259	19,119	0.580	124,837	2,247,059	27,933	49,659
FM 751	0.0205	15,768	0.494	85,403	1,537,255	19,110	33,972

$$PL_t = 18 \times ESAL_t \tag{11}$$

For a design period of 10 years, the total payload determined for each section is given in Table 20. The sum of the expected single and tandem axle loads must equal the total payload during this period, as expressed by the following equation:

$$P_s n_s + P_t n_t = PL_t \tag{12}$$

where,

n_s = expected number of applications of single axle load P_s in kips, and

n_t = expected number of applications of tandem axle load P_t in kips.

To evaluate the need for load restrictions, the legal load limits are used in Eq. (12). These limits are 20 kips for a single axle and 34 kips for a tandem. In evaluating the need for posting load limits, the analysis is carried out assuming that all trucks are running at the legal load limits. The number of allowable axle load applications for a given legal load limit is then predicted using the corresponding Asphalt Institute performance equation for a given pavement and failure criterion. The load-zoning procedure then uses Miner's hypothesis to predict service life, given the distribution of the legal axle loads. This prediction will require estimates of n_s and n_t. In practice, the pavement engineer will have to characterize the distribution of the vehicles that use the route to get these estimates.

For this demonstration, information on the distribution of vehicles by class was not available. However, it is known that the tractor-semitrailer (3S2) is the predominant vehicle used by today's carriers. Consequently, in the load-zoning analysis, researchers made the following assumptions on the distribution of trucks using the routes:

1. 75 percent of the trucks are 3S2s, and
2. the remaining 25 percent are single unit trucks with tandem drive axles (3As), representing vehicles used for local deliveries and buses.

Given this distribution, the engineer can determine the average number of axle groups per truck, the percent of single axles, and the percent of tandem axles, as illustrated in Table 21. From this table, the ratio of n_s to n_t is determined to be:

$$\frac{n_s}{n_t} = \frac{percent\ single\ axles}{percent\ tandem\ axles} = \frac{36}{64} = 0.56 \qquad (13)$$

The above ratio is used, in conjunction with Eq. (12), to compute the expected number of applications for each legal load limit that will maintain the total payload predicted during the design period. The resulting values are given in Table 20.

This method of determining n_s and n_t (corresponding, respectively, to the legal single and tandem axle load limits) is necessary since TxDOT's current design practice uses 18-kip ESALs to account for the axle load distribution along a given route. It is conceivable that this practice will change when TxDOT decides to implement the 2002 AASHTO pavement design procedure, which uses the axle load spectrum. At that time, the standard "Traffic Analysis for Highway Design" tables will have to be replaced by axle load distribution tables, and PLZA will have to be modified accordingly, so that users may input the axle load distribution directly.

Evaluation of Need for Load Restrictions

At each FWD station, researchers predicted the number of allowable load applications corresponding to the legal axle load limits. These predictions were then used with the expected number of load applications to determine the service life consumption for each axle load and configuration. The remaining life (in years) at each station was then determined assuming Miner's rule of cumulative damage. The authors then used these predictions to estimate the probability that the test section will last at least 10 years to establish the need for load restrictions. Table 22 summarizes the results from this evaluation.

Table 21. Calculation of Average Axle Groups per Truck, Percent Single Axle Groups, and Percent Tandem Axle Groups.

Truck Category	Number of Single Axle Groups	Number of Tandem Axle Groups	Percentage of Truck Distribution	Number of Axle Groups[1]	Average Number of Axle Groups per Truck[2]	Average Number of Single Axle Groups per Truck[3]	Average Number of Tandem Axle Groups per Truck[4]
3S2	1	2	75	3	2.25	0.75	1.50
3A	1	1	25	2	0.50	0.25	0.25
Total					2.75	1.00	1.75
Percent single axle groups						$\frac{1.00}{2.75} \times 100 = 36$	
Percent tandem axle groups						$\frac{1.75}{2.75} \times 100 = 64$	

[1] Sum of columns 2 and 3
[2] Product of columns 4 and 5 divided by 100
[3] Product of columns 2 and 4 divided by 100
[4] Product of columns 3 and 4 divided by 100

Table 22. Predictions of Service Life and Reliability on Test Sections.

Location of Test Section	Station	Service Life (years)		Reliability (percent)	
		Fatigue Cracking	Rutting	Fatigue Cracking	Rutting
FM 437	1+900	> 40	> 40	99.9	98.9
	2+000	> 40	> 40		
	2+050	> 40	> 40		
	2+100	> 40	> 40		
	2+150	> 40	> 40		
	2+200	> 40	> 40		
FM 933	30+460	> 40	> 40	44.0	97.9
	30+260	5	> 40		
	30+060	3	27		
	29+860	23	> 40		
	29+660	3	> 40		
	29+460	3	> 40		
FM 1805	0	> 40	9	92.5	85.1
	100	> 40	> 40		
	200	> 40	> 40		
	300	> 40	> 40		
	400	> 40	> 40		
	500	> 40	6		
	600	9	12		
	700	11	> 40		
	800	36	> 40		
FM 751	0	> 40	> 40	95.2	58.8
	100	24	> 40		
	200	> 40	17		
	300	20	18		
	400	14	6		
	500	23	4		
	600	22	4		
	700	20	25		
	800	20	6		
	900	20	14		
	1000	14	3		

For reporting purposes, PLZA uses an upper limit of 40 years on the performance predictions. However, in evaluating reliability, the actual predictions are used in the computer program. With respect to the potential for pavement failure within the prescribed analysis period, the results presented in Table 22 indicate that the sections may be ranked as follows (from greatest to least potential for premature failure):

1. FM 933,
2. FM 751,
3. FM 1805, and
4. FM 437.

Based on these results, the need for axle load restrictions are strongly indicated for FM 933. The predicted reliability for this section (44 percent) is less than the minimum recommended reliability level of 50 percent for this class of road.

To check the predictions from the load-zoning program, researchers also conducted a remaining life analysis using MODULUS. The results from this evaluation are given in Table 23. Note that the MODULUS program classifies the remaining life estimates into 0 – 2 years, 2 – 5 years, 5 – 10 years, and over 10 years. For this comparison, the authors note that the fatigue and rutting models are different between MODULUS and PLZA. Consequently, to assess the results from the load-zoning program, researchers examined the trends in the performance predictions instead of directly comparing the remaining life estimates. Based on the results in Table 23, the following observations are noted:

1. In terms of the potential for pavement failure, the MODULUS results lead to the same ranking of the pavement sections that PLZA determined based on the predicted reliability levels. The best section, in terms of remaining life, is FM 437, while the worst section is FM 933.
2. On the worst section (FM 933), both the MODULUS and load-zoning programs predict that fatigue cracking is the critical distress in terms of pavement life. The service life estimates based on this distress also show a consistent trend between FWD stations.
3. On the next best section in terms of pavement life (FM 1805), both the MODULUS and load-zoning programs suggest that rutting is likely to govern the performance of the pavement. However, load-zoning is not indicated.

Table 23. Comparison of Performance Predictions from MODULUS and PLZA.

Location of Test Section	Station	Predicted Service Life (years)			
		MODULUS		PLZA	
		Fatigue	Rutting	Fatigue	Rutting
FM 437	1+900	10+	10+	> 40	> 40
	2+000	10+	10+	> 40	> 40
	2+050	10+	10+	> 40	> 40
	2+100	10+	10+	> 40	> 40
	2+150	10+	10+	> 40	> 40
	2+200	10+	10+	> 40	> 40
FM 933	30+460	10+	10+	> 40	> 40
	30+260	2 – 5	10+	5	> 40
	30+060	2 – 5	10+	3	27
	29+860	10+	10+	23	> 40
	29+660	0 – 2	5 – 10	3	> 40
	29+460	0 – 2	5 – 10	3	> 40
FM 1805	0	10+	10+	> 40	9
	100	10+	10+	> 40	> 40
	200	10+	10+	> 40	> 40
	300	10+	10+	> 40	> 40
	400	10+	10+	> 40	> 40
	500	10+	5 – 10	> 40	6
	600	10+	10+	9	12
	700	10+	5 – 10	11	> 40
	800	10+	10+	36	> 40
FM 751	0	10+	10+	> 40	> 40
	100	10+	10+	24	> 40
	200	10+	10+	> 40	17
	300	10+	10+	20	18
	400	10+	10+	14	6
	500	10+	10+	23	4
	600	10+	10+	22	4
	700	5 – 10	10+	20	25
	800	2 – 5	10+	20	6
	900	5 – 10	10+	20	14
	1000	2 – 5	5 – 10	14	3

4. On the remaining section (FM 751), the performance predictions from MODULUS and PLZA rank it as the next critical section after FM 933. However, the results show that the critical distress is different between the two programs. In particular, the results from MODULUS predict that cracking will govern pavement life, while those from the load-zoning program suggest rutting to be the critical distress. In either case, the performance predictions from both programs suggest the need to consider load restrictions on the route.

Evaluation of Axle Load Limits

Researchers evaluated axle load limits at different reliability levels on the FM 933 section. In this analysis, they assumed that the expected number of load applications would remain the same. Figure 24 shows the results from this evaluation. From this figure, the pavement engineer selects appropriate axle load limits for the given pavement based on the desired level of reliability. Thus, if the minimum recommended reliability level of 50 percent is used, Figure 24 shows that the corresponding single and tandem axle load limits are 15.5 and 31 kips, respectively.

As expected, the axle load limits decrease with increase in the desired reliability level. For example, at 60 percent reliability, the load limits are 12 kips for a single axle and 24 kips for a tandem. These load limits result in a GVW of 60 kips for a 3S2 truck, which is close to the standard gross vehicle weight limit of 58,420 lbs presently applied on all load-zoned roads in Texas. This observation suggests that the existing gross vehicle weight restriction corresponds to a reliability level of about 60 percent for the FM 933 section.

If the higher reliability level of 70 percent is used, the single and tandem axle load limits reduce further to about 10 and 19 kips, respectively, from Figure 24. These load limits are rather restrictive, in the opinion of the researchers, suggesting that if a reliability level of 70 percent is desired, the engineer should consider rehabilitating the pavement section to upgrade its structural capacity. Note that the reliability level should be consistent with the level of use of the facility. If the engineer believes that 70 percent is warranted for the amount of traffic using the facility, then, in the authors' opinion, the pavement needs to be upgraded as the results indicate the pavement to be structurally inadequate for the level of traffic it serves.

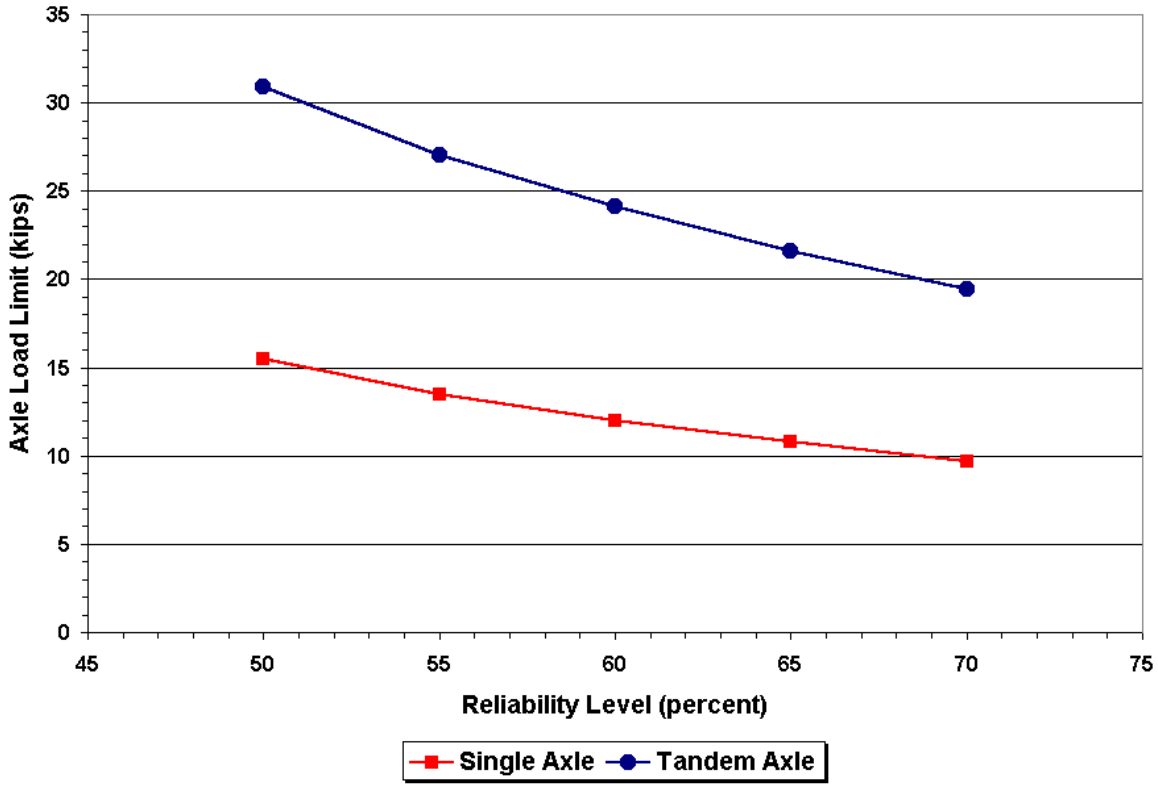

Figure 24. Axle Load Limits Evaluated at Different Reliability Levels (FM 933).

Researchers conducted a similar evaluation of axle load limits for FM 751. The results of this evaluation are presented in Figure 25, where axle load limits corresponding to reliability levels of 60 to 95 percent are plotted. Recall that the reliability level for this section is about 59 percent under existing legal load limits, as shown in Table 22. Assuming that 60 percent reliability is appropriate, single and tandem axle load limits of 18 and 36 kips are determined, respectively, from Figure 25. It is interesting to note that the 2-kip reduction from the 20-kip legal single axle load is compensated by the 2-kip increase in the allowable tandem axle load. This result brings up the importance of posting load limits on the basis of axle load and axle configuration. For one thing, it shows that single and tandem axle configurations have different damaging effects on pavements. For another, it suggests how axle load limits may actually help TxDOT preserve the highway network in a way that will maintain or have the least negative impact on trucking productivity. Consider, for example, a tractor-semitrailer with a single drive axle (2S2). Instead of having 20 kips on the drive axle and 34 kips on the trailer tandem, the trucker could distribute his payload such that 18

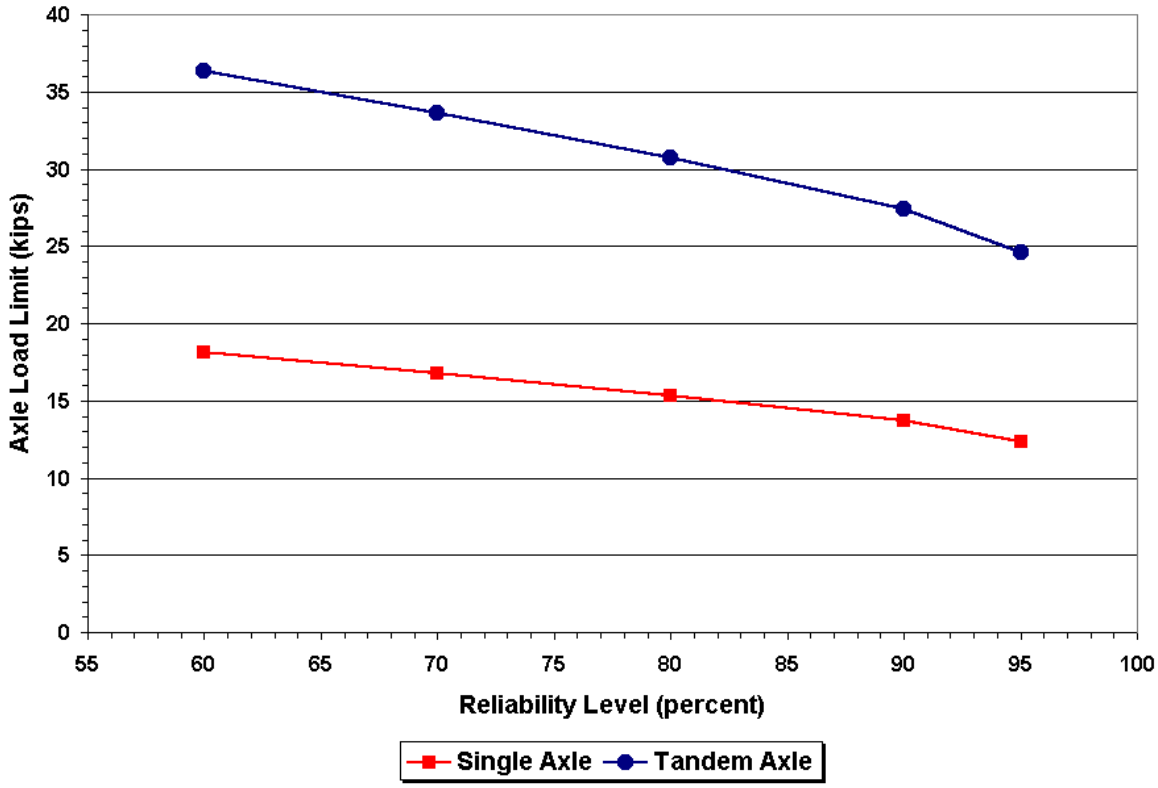

Figure 25. Axle Load Limits Evaluated at Different Reliability Levels (FM 751).

and 36 kips are carried, respectively, on the drive and trailer axles. This example assumes that TxDOT permits posting of axle load limits higher than the legal limits. Alternatively, the legal tandem axle load may be specified, in lieu of 36 kips, in the example given.

CHAPTER V
SUMMARY AND RECOMMENDATIONS

The previous chapters have explained and demonstrated the load-zoning analysis procedure incorporated in the PLZA program developed in this project. Based on the investigations conducted, the authors note the following findings:

1. The sensitivity analysis of predicted performance based on the Asphalt Institute equations showed that pavement life varies directly with layer moduli and thicknesses for the pavement structures considered in the analysis.
2. Overall, the results from the sensitivity analysis showed that pavement life (based on the Asphalt Institute fatigue equation) is influenced the most by surface thickness and base modulus, and to a lesser degree, by the base thickness and surface modulus. Among the variables considered, the subgrade modulus showed the least effect on the predicted fatigue life, exhibiting an appreciable effect only for the thin pavement.
3. On the basis of rutting, the analysis showed that predicted pavement life is influenced significantly by the layer moduli and thicknesses. In particular, the surface thickness, base thickness, and subgrade modulus are observed to have the most impact on the predicted life, which varied in the same direction as the change in each design variable.
4. The rut depth criterion was observed to govern the predicted pavement life for the thin and medium pavements, while the fatigue criterion governs the service life for the thick pavement. Since most roads that undergo a load-zoning analysis fall under the thin and medium categories, this observation implies that, for roads comparable to the pavements analyzed, rutting will likely control the load restrictions, based on the Asphalt Institute performance equations.
5. In terms of options to rehabilitate existing load-zoned roads to carry legal load limits, the results from the sensitivity analysis imply that increasing the surface thickness and/or improving the base material are primary options an engineer

should consider to improve the expected fatigue life of the pavement. The effect of these changes on predicted pavement response is to reduce the bending effect under load, and the tensile strain at the bottom of the surface mix. Theoretically, this reduction in tensile strain translates to a higher number of load repetitions prior to crack initiation. In addition, the increase in surface thickness adds to the number of load repetitions for crack propagation. On the basis of the rut depth criterion, the primary options an engineer should consider are to increase the surface thickness and/or base thickness, and to improve the subgrade through stabilization or replacement with a better material. The effect of these changes is to reduce the compressive strain at the top of the subgrade, resulting in a predicted increase in pavement life.

6. Researchers also used the load-zoning procedure to evaluate the need for load restrictions on four in-service pavements located in the Waco and Tyler districts. This evaluation was conducted using pavement evaluation techniques already implemented within TxDOT, specifically, the GPR, FWD, DCP, COLORMAP, and MODULUS, and using standard traffic information employed in pavement design. The experience from this demonstration indicates that PLZA can be readily implemented within the department, in the researchers' opinion.
7. Service life predictions from PLZA were also assessed against corresponding predictions from the MODULUS program. The results of this comparison showed that, in terms of the need for load restrictions, both programs produce the same ranking of the pavement sections tested and analyzed.
8. Results from the demonstration of PLZA brought up the importance of posting load limits on the basis of axle load and axle configuration. The evaluation of axle load limits indicated that single and tandem axle configurations have different damaging effects on pavements, and that posting load limits in terms of axle load may actually help TxDOT preserve the highway network in a way that will maintain or have the least negative impact on trucking productivity.

IMPLEMENTATION OF THE LOAD-ZONING PROCEDURE

As previously noted, using PLZA requires, for the most part, the application of pavement evaluation tools already implemented within TxDOT. Researchers recommend that the load-zoning procedure be initially implemented through the Materials and Pavements section of the Construction Division, which is staffed with engineers trained to operate GPR, FWD, and DCP equipment, and to analyze GPR and FWD data using COLORMAP and MODULUS, respectively. As the need arises, implementation of the analysis program may be phased into the districts, particularly those with significant mileage of load-zoned pavements. The implementation of the program within the districts may be realized through training sessions conducted in-house or through an interagency agreement.

With respect to the field application of the load-zoning methodology, specific instructions on the use of PLZA are given in the user's guide prepared by Fernando and Liu (*10*). In actual applications, users must first characterize the route to be analyzed. This will require characterizing the truck traffic on the route, determining pavement layer thicknesses, and evaluating material properties. Truck traffic data may be requested from the Transportation Planning and Programming division of TxDOT. The beginning and ending ADTs, directional factor, percent trucks, and 18-kip ESAL estimates are normally reported by TP&P in the "Traffic Analysis for Highway Design" tables that it provides in response to requests from the districts or the Materials and Pavements section. These data are used in PLZA to evaluate the need for load restrictions and to determine, as appropriate, the applicable single and tandem axle load limits on a given route.

Pavement layer thicknesses may be determined nondestructively using GPR supplemented, as necessary, by coring or DCP measurements. Researchers strongly suggest a GPR survey on the route to establish the variations in layer thicknesses. This survey should be conducted at the beginning of the evaluation for the reasons given in Chapter II of this report. Additionally, a video log may be made during the radar survey to provide a record of the pavement surface condition at the time of the evaluation.

GPR data should be used to subdivide the route into homogeneous segments using the cumulative difference method as described by AASHTO (*17*), and as illustrated by Fernando and Chua (*24*). Because of the strong influence of layer thickness on predicted pavement response, and on layer moduli backcalculated from FWD deflections, it is important to

establish the variability in layer thickness along the route to minimize the inaccuracies attributed to layer thickness variations. The segments delineated from the GPR data are subsequently used to plan the FWD survey, the purpose of which is to characterize the materials that comprise the pavement in terms of the resilient modulus.

FWD data are collected following the protocol established by TxDOT (*25*). For load-zoned pavements with surface thicknesses greater than three inches, pavement temperature measurements should be made to correct backcalculated asphalt concrete moduli to a standard temperature. Alternatively, infrared surface temperatures may be measured during the survey for the purpose of predicting pavement temperatures at the time of test using the Texas-LTPP equation implemented in the Modulus Temperature Correction Program (*26, 27*). Use of this equation requires the previous day's maximum and minimum air temperatures, which are readily obtained from the local weather service.

The authors recommend that the FWD data be stored in a separate file for each segment of the route surveyed. Each file is then analyzed with the MODULUS program to estimate the stiffness of each pavement layer. The output file of the backcalculated moduli for each segment is directly input to PLZA for the load-zoning analysis.

For the prediction of pavement response under loading, PLZA permits the engineer to model pavement materials as linear or nonlinear. To model materials as linear elastic, the coefficients K_2 and K_3 in Eq. (1) are set to zero. For these materials, K_1 is directly determined from the FWD backcalculated moduli that are input to the computer program. Alternatively, the pavement engineer may choose to model the materials as nonlinear. For this case, he or she must specify the K_2 and K_3 coefficients for each nonlinear material. The program then estimates the coefficient K_1 using these values with the backcalculated layer modulus for the material. The nonlinear material coefficients may be obtained from laboratory testing of compacted base and subgrade specimens following AASHTO T 292-91. Alternatively, the pavement engineer may use the data given in Tables 1 and 2 of this report as a guide in specifying nonlinear material coefficients when resilient modulus data from laboratory tests are not available.

In view of the possible variations in layer thickness and materials along the route, different results may be obtained for the different segments delineated from the GPR data. In practice, it will be difficult to implement numerous postings on a given route. Thus, the

pavement engineer must still use his or her judgment in taking the results of the load-zoning analysis to establish how a given route should be posted. For example, the engineer may make the decision to post the route based on the weakest segment. This decision should also consider the current truck use of the particular route, alternative roadways that trucks may take, the presence of load-zoned bridges, and the need to upgrade the route to carry truck traffic at the legal load limits.

ADDITIONAL RESEARCH NEEDS

The load-zoning procedure developed from this project uses the standard traffic information for pavement design that is provided by TP&P. In current design practice, truck traffic is quantified by the predicted 18-kip ESALs during the design period. This practice is likely to change in the future when the AASHTO 2002 pavement design procedure is implemented by TxDOT. When this occurs, the axle load distribution will have to be characterized in order to use the new design method. Consequently, it will be necessary to modify the load-zoning program at that time so that the user may directly input the axle load distribution data provided by TP&P into the analysis.

In addition, the authors recommend that research be conducted to investigate moisture effects on pavement load carrying capacity. The moduli of unbound pavement layers are affected by moisture, and to the extent that moisture variations occur within the pavement, significant changes in load-carrying capacity may take place. Thus, the capabilities for measuring or estimating the moisture content in the underlying base and subgrade materials, and determining the effects of moisture variations on layer stiffness become important to the evaluation of rehabilitation alternatives, load-carrying capacity for superheavy load moves or overweight truck traffic, and the need for load restrictions.

REFERENCES

1. Crockford, W. W. *Weight Tolerance Permits.* Research Report 1323-2F, Texas Transportation Institute, Texas A&M University, College Station, TX, 1993.

2. Fernando, E. G. and R. L. Lytton. A System for Evaluating the Impact of Truck Characteristics and Use on Flexible Pavement Performance and Life-Cycle Costs. In *Proceedings*, Seventh International Conference on Asphalt Pavements, Nottingham, England, Vol. 3, Design and Performance, 1992, pp. 110–131.

3. *Truck Weight Limits – Issues and Options.* Special Report 225, Transportation Research Board, Washington, D.C., 1990.

4. *New Trucks for Greater Productivity and Less Road Wear – An Evaluation of the Turner Proposal.* Special Report 227, Transportation Research Board, Washington, D.C., 1990.

5. Kilareski, W. P. Heavy Vehicle Evaluation for Overload Permits. In *Transportation Research Record 1227*, Transportation Research Board, National Research Council, Washington, D.C., 1989, pp. 194–204.

6. Middleton, D. R., A. Villareal, and J. D. Blaschke. *Evaluation of Oversize/Overweight Permit Policy and Fee Structure.* Research Report 1109-1F, Texas Transportation Institute, Texas A&M University, College Station, TX, 1988.

7. Terrell, R. L. and C. A. Bell. *Effects of Permit and Illegal Overloads on Pavements.* NCHRP Synthesis 131, National Cooperative Highway Research Program, Washington, D.C., 1987.

8. Mason, J. M., Jr. Effect of Oil Field Trucks on Light Pavements. *Journal of Transportation Engineering*, American Society of Civil Engineers, Vol. 109, No. 3, 1983, pp. 425–439.

9. Park, S. and E. G. Fernando. *Development of a Methodology for Posting Load Limits on Load-Zoned Pavements: Interim Report*. Research Report 1701-1, Texas Transportation Institute, Texas A&M University, College Station, TX, 1997.

10. Fernando, E. G. and W. Liu. *Program for Load-Zoning Analysis (PLZA): User's Guide*. Research Report 2123-1, Texas Transportation Institute, Texas A&M University, College Station, TX, 1999.

11. Jooste, F. J. and E. G. Fernando. *Development of a Procedure for the Structural Evaluation of Superheavy Load Routes*. Research Report 1335-3F, Texas Transportation Institute, Texas A&M University, College Station, TX, 1995.

12. Uzan, J. Granular Material Characterization. In *Transportation Research Record 1022*, Transportation Research Board, National Research Council, Washington, D.C., 1985, pp. 52–59.

13. Titus-Glover, L. and E. G. Fernando. *Evaluation of Pavement Base and Subgrade Material Properties and Test Procedures.* Research Report 1335-2F, Texas Transportation Institute, Texas A&M University, College Station, TX, 1995.

14. Asphalt Institute. *Research and Development of the Asphalt Institute's Thickness Design Manual (MS-1) Ninth Edition.* Research Report No. 82-2, Asphalt Institute, Lexington, KY, 1982.

15. Asphalt Institute. *Thickness Design–Asphalt Pavements for Highways and Streets.* Manual Series No. 1, Asphalt Institute, Lexington, KY, 1981.

16. Miner, M. A. Cumulative Damage in Fatigue. *Journal of Applied Mechanics*, Vol. 12, No. 1, 1945.

17. American Association of State Highway and Transportation Officials. *AASHTO Guide for Design of Pavement Structures.* AASHTO, Washington, D.C., 1993.

18. Scullion, T. and Y. Chen. *COLORMAP Version 2 User's Guide with Help Menus.* Research Report 1702-4, Texas Transportation Institute, Texas A&M University, College Station, TX, 1999.

19. Michalak, C. H. and T. Scullion. *MODULUS 5.0: User's Manual.* Research Report 1987-1, Texas Transportation Institute, Texas A&M University, College Station, TX, 1995.

20. United States Department of Agriculture. *Soil Survey of Bell County, Texas.* Soil Conservation Service, Washington, D.C., 1977.

21. United States Department of Agriculture. *Soil Survey of Hill County, Texas.* Soil Conservation Service, Washington, D.C., 1977.

22. United States Department of Agriculture. *Soil Survey of Smith County, Texas.* Soil Conservation Service, Washington, D.C., 1993.

23. United States Department of Agriculture. *Soil Survey of Van Zandt County, Texas.* Natural Resources Conservation Service, Washington, D.C., 1998.

24. Fernando, E. G. and T. Chua. Development of a Route Segmentation Procedure Using Predicted Layer Thicknesses from Radar Measurements. In *Proceedings*, Fifth International Conference on Ground Penetrating Radar, Vol. 1, Ontario, Canada, 1994, pp. 335–349.

25. Texas Department of Transportation. *Falling Weight Deflectometer Operator's Manual.* Austin, TX, 1996.

26. Fernando, E. G. and W. Liu. *User's Guide for the Modulus Temperature Correction Program (MTCP)*. Research Report 1863-1, Texas Transportation Institute, Texas A&M University, College Station, TX, 2001.

27. Fernando, E. G., W. Liu, and D. Ryu. *Development of a Procedure for Temperature Correction of Backcalculated AC Modulus*. Research Report 1863-2, Texas Transportation Institute, Texas A&M University, College Station, TX, 2001.

APPENDIX

PENETRATION CURVES FROM DCP TESTS

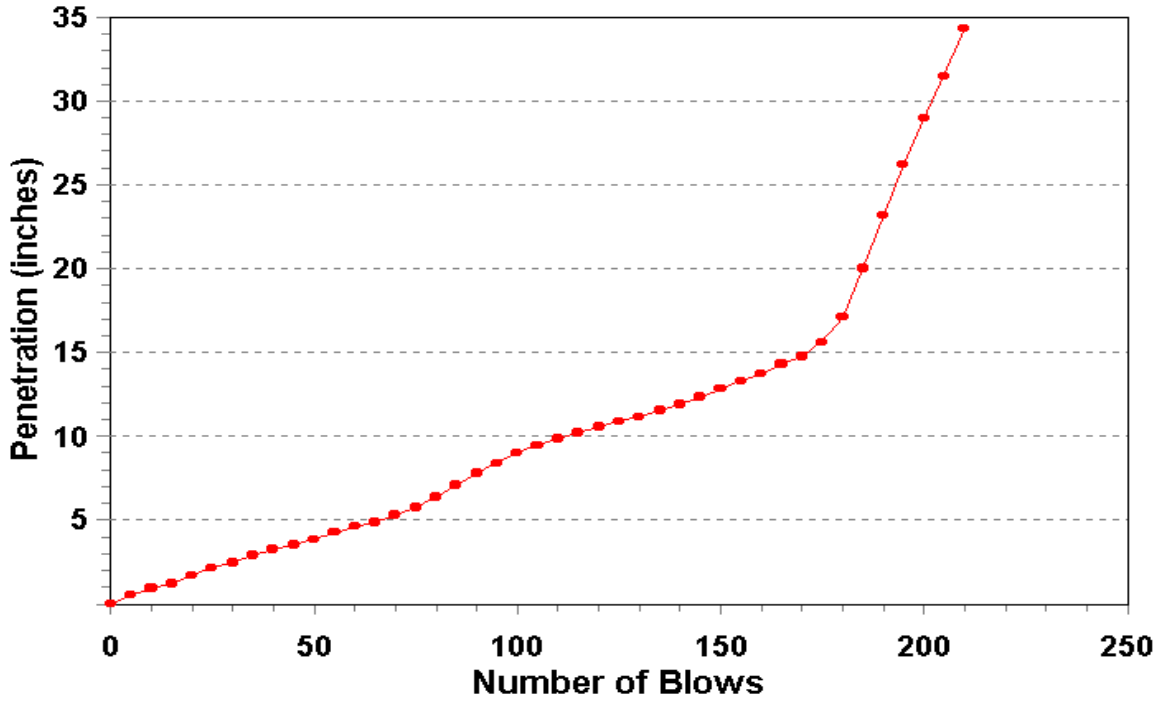

Figure A1. DCP Data Starting from Base at Station 30+460 along FM 933.

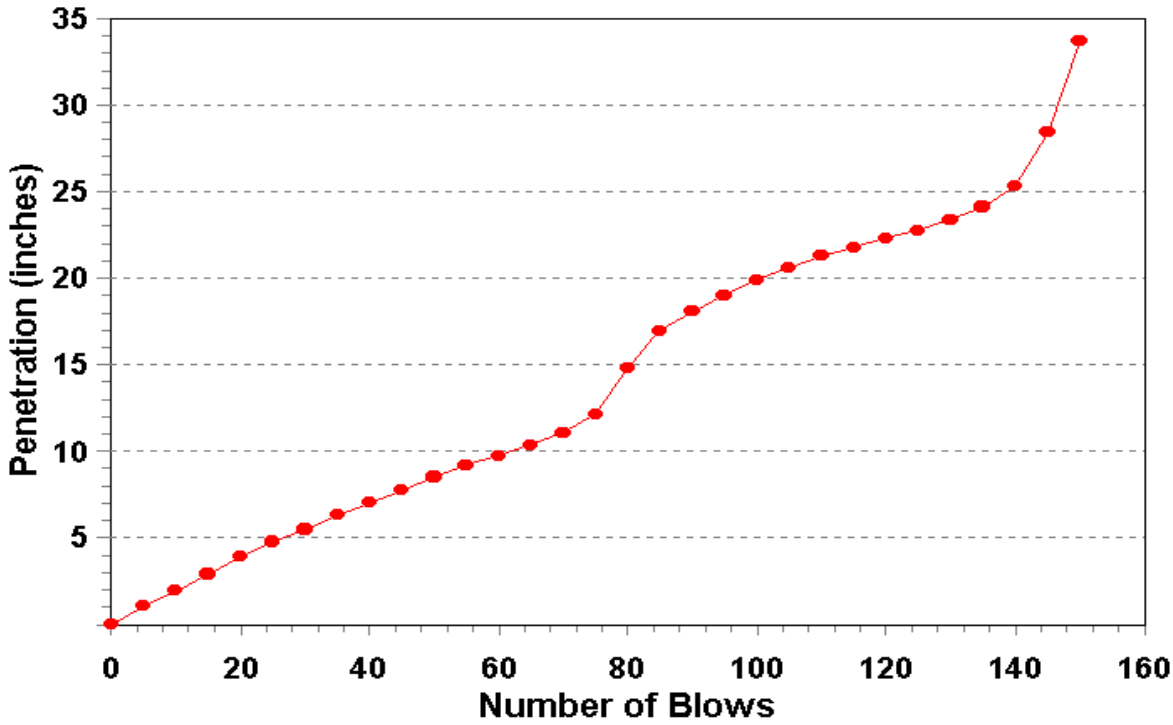

Figure A2. DCP Data Starting from Base at Station 30+260 along FM 933.

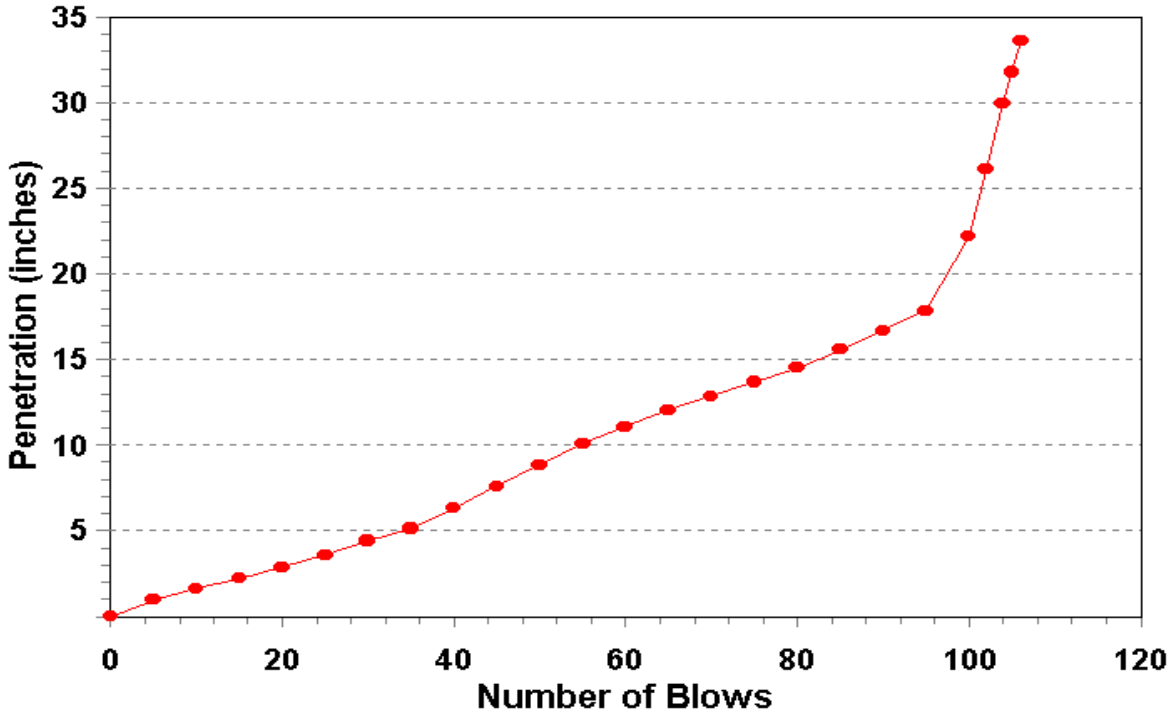

Figure A3. DCP Data Starting from Base at Station 30+060 along FM 933.

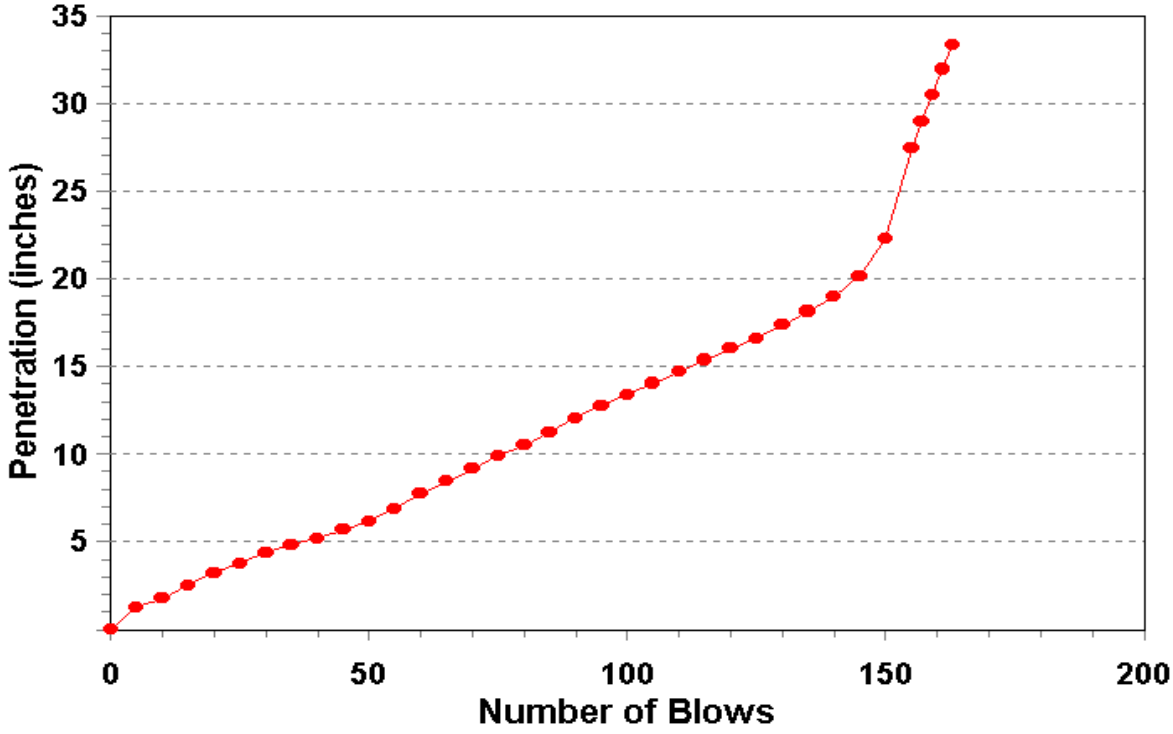

Figure A4. DCP Data Starting from Base at Station 29+860 along FM 933.

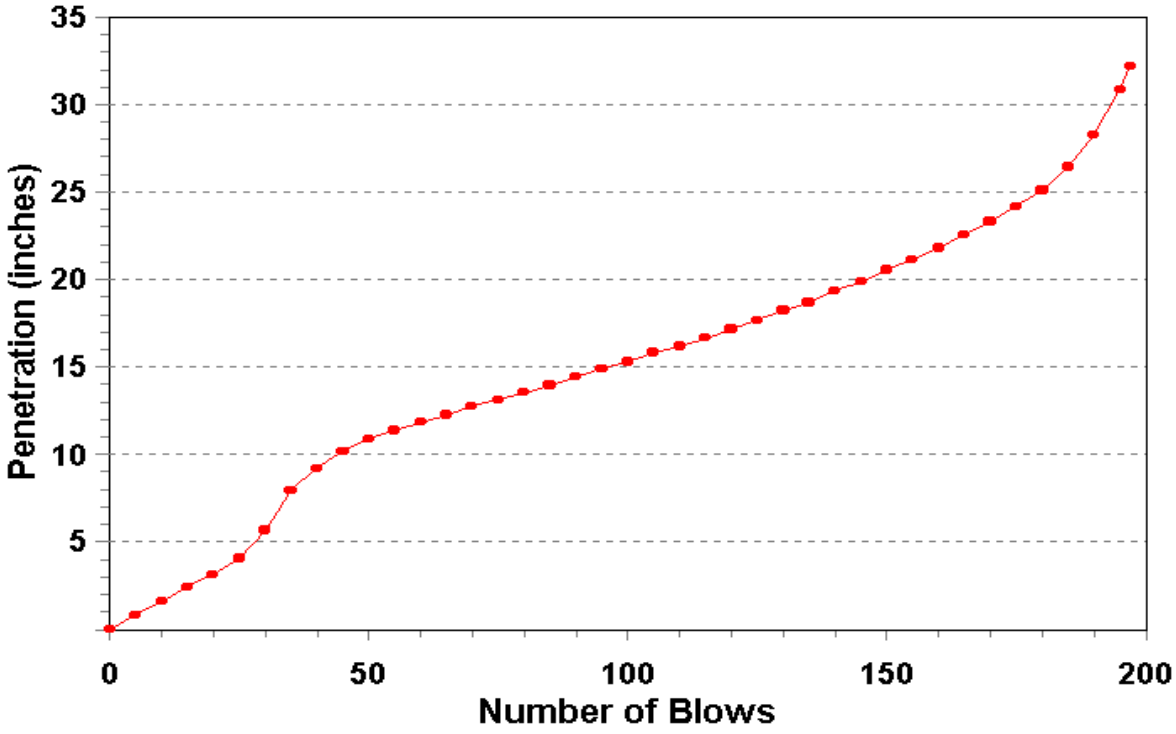

Figure A5. DCP Data Starting from Base at Station 29+660 along FM 933.

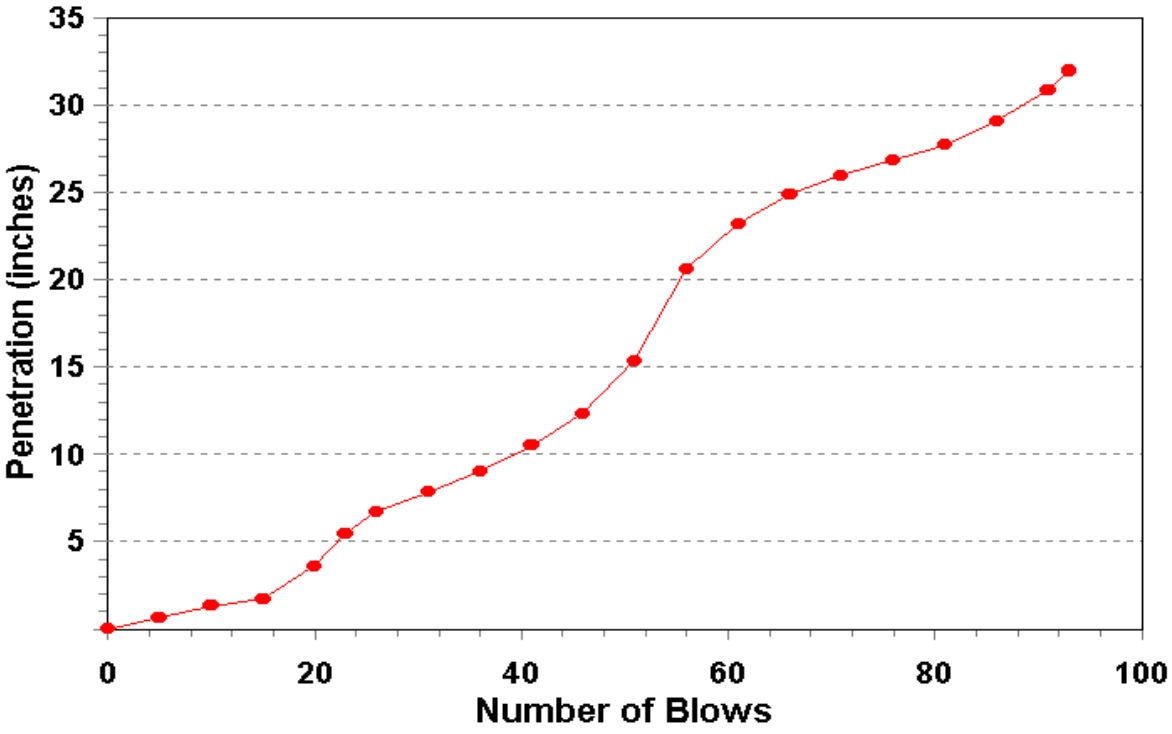

Figure A6. DCP Data Starting from Base at Station 29+460 along FM 933.

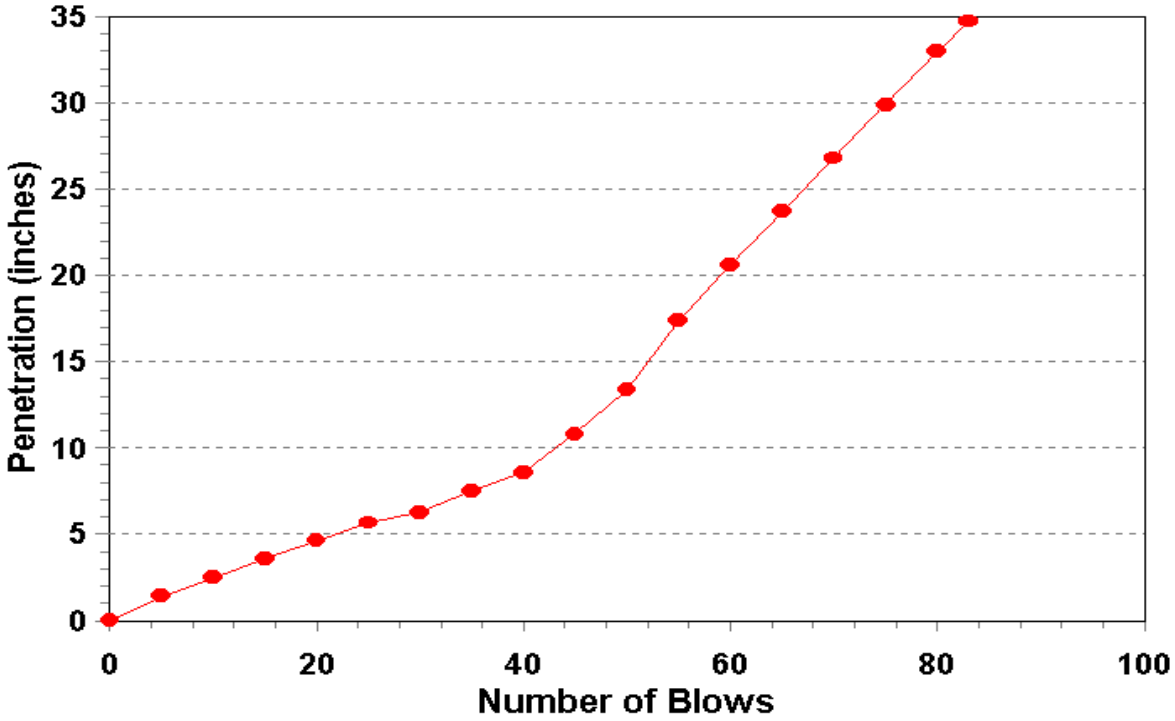

Figure A7. DCP Data Starting from Base at Station 0 along FM 1805.

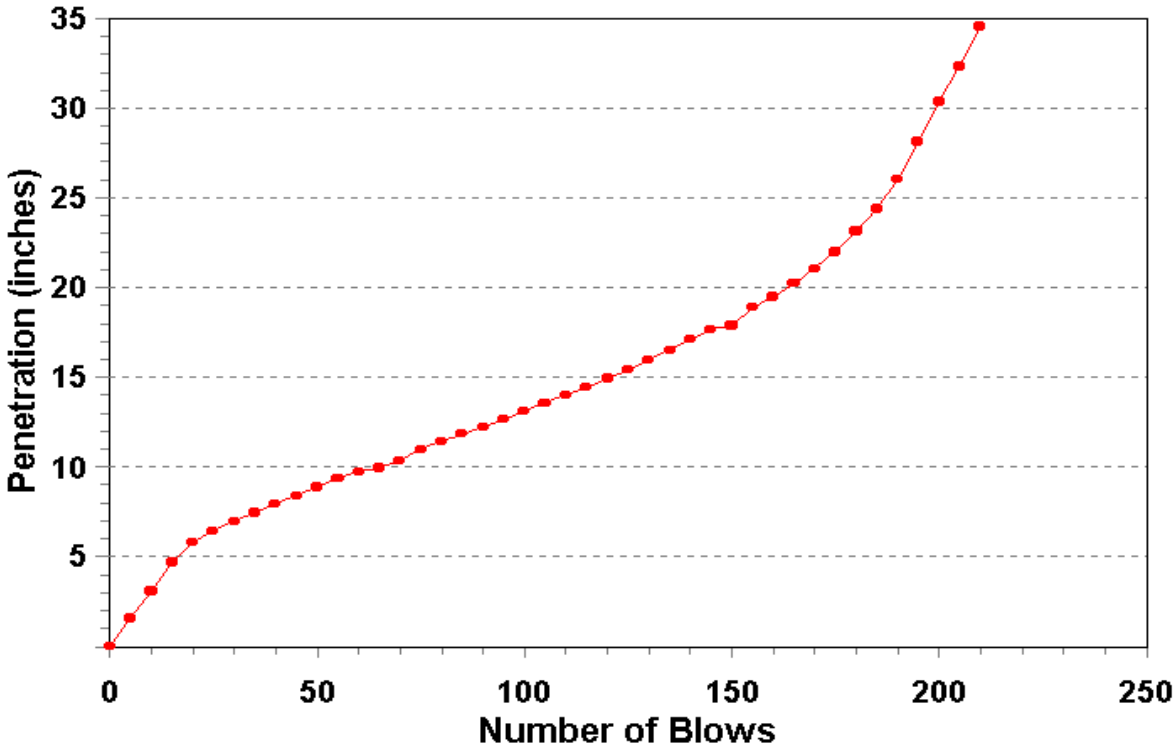

Figure A8. DCP Data Starting from Base at Station 100 along FM 1805.

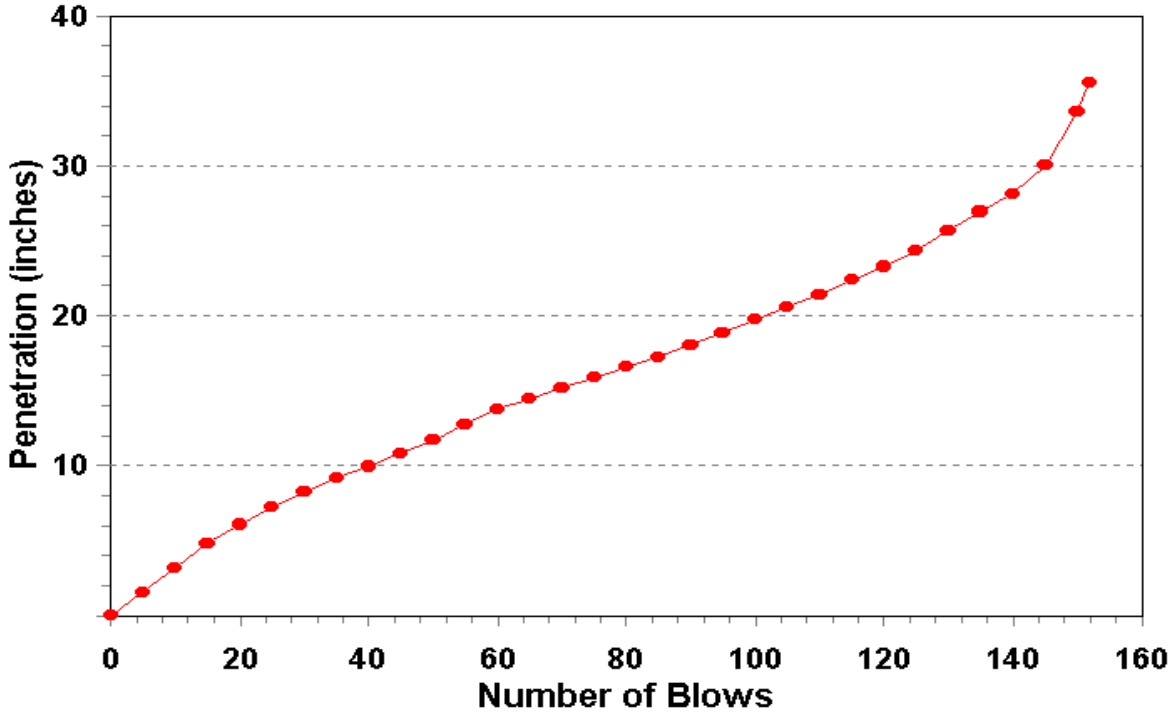

Figure A9. DCP Data Starting from Base at Station 200 along FM 1805.

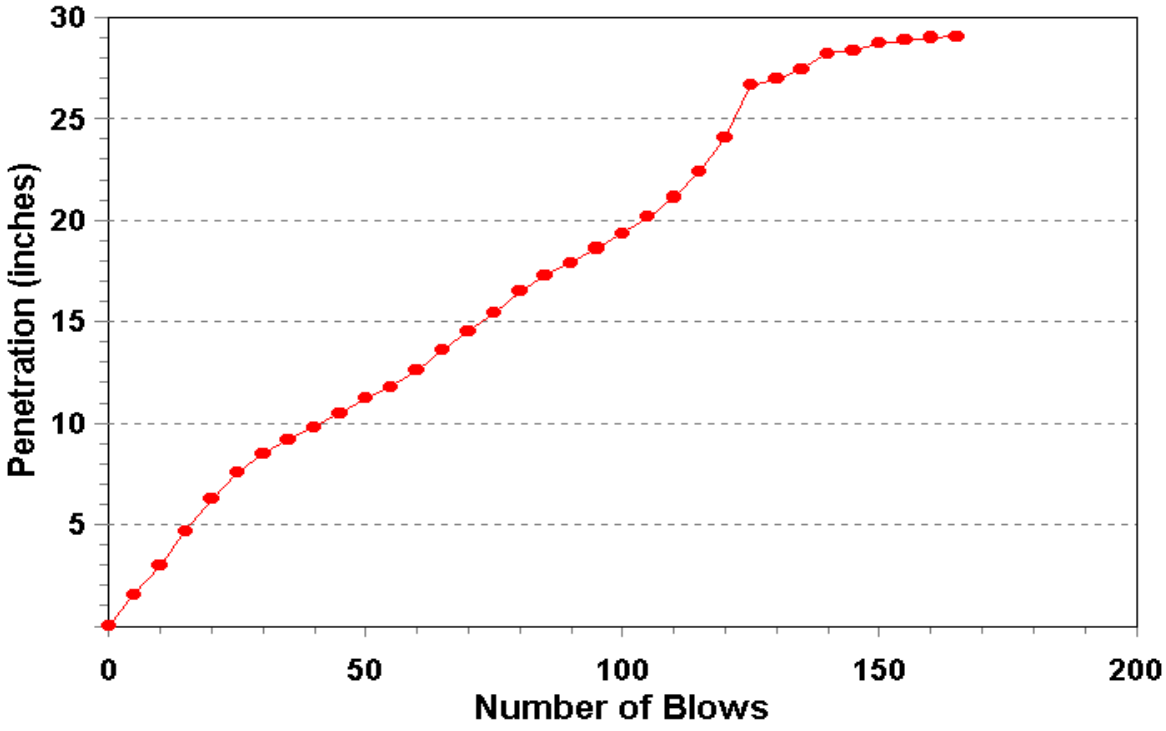

Figure A10. DCP Data Starting from Base at Station 300 along FM 1805.

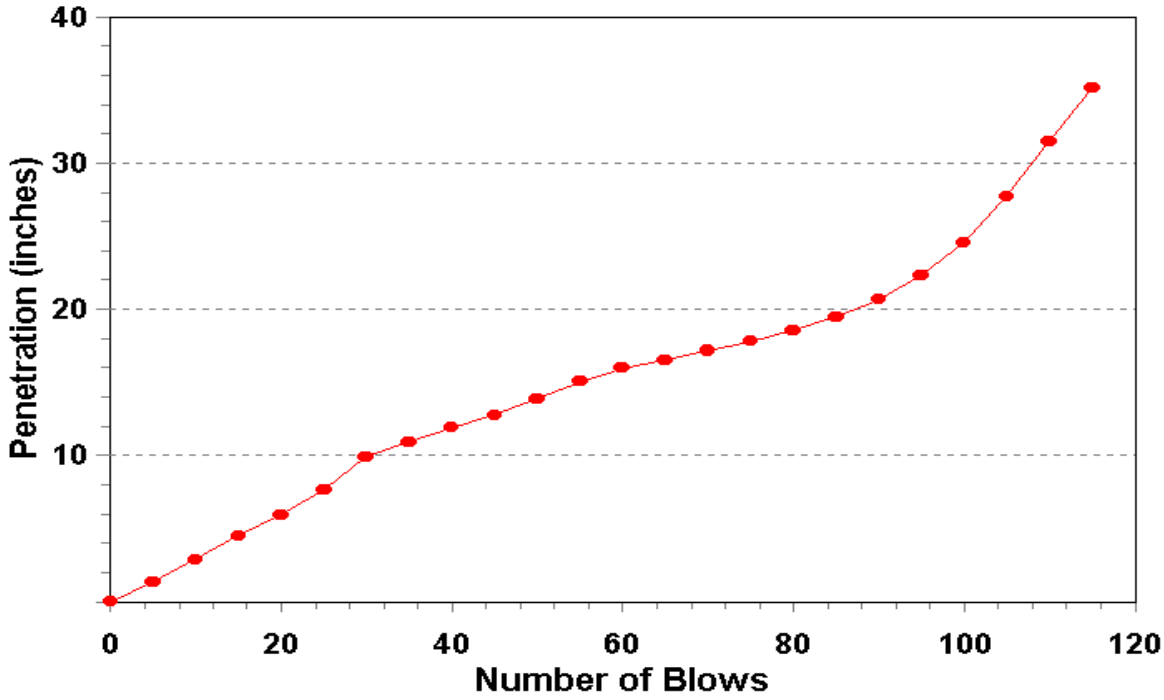

Figure A11. DCP Data Starting from Base at Station 400 along FM 1805.

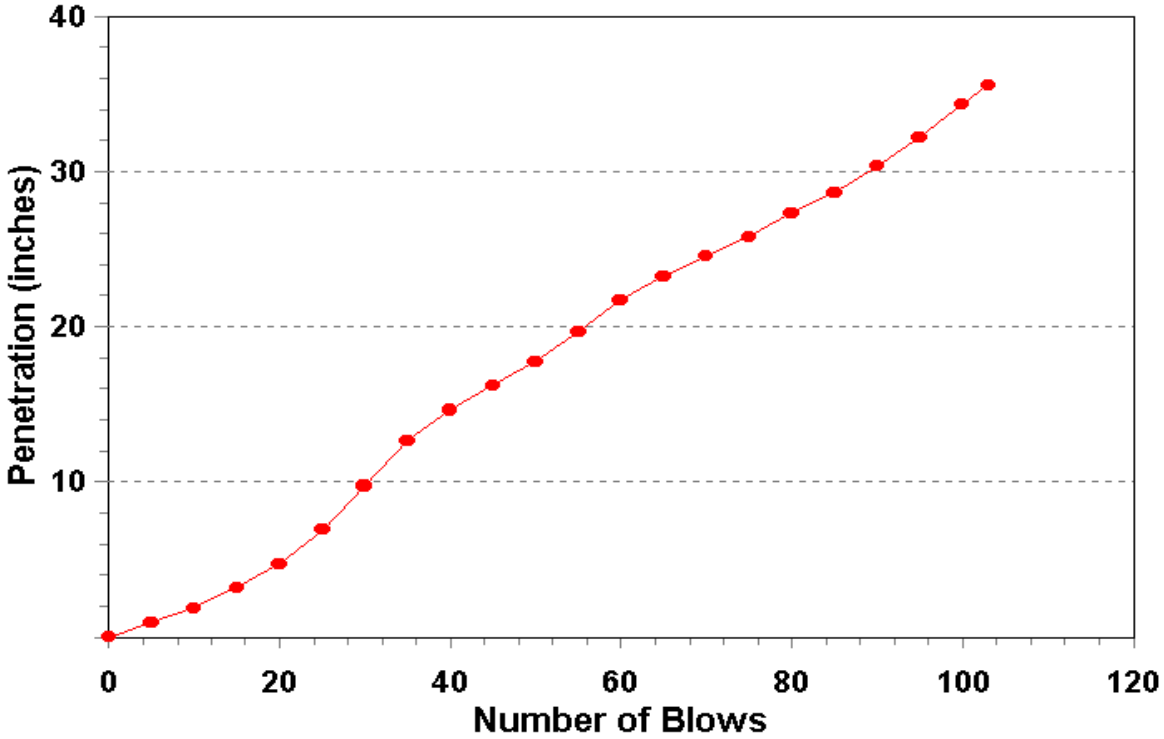

Figure A12. DCP Data Starting from Base at Station 500 along FM 1805.

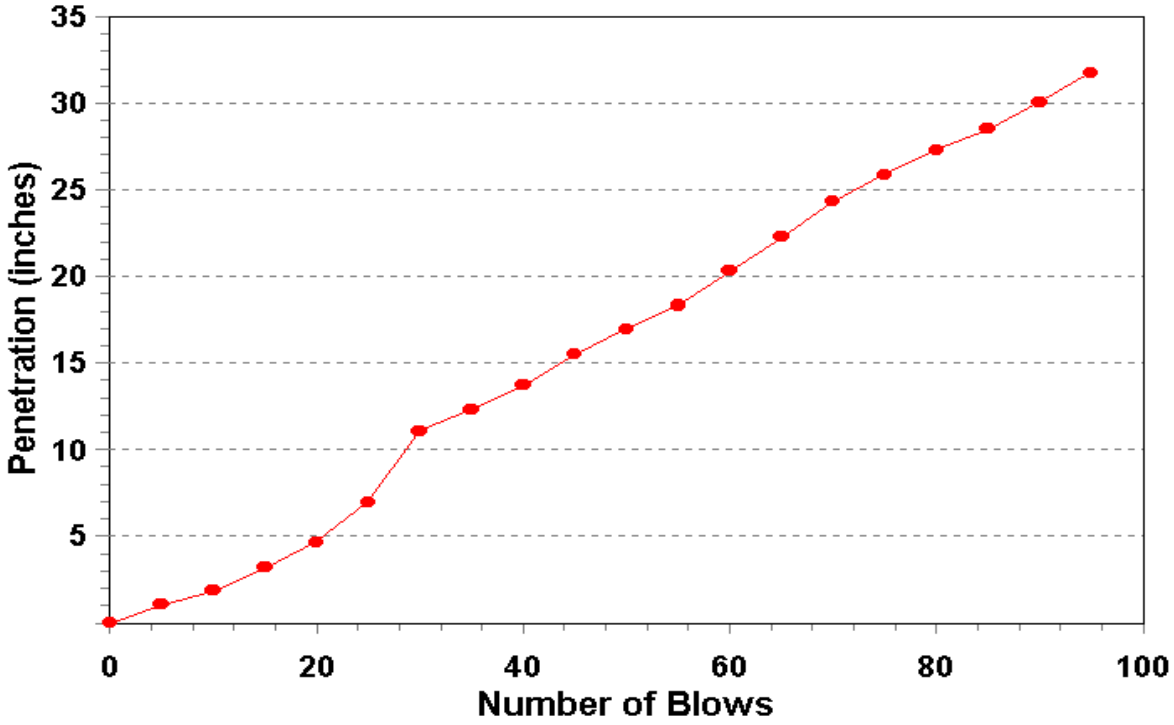

Figure A13. DCP Data Starting from Base at Station 600 along FM 1805.

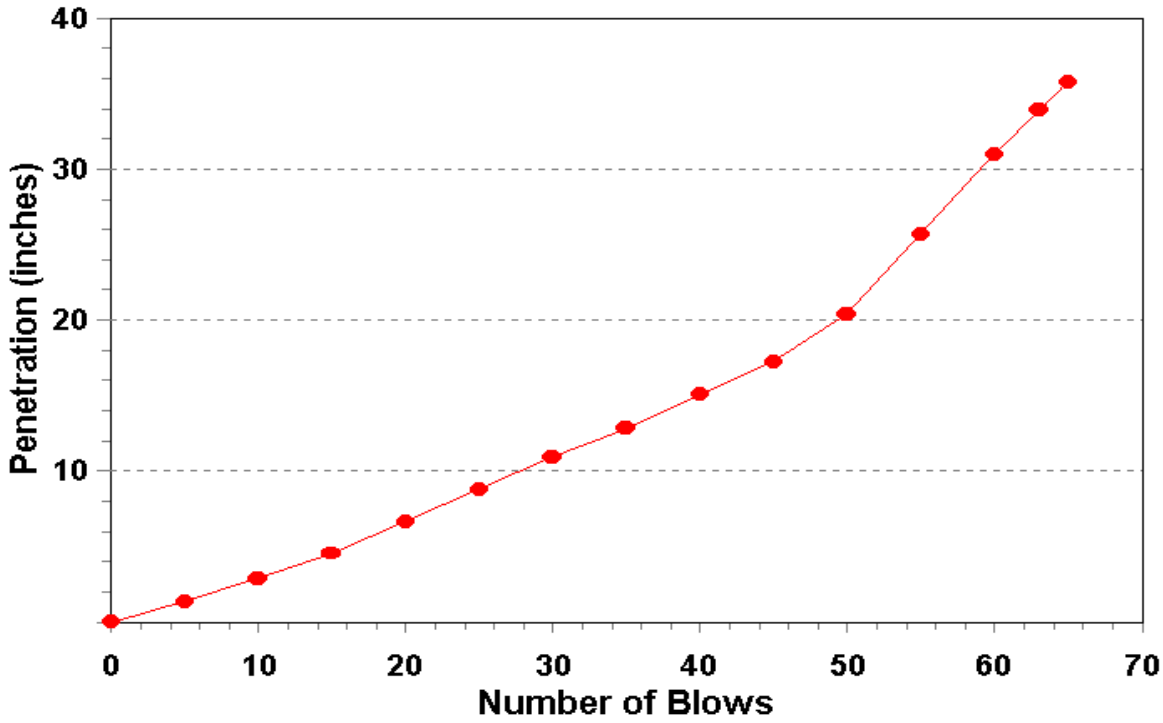

Figure A14. DCP Data Starting from Base at Station 700 along FM 1805.

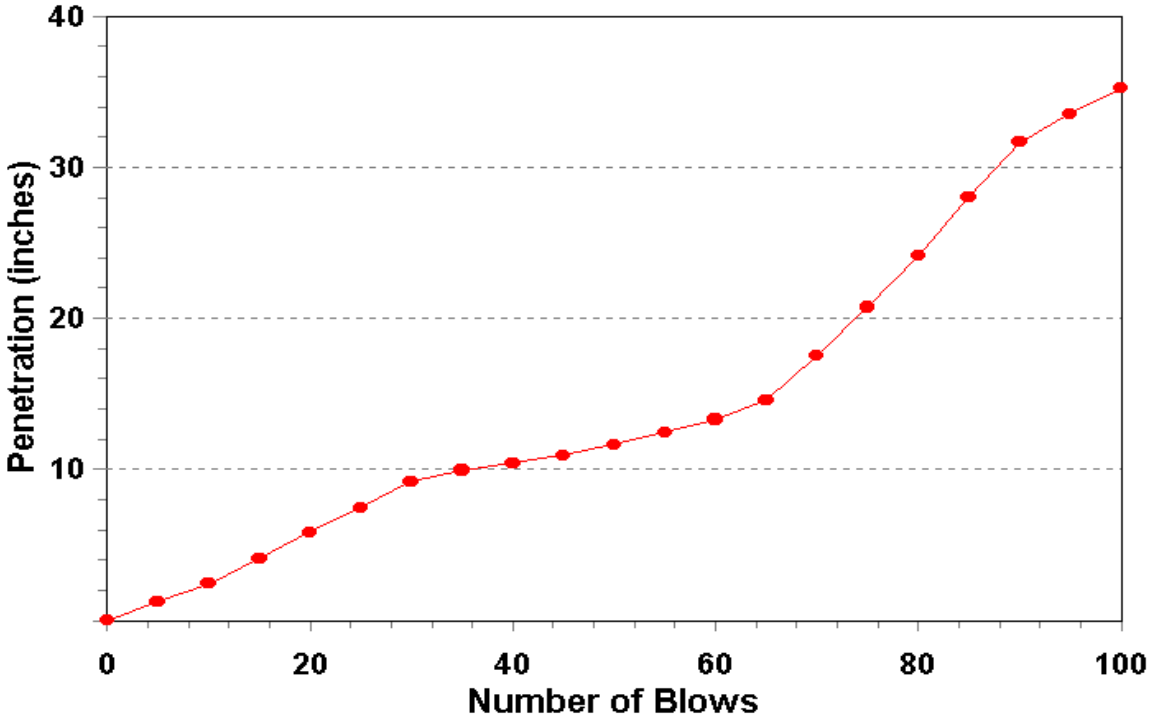

Figure A15. DCP Data Starting from Base at Station 800 along FM 1805.

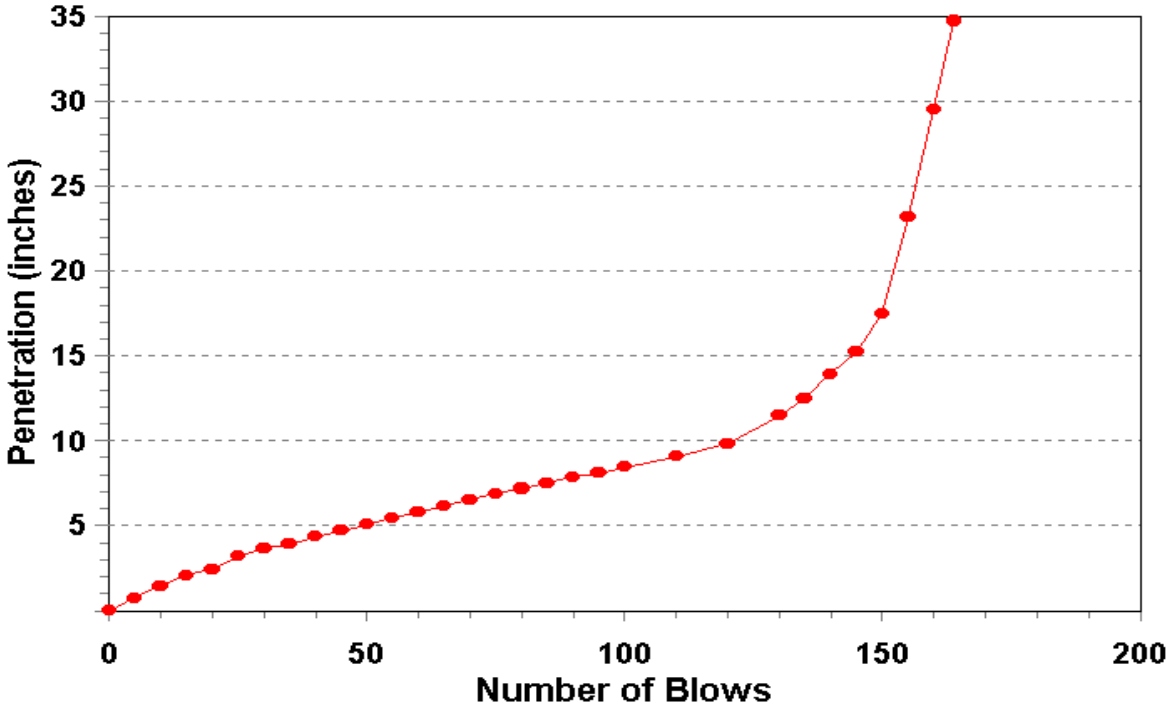

Figure A16. DCP Data Starting from Base at Station 0 along FM 751.

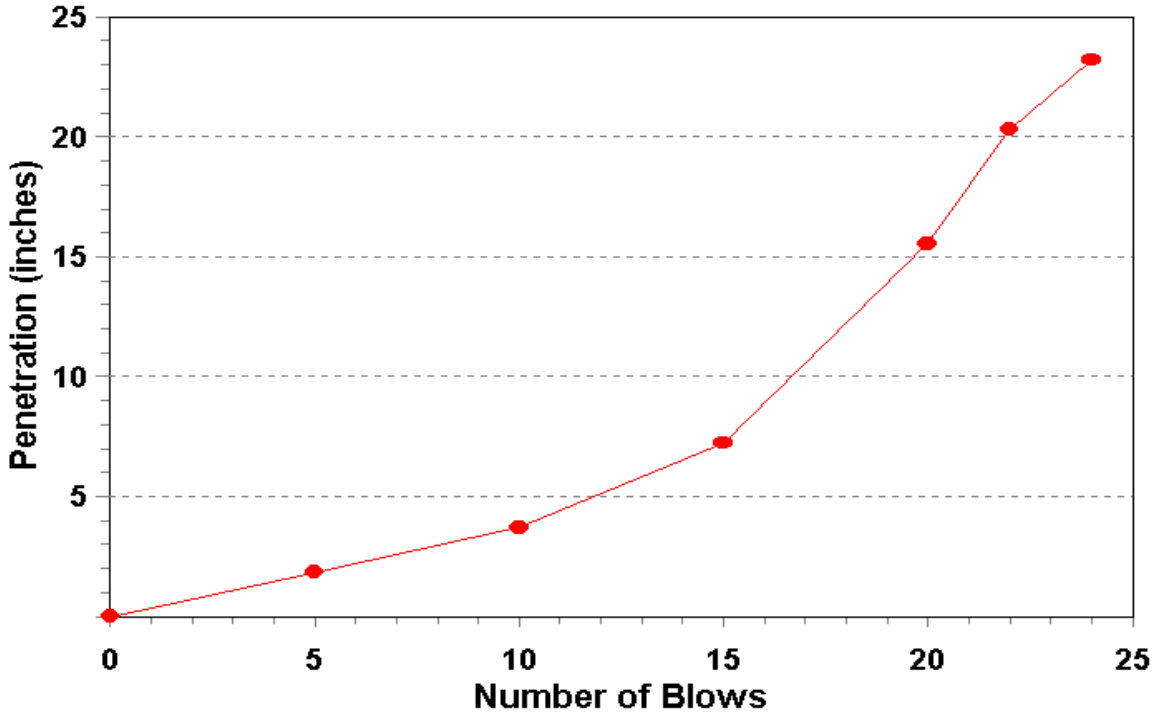

Figure A17. DCP Data Starting from Base at Station 100 along FM 751.

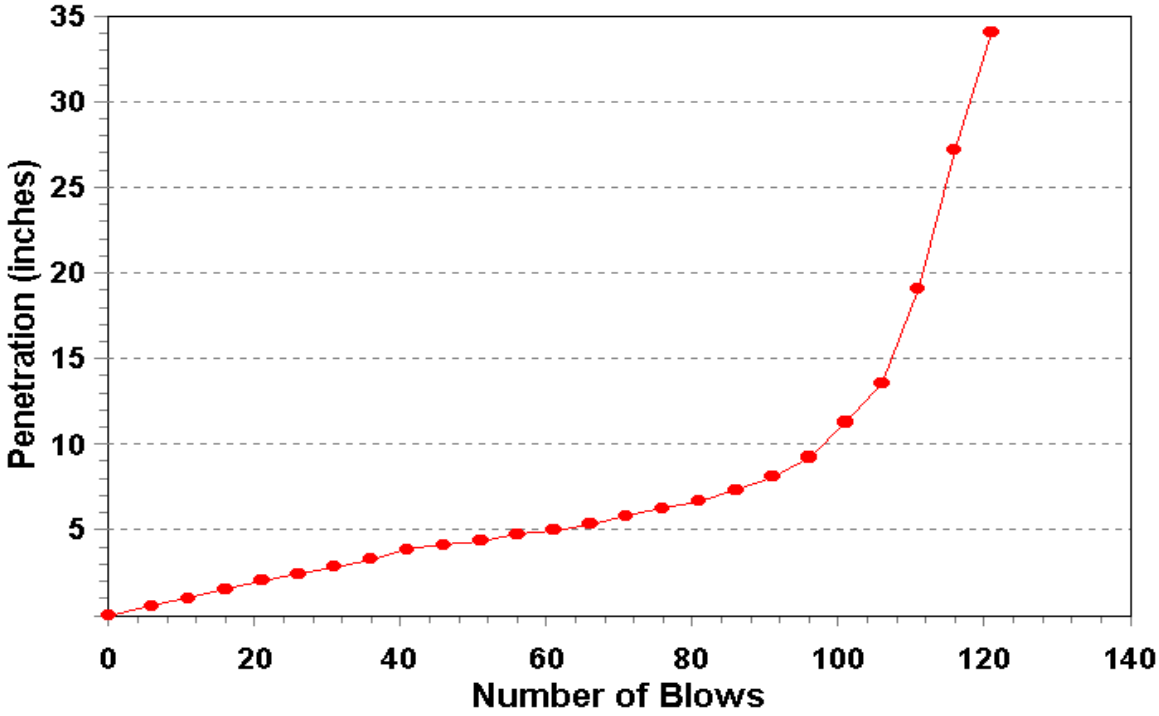

Figure A18. DCP Data Starting from Base at Station 200 along FM 751.

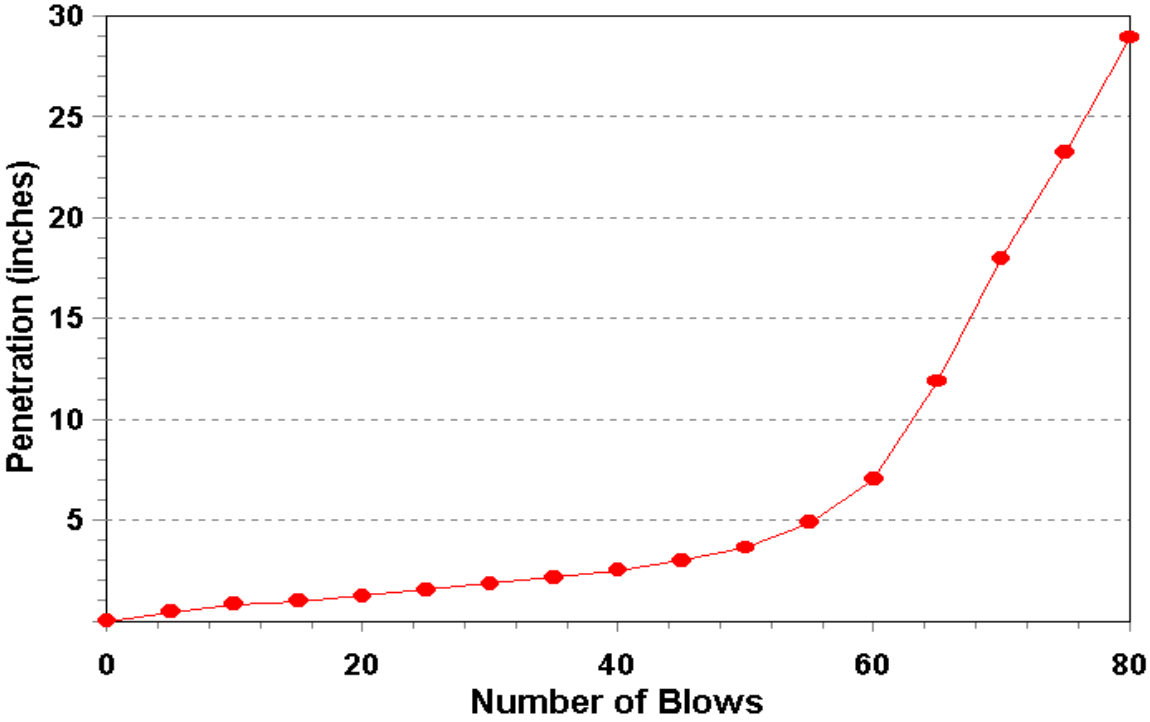

Figure A19. DCP Data Starting from Base at Station 300 along FM 751.

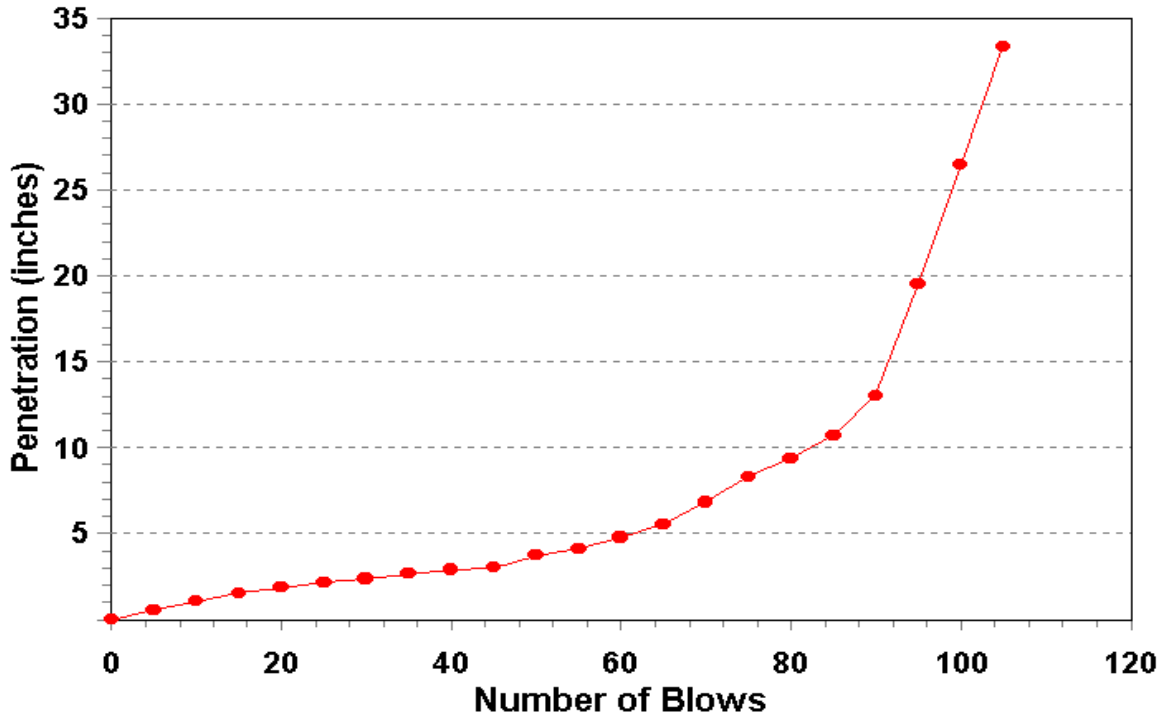

Figure A20. DCP Data Starting from Base at Station 400 along FM 751.

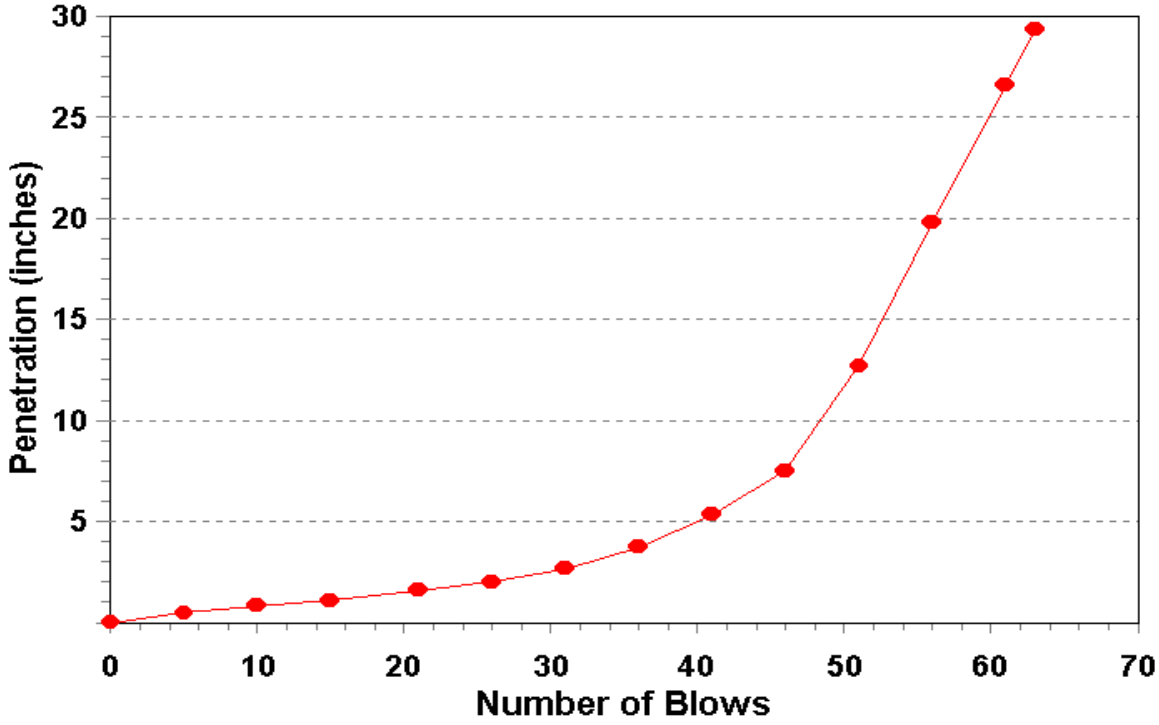

Figure A21. DCP Data Starting from Base at Station 500 along FM 751.

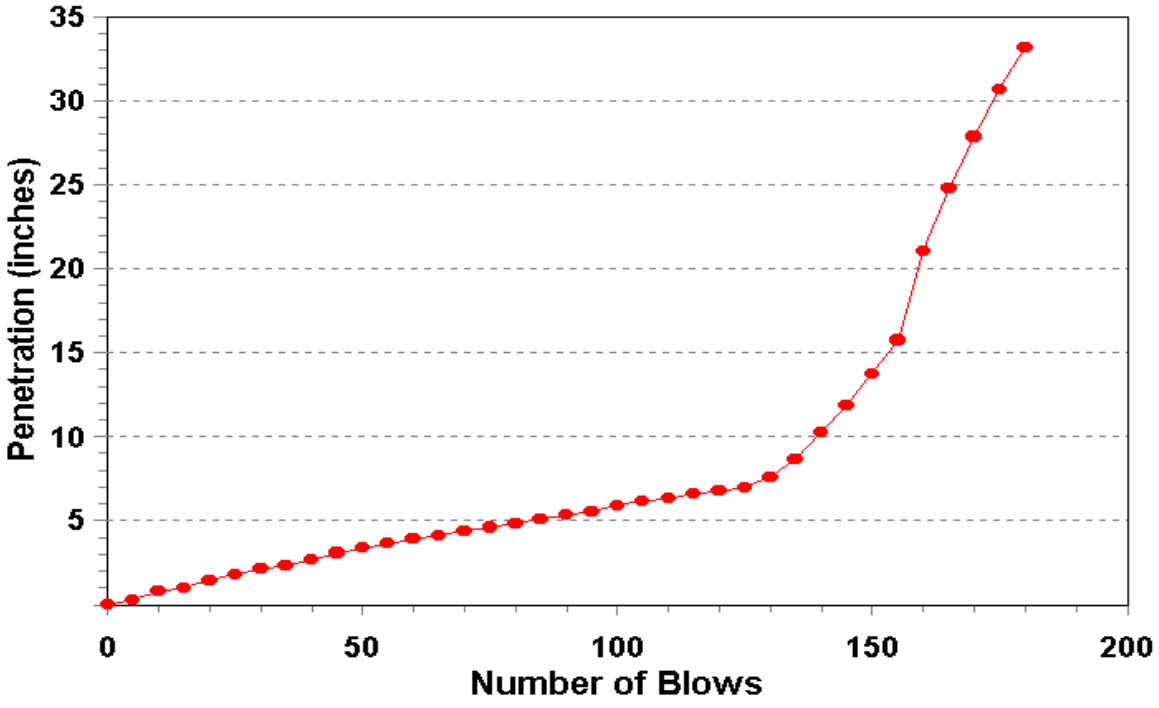

Figure A22. DCP Data Starting from Base at Station 600 along FM 751.

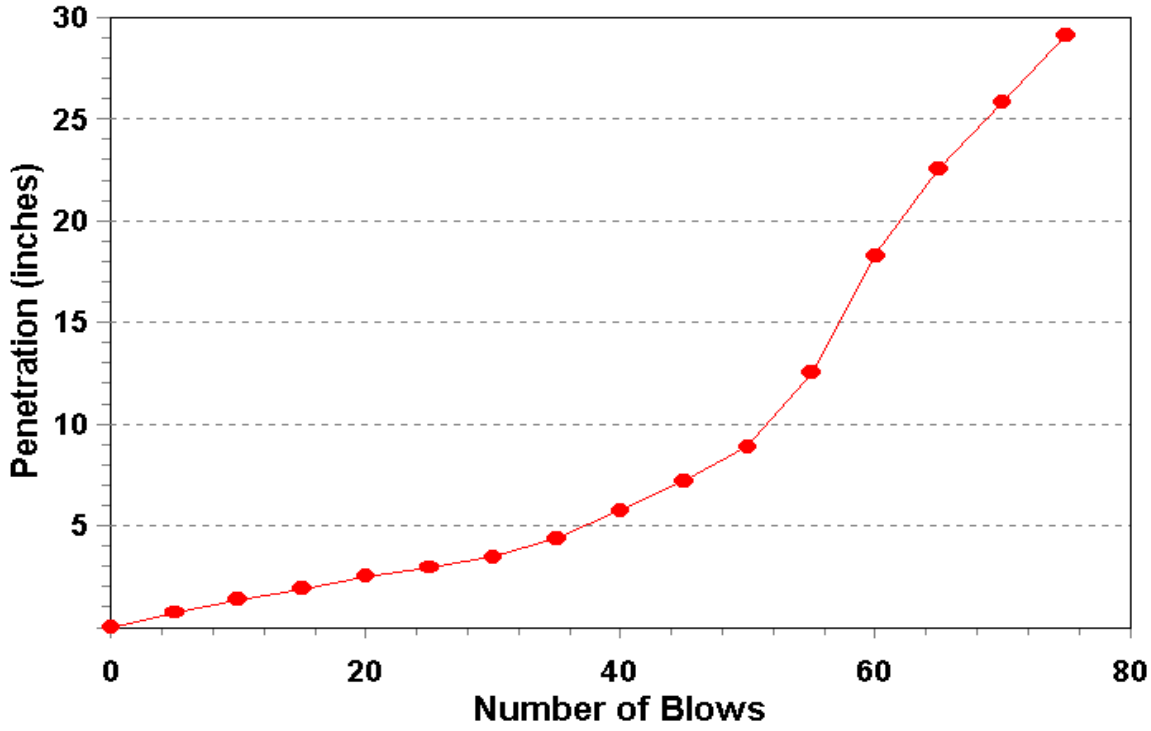

Figure A23. DCP Data Starting from Base at Station 700 along FM 751.

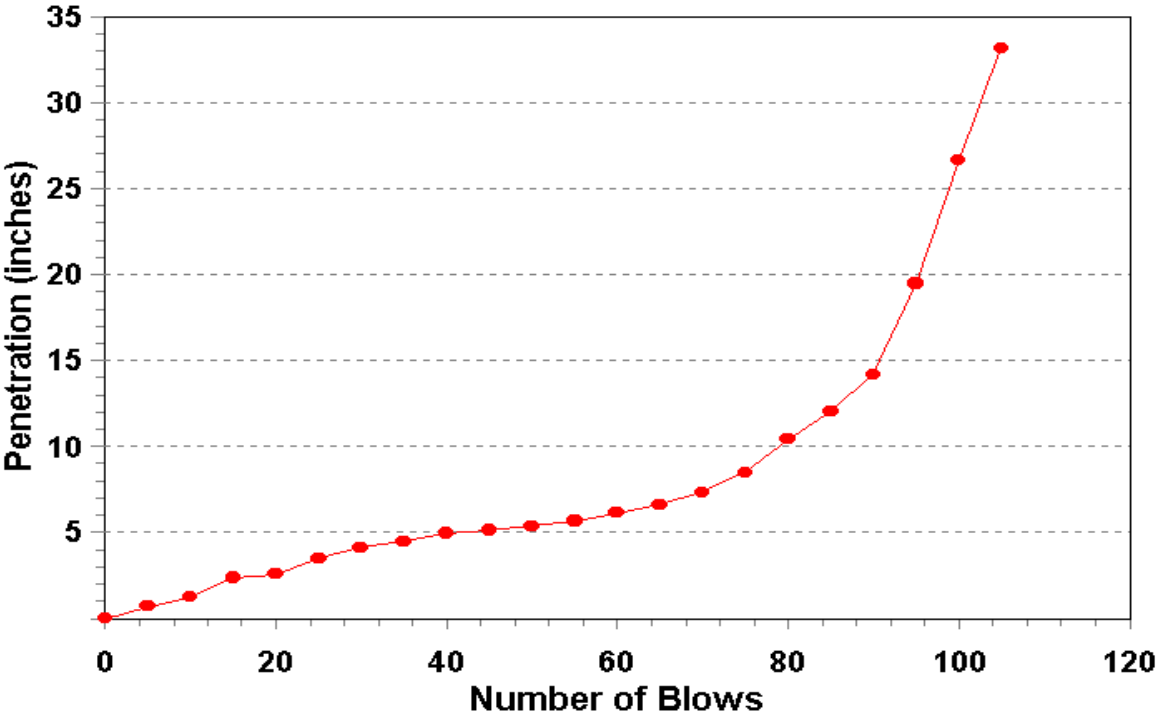

Figure A24. DCP Data Starting from Base at Station 800 along FM 751.

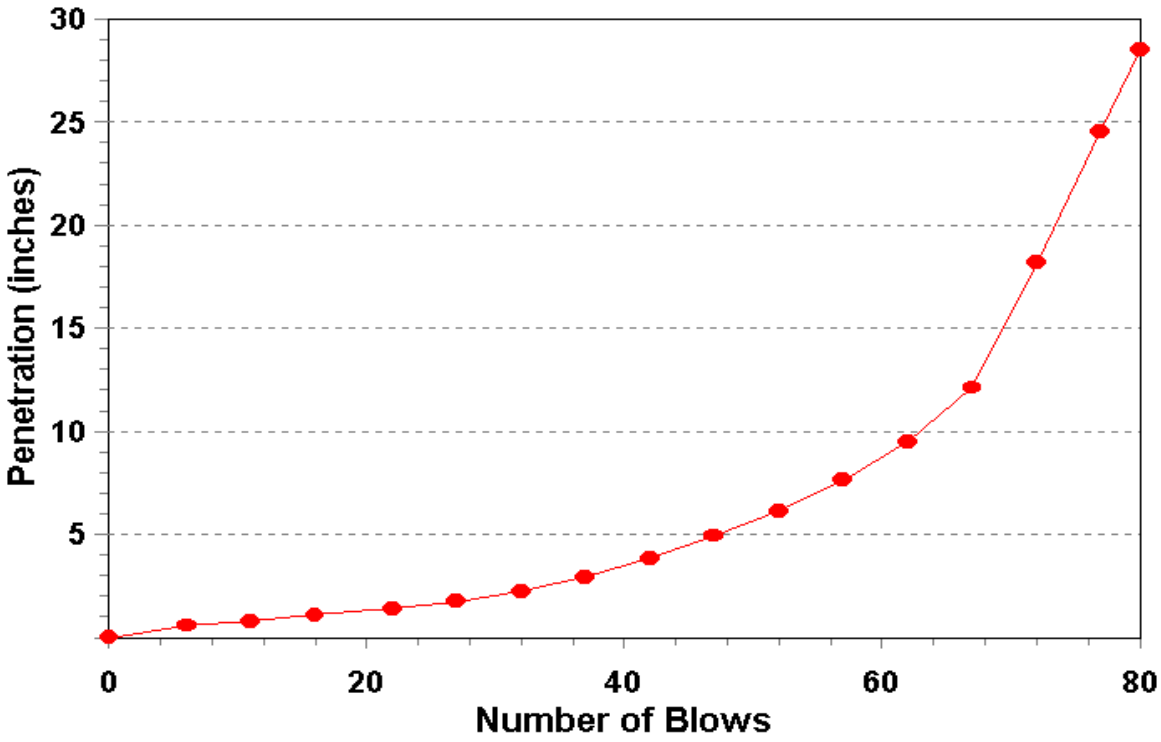

Figure A25. DCP Data Starting from Base at Station 900 along FM 751.

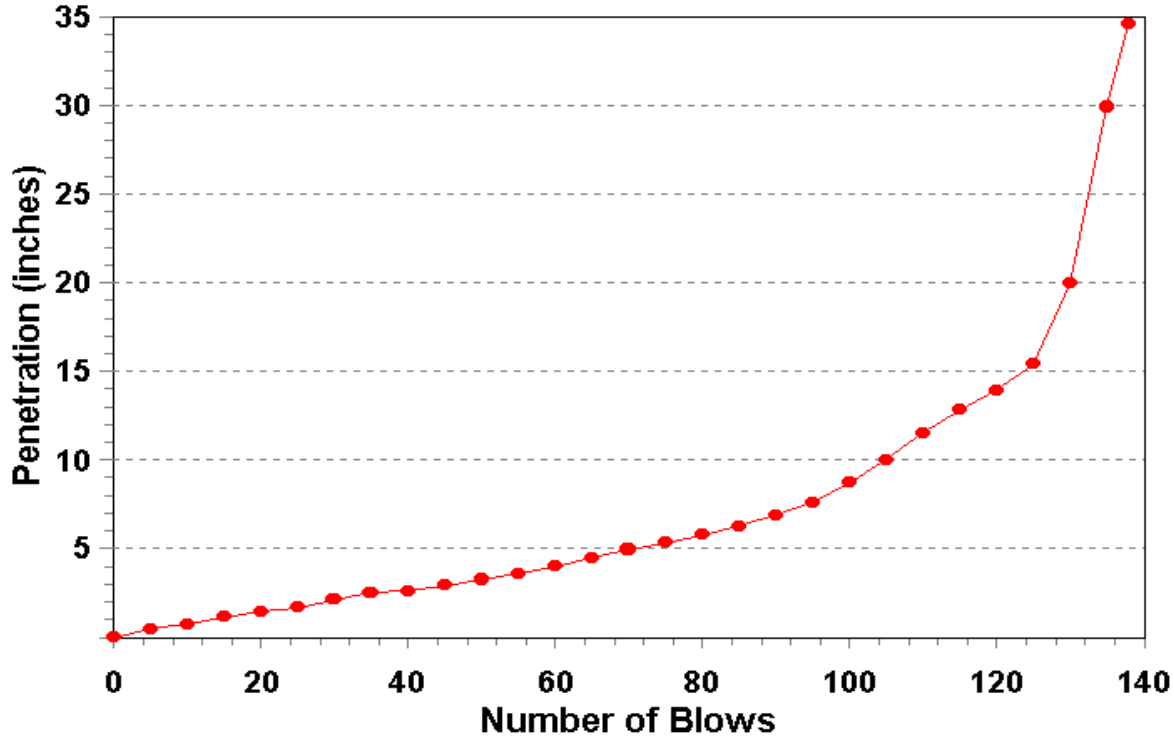

Figure A26. DCP Data Starting from Base at Station 1000 along FM 751.